Use of Particulate Material for the Formulation of Diagnostic Products

Inauguraldissertation

Zur

Erlangung der Würde eines Doktors der Philosophie

vorgelegt der

Philosophisch-Naturwissenschaftlichen Fakultät

der Universität Basel

von

Marine Hélène Mathilde CAMBLIN

aus Frankreich

Basel, 2018

Genehmigt von der Philosophisch-Naturwissenschaftlichen Fakultät

auf Antrag von

Prof. Dr. Jörg Huwyler

Dr. Bernd Herzog

Basel, den 13. Dezember 2016

Prof. Dr. Jörg Schibler

Dekan der Philosophisch-Naturwissenschaftlichen Fakultät

« Il n'y a pas de meilleure récompense que la sensation du travail accompli »

☑ PhD Thesis

TABLE OF CONTENTS

ACKNOWLEDGMENTS

First, I would like to express my gratitude to Prof. Dr. Jörg Huwyler. Thank you for giving me the opportunity to spend the 4 years of my PhD thesis in pharmaceutical technology in your research group. Thank you for being an attentive ear during difficult times, for motivating and trusting me and giving me the chance to take a step forward with a new project.

I would like to thank Prof. Dr. Matthias Hamburger for taking the chair of my PhD thesis and Dr. Bernd Herzog for being the co-referee.

I would like to thank Dr. Vimalkumar Balasubramanian and Dr. Fabiola Porta their supervision during the first 2.5 years of my thesis in drug targeting. My deepest acknowledgment to Dr. Maxim Puchkov, for his great supervision during the last part of my PhD. Thank you giving me the opportunity to work in your team, for sharing your knowledge, expertise and ideas for my project. Thank you for our long discussions and for your advice about professional and personal life.

Many thanks to all my colleagues: Pascal, LeHa, Helene, Dominik, Philip, Klara, Sandro, Gabriella, Tanja, Veronika, Daniel, Reiji, Leonie, Roger, Andreas, Anacelia, Emilien, Andrea, Tobias, Dominique, Tim, Jonas, Emre for bringing such a nice atmosphere in our team. Thank you, Isabel, for being my friend and running partner during lunch breaks. I also would like to thank Susanne Schenk, Darryl Boreland, Denise Ruolf, Christina Erb and Stefan Winzap for their help and support at the Pharmacenter and during the student practical works.

This work is dedicated to my parents Marie and Philippe. I would have not been able to go so far in my studies without their support. Maman, Papa, merci de m'avoir permis d'étudier la pharmacie dans les meilleures conditions, d'avoir cru en moi et de m'avoir supporté toutes ces années. Merci pour votre présence et votre soutien dans les moments heureux, mais aussi lors des moments plus difficiles que j'ai eu à traverser. C'est aussi grâce à vous que je suis arrivée jusque-là et que je suis épanouie dans ma vie personnelle et professionnelle.

I would like to thank all my friends and my entire family for being who they are, for the good moments spent together. Je voudrais particulièrement remercier Maëlle, Rose-Emilie, Pierre-Jean et Yann d'être des frères et sœurs au top !

Finally, I would like to thank my husband, Jean-Philippe. Merci d'être toi, de partager ma vie et d'avoir confiance en moi. Merci pour tous ces bons moments passés en à tes côtés et tous ceux à venir dans les 70 prochaines années. Merci d'avoir été présent pour me motiver dans les moments difficiles de la rédaction de ce manuscrit, de m'avoir soutenue et encouragée.

SUMMARY

Diagnosis is the medical act that identifies the signs and the symptoms of an illness. It is an unavoidable step before the prescription of any medical treatment. Over the last decades, the increasing desire of more precise diagnosis, led to the emergence of new tools: the diagnostic products.

These products are used to identify and monitor the cause of disorders to facilitate and specify the diagnosis, and thus, allow an adaptation of the medical treatment. Diagnostic products can be imaging probes, labels for immunoassays, reagents, contrast agents, or radiopharmaceutical products. As a part of diagnostic products, companion diagnostics are specific of a treatment and are mostly used in cancer therapies. They help determining if the patient would profit from a medication, depending on his genotype and possible genetic mutations. Phenotyping cocktails are diagnostic products that are used in phenotyping to obtain additional information, considering the effect of external environmental factors which can also influence the response to a treatment.

Diagnostic products permit the personalization of medicine, by adapting the medications to the patient, optimize the treatment, and reduce potential side effects. Despite their great benefit, only a few diagnostic products are developed, limiting the possibility to improve diagnosis and therapeutics. In this manuscript, we present 2 diagnostic products formulated with nanoparticulate and microparticulate material. The first formulation consists in "polymersomes containing quantum dots (QDs) for cellular imaging". These polymeric vesicles have the capacity to encapsulate highly fluorescent probes like QDs to prevent the toxic effect of the latter without altering their imaging properties. The second diagnostic product is the "CombiCap, a novel drug formulation for the Basel phenotyping cocktail". This unique formulation is equivalent to the 6 dosage

forms composing the Basel cocktail and presents many advantages that facilitate its diagnostic use.

Both formulated products are intended for diagnostic purposes. They are safe, reliable, specific, customizable, easy to formulate and easy to use. They bring precise information on the health status of the patient in order to give a better diagnosis, to adapt the medical treatment and to monitor the therapeutic response. The interest for individualized therapies is growing, and therefore, the development of new diagnostic products needs to increase. In the future, the personalization of diagnosis and therapeutics will be a common medical practice.

ABBREVIATIONS

ATC	Anatomical Therapeutic Chemical
CT	Computer Tomography
FDA	Federal Drug Agency
FEV	Forced Expiratory Volume
LFA	Lateral Flow Assay
MRI	Medical Resonance Imaging
NMR	Nuclear Magnetic Resonance
PET	Positron Emission Tomography
QD	Quantum Dot
SPECT	Single Photon Emission Computer Tomography
SPION	SuperParamagnetic Iron Oxide Nanoparticle
WHO	World Health Organization

TABLE OF FIGURES

1 GENERAL INTRODUCTION

1.1 Definitions and origins

1.1.1 Diagnosis

Diagnosis is defined as the identification of the nature of an illness or other problem by examination of the symptoms. The word diagnosis derives from the ancient Greek *διάγνωσις*. It is composed by the prefix *δια-* (dia-) meaning "through" and *γνῶσις* (gnosis) meaning "knowledge" (1). Literally, diagnosis is related to the ability to get the knowledge through the observation of symptoms.

Every medical treatment results from the diagnosis of a disease or a special health condition. Most diagnoses are made on a daily basis in the doctor's office in the case of minor sicknesses such as a cold, a migraine, a stomach flu or a depression. These common diagnoses consist in identifying a disease, based on the observation of physical and mental symptoms; and paying heed to the medical history of the patient (2). However, some diseases require more thorough examinations in order to be diagnosed. To evaluate precisely the health condition of a patient, it is possible to rely on *in vivo* or *in vitro* diagnostic methods. On the one hand, *in vivo* diagnosis is made directly on the patient and often relays on medical imaging such as X-rays, computerized tomography (CT), medical resonance imaging (MRI), ultrasounds, or nuclear magnetic resonance (NMR). On the other hand, *in vitro* diagnosis consists on the examination of body fluids, cells, tissues, or organs taken ahead from the patient's body.

1.1.2 Diagnostic products

Both types of diagnosis require the use of diagnostic products. The latter are defined by the FDA as reagents, instruments and systems intended to be used in the diagnosis of an illness or other health condition to cure, treat or prevent diseases (3). In other words, diagnostic products help physicians in the observation and interpretation of a patient's clinical status, and allow identifying and measuring normal or abnormal constituents of body fluids or tissues. *In vitro* diagnostic products are usually reagents (e.g. chemical, biological or radioactive substances), and are "*intended for use in the collection, preparation and examination of specimens taken from the human body*" (3). The main advantage of *in vitro* diagnostic tests is the possibility to analyze the samples after their

collection, without requiring the presence of the patient. Meanwhile, *in vivo* diagnostic tests are done *in situ* by analyzing a physical feature of the patient with electromedical or imaging instruments. Most *in vivo* diagnostic products are contrast agents that are used in medical imaging to enhance the visualization of fluids or structures such as organs or tumors.

Since a few times, diagnostic products are increasingly developed. They are used to obtain more accurate diagnosis and to further prescribe treatments adapted to the patients, in the view of a personalization of the therapies.

1.1.3 Brief history of diagnosis

In the early years of civilization, the first healers observed clinical symptoms to make diagnoses before recommending any kind of treatments. The first written trace of diagnosis was discovered by Edwin Smith on a papyrus dated from circa 1600 B.C. It compiled older papyruses on surgery; giving anatomical observations, the diagnostic method of 48 health injuries and their possible treatments (4). Many years later, around 300 B.C., Hippocrates, also known as the "Father of Medicine", diagnosed diabetes mellitus for the first time by tasting the sweetness of patient's urine when coupled with other symptoms like polyuria, polydipsia and polyphagia (5). During the middle age in Europe, Christianism rejected any type of science or medicine. The "water casting", a technique for urine analysis was the only authorized diagnostic method (6). From 1300, uroscopy became the most commonly performed test to detect diseases and abnormal health conditions from the observation of the color, consistency, smell and even taste of the urine. A colorimetric wheel (Figure 1) was created to help the physicians making their diagnosis (7). Uroscopy is a diagnostic method that was used over centuries. This method can be considered as the starting point of modern laboratory diagnosis, and is still used in the early detection of urinary tract infections, kidneys disorders, liver problems, diabetes or other metabolic conditions and pregnancy (8).

Figure 1: Urinary wheel from circa 1500.

Physicians were referring to this organoleptic wheel to make their diagnosis based on the patient's urine taste and color.

The Renaissance brought a new vision on sciences and particularly in medicine with the emergence of body dissection to learn about human anatomy. During the following centuries, the invention of several medical instruments such as microscope, thermometer, stethoscope, ophthalmoscope, and laryngoscope, expended the precision of medical diagnosis. Chemical and bacteriological laboratory tests were also developed to diagnose diseases such as tuberculosis, cholera, typhoid and diphtheria (6). In the early 20th century, J.C. Todd published the first edition of the manual entitled "Clinical diagnosis by laboratory methods", to give a description of laboratory diagnosis techniques. This manual was completed by J. Henry and has remained a reference book over the years. The 23rd edition is scheduled in 2017 (9). From the 20th century, huge progresses were made in the field of diagnosis; many imaging techniques were discovered such as fluorescence microscopy, X-ray spectroscopy, mass spectrometry, electron microscopy. New diagnostic methods were invented like radio-immunoassays and immune-electrophoresis (10). Diagnostic products were also developed to enhance the results of diagnostic procedures, for instance, contrast agents, radiolabels, lateral flow assays, and medications for diagnostic purpose (11). For some time now, the field of medical diagnosis has experienced extensive development with the emergence of personalized medicine, to improve early diagnosis and to adapt treatments to each patient (12). This project requires advanced technologies and products to give the possibility to make precise

diagnosis and deliver the accurate drug to the right person, at the right time, with the appropriate pharmaceutical form, with the correct dose and with a good quality. For this purpose, the application of particulate material such as nanoparticles and microparticles is a great benefit.

1.2 Nanoparticles for imaging and diagnostics

Nanotechnology applied to molecular diagnosis is known as nanodiagnostics (13). With the increase of interest in the field of nanotechnologies, several nanoparticles were developed for a diagnosis purpose. These nanodiagnostics products have 2 main functions; the first one as imaging agents to enhance visualization of body tissues (14) and the second one as labels for diagnostic immunoassays (15) . Even potential diagnostic applications of nanoparticles are very broad, current applications are only developed in the fields of medical imaging, biomarker research, cancer diagnosis and detection of infectious diseases (16).

1.2.1 Medical molecular imaging

For the past 40 years, the evolution of molecular imaging has improved the early detection of diseases (17). Medical imaging consists in the non-invasive evaluation of anatomical and functional characteristics to facilitate the early diagnosis, identify the stage of disease, provide information on physiological abnormalities and can help in following the efficacy of a medical treatment (18). The most common imaging procedures for clinical diagnosis are MRI and ultrasounds to get information about soft tissues. Computer tomography gives information about structures and particularly bones. Positron emission tomography (PET) and single photo emission computer tomography (SPECT) are used to obtain information about metabolic parameters. Optical imaging is as well a common procedure used to get precise images of soft tissues (17,19).

For a better visualization and characterization of biological processes during molecular imaging, it is recommended to use sensitive molecular imaging probes (13). Nanoparticles are well described in the literature for imaging purposes. There is a variety of nanoprobes such as polymeric particles and vesicles, liposomes, superparamagnetic iron oxide nanoparticles (SPIONs), and metallic nanoparticles i.e. ytterbium, bismuth, and gold nanoparticles (19,20).

Generally, nanoparticles for diagnosis range between 5-100 nm and are combined with low molecular weight contrast agents to optimize their pharmacokinetic properties, biodistribution and tissue penetration (14). As they are not therapeutics, diagnostic products should not induce any physiological effect; have a short circulation time, a fast biodegradation and elimination as well as a low toxicity (19,21). However, to reach the structure that needs to be visualized, the imaging nanoparticles can be labeled with targeting ligands (18). Unlike for therapeutics, nanoparticles for diagnostic are not well developed and only few are commercialized and used in clinical imaging (22).

1.2.2 Examples of nanoparticles for imaging

1.2.2.1 Superparamagnetic iron oxide nanoparticles (SPIONs)

SPIONs find their application in MRI and are considered as highly effective contrast agent to monitor anatomical, physiological, and molecular changes during the evolution of a disease or a treatment. The superparamagnetism is given by their reduced size that is below a single magnetic domain (23). SPIONs present several advantages as compared to traditional contrast agents. They have a stronger magnetic signal strength, their toxicity is relatively low, their contrast enhancement last longer, their sensitivity is increased, and they do not retain their magnetization after the removal of the external magnetic field (14,24).

SPIONs are commonly used as a core material for passive and active targeting. They can be coated with biocompatible polymers such as polyethylene glycol, dextran, alginate, or other synthetic polymers. For active targeting, ligands like proteins, peptides, nucleosides, or antibodies can be attached to the magnetic iron oxide core via an anchor arm. The advantage of the targeting is the accumulation of the SPIONs in the defined cells, mostly cancer cells. This accumulation permits a better differentiation between tumors and healthy tissues on the MRI pictures (25). Only passive-targeting SPIONs are currently on the market, e.g. Ferristene (Abdoscan®, GE Healthcare, UK) that is used per oral for gastrosintestinal MRI (26), and Ferrixan (Resovist®, Bayer Schering, Germany) for liver and spleen imaging (27) or at different phases of clinical trials. Actively targeted SPIONs for tumor cells imaging by MRI are still on development. For instance, Fu at al. developed an anti-IL-1β monoclonal antibody

functionalized SPIONs for the diagnosis and the treatment of acute temporal lobe epilepsy (28). Wan et al. worked on active targeting of the lung adenocarcinoma cells. They coated SPIONs with oleic acid and carboxymethyl dextran and then, functionalized them with anti-CD44v6 monoclonal antibody (29).

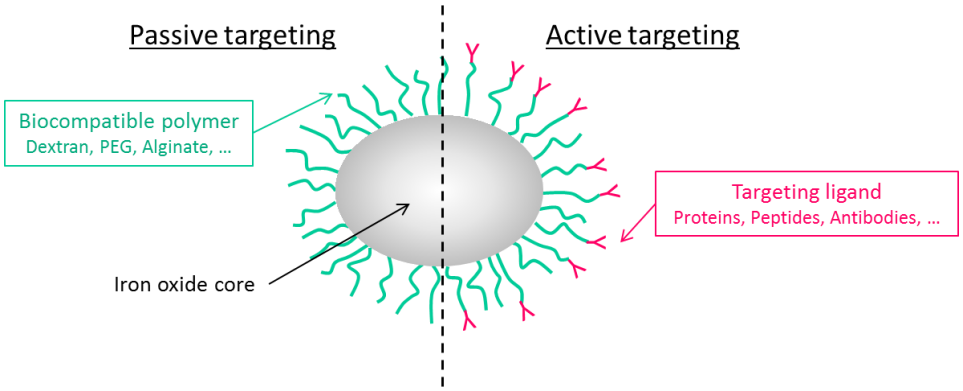

Figure 2: Strategy of passive or active targeting of SPIONs.
Iron oxide core can be coated with biocompatible polymer and labeled with ligands to assess the targeting of cells or tumors. Adapted from Rosen et al (24)

1.2.2.2 Quantum dots

Quantum dots (QDs) are fluorescent nanoparticles with higher optical properties compared to organic dyes. Most of the QDs are made of semiconductor materials, usually cadmium (Cd) associated with sulfur (CdS), selenium (CdSe) or tellurium (CdTe). The size of these nanocrystals is in the range of 2-10 nm range. The wavelength of fluorescence emission (450nm - 850nm) is related to the dimension of the QD, allowing all colors for imaging and diagnostic assays. Main advantages of QDs are a long fluorescence lifetime and an imperceptible photo bleaching over hours (30).

QDs are generally used as fluorophores in diagnostic optical imaging for cancer applications, including the cellular and molecular imaging of tumors. This imaging method has a good sensitivity and is non-invasive, but such optical technique is limited in term of tissue penetration depth (31). In order to increase the residence time of the QDs in the body, a polymeric coating can be applied on their surface and it is possible to target a defined cell line after conjugation with bioactive molecules. For instance, Akerman et al. labeled QDs with different peptides specific to vascular sites: one peptide bonded cells in lung blood

vessels; the other bounded to lymphatic vessels and tumor cells. Each peptide targeted the dedicated site in mice, showing that the QDs can be targeted *in vivo* with a good specificity (32). However, the use of QDs is limited by the toxicity of their heavy-metal core (33). It is essential to prevent this toxic effect for *in vivo* imaging and diagnostic use. In chapter 3, the article "Polymersomes containing quantum dots for cellular imaging" describes a method for isolating the QDs in polymeric nanovesicles called polymersomes, while preserving their imaging properties. The polymer shell could protect the cells from death without altering the fluorescent optical features of the QDs (34).

1.2.2.3 Gold nanoparticles

Gold nanoparticles are largely used in multiple imaging procedures because they present many benefits. They are easy to synthetize with a precise control of the particle size and shape. They have a low short term toxicity and can be tuned by surface modification or bio-conjugation (14). The use of gold nanoparticles for computer tomography was established 10 years ago, by Hainfeld et al. to detect breast tumors in mice. They showed that gold nanoparticles can be used as contrast agents with properties that overcome the limitations of iodine-based agents. Few minutes after injection, they obtained high-resolution pictures of the tumor, kidneys, and blood vessels (Figure 3). No toxic effect was detected after renal excretion, indicating the safety of gold nanoparticles as a contrast agent (35). The contrast of pictures and the time of circulation in the blood can be extended by a pegylated coating of the gold nanoparticles (36,37).

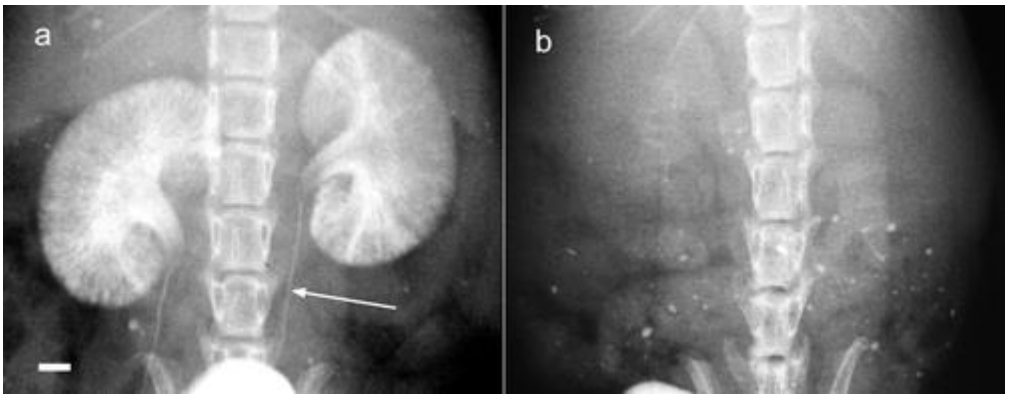

Figure 3: X-ray picture of mouse kidneys.
1h after IV injection of gold nanoparticles (a) and conventional iodine contrast agent (b).

The arrow shows the ureter (100 µm diameter). The bar represents 1 mm. Source Hainfeld et al. (35).

1.2.2.4 Lipid nanoparticles

Liposomes have mostly been developed for drug delivery; however, a few formulations were developed for diagnosis. In the 1980s, the first liposomal radiotracer VesCan® (Vestar Inc., USA) was developed for *in vivo* imaging. The liposomes were loaded with the radionucleotide ^{111}In and were used as diagnostic agents for scintigraphy of tumors in clinical trials (38,39). Despite the broad development of liposomes in drug delivery, few researches are focused on liposomes for the diagnostic purpose. Most diagnostic liposomes are labeled with radionucleotides such as ^{67}Ga, ^{111}In, ^{99m}Tc, and ^{18}F for PET and SPECT imaging in the diagnosis of tumors (40–43).

1.2.3 Nanoparticles as labels in immunoassays: lateral-flow assays

A lateral-flow assay (LFA) (also called immunodipsticks) is a diagnostic tool intended to reveal the presence or the absence of a compound indicating a health condition like a pregnancy (44,45), a metabolic disorder such as cardiovascular disease (46–48), a kidney failure (49,50), or diabetes (51–53). These LFAs can also be used to detect pathogenic infections (54–60), bio-warfare agents (61,62), toxins in food or water (63–68) as well as the presence of drugs of abuse in body fluids(69,70). The first immunodipstick was described in 1986 by Pappas as an improvement of a dot-ELISA assay for the diagnosis of echinococcosis (71).

The LFA consists of a strip containing a sample pad, a conjugate pad, a detection zone and an absorption pad (Figure 4)(72). At one extremity, the sample pad permits the inlet of the sample on the strip, the conjugate pad contains the reactive agents (antibodies) labeled with detection molecules (colored nanoparticles). The detection zone has 2 lines, one for the validation of the test (T) and the other to control (C) the functionality of the test (73). At the other extremity, the absorption pad captures the excess of sample. The LFA combines the principle of chromatography and immunology (74). Indeed, the antigens contained in the liquid sample (blood, urine, tears, or saliva)(75) are carried by capillarity to the conjugate pad where they bind to specific antibodies labeled with nanoparticles. The complex analyte-antibody-nanoparticle is then

recognized by the antibodies that are immobilized at the test line. The remaining labeled antibodies bind to the immobilized antibodies at the control line. Upon the antigen binding, the nanoparticles aggregate along the line and produce a visible signal (76). If the test is positive, 2 colored lines arise on the detection zone, however, in the case of a negative result, only the control line appears because no antigen could bind the antibodies from the test line (15).

The labels are colored or fluorescent nanoparticles. The visible color comes from the immune reaction at the test or control line (76). These nanoparticulate labels are smaller than the pore size of the membrane to avoid any obstruction, and are generally gold nanoparticles (77–81), latex particles (82), carbon nanoparticles (83,84), quantum dots (85,86) or liposomes (63,87–89).

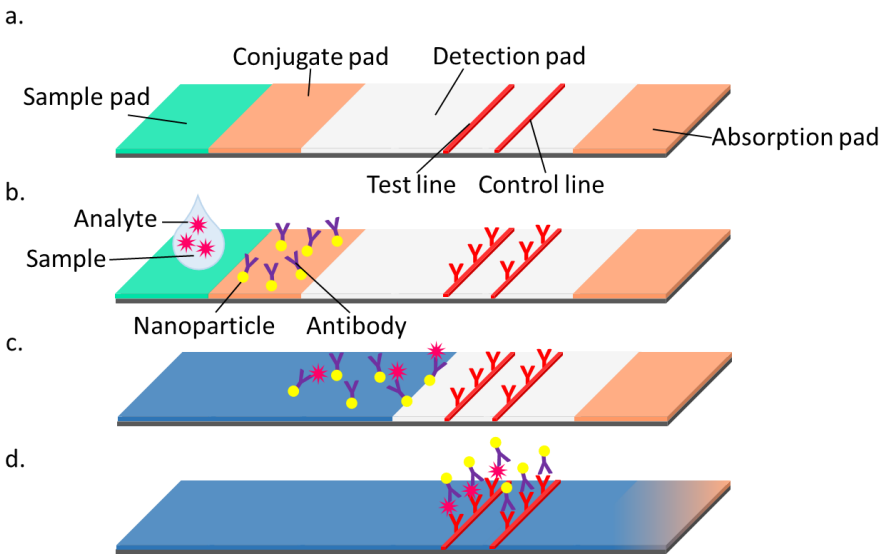

Figure 4: Schema of a lateral flow assay

(a). Start of assay by adding liquid sample (b). Antibodies labeled with colored nanoparticles bind the antigen from the sample to form a complex (c). Complexes (antigen-antibody-nanoparticle) move by capillarity on the detection pad and bind to test line (positive result), labeled antibodies without antigens bind to control line (d). Schema adapted from Mark et al (72)

Lateral flow assays are widely developed as diagnostic products because they offer many advantages. They are easy to use and do not need sophisticated machines for the interpretation of the results, meaning they can be used at a point-of-care (e.g. in the doctor's office, at home or even in a remote area from Amazonia). The time needed to give a diagnosis with a LFA is short because the result of the test is visible within 3 to 20 minutes(65). The cost of diagnosis is

also reduced because LFAs are relatively inexpensive (less than 1€ for the cheapest) compared to the analyses performed at the hospital or in a laboratory. A small sample (few microliters) is enough to perform the test.

However, this small sample size can lead to a reduced sensitivity and specificity that makes the test more difficult to interpret. Another weakness of LFAs is the qualitative or semi-quantitative aspect of the result. Indeed, it is difficult to quantify a response based on a visual observation. Nonetheless, researches are improving the sensitivity of LFAs with new labels such as superparamagnetic nanoparticles (74), indigo precursor nanoparticles (90), platinum nanoparticles (91), modified gold nanoparticles (64,92–94). The principle of the LFA itself can also be improved by electrochemical detection (95,96), magnetic detection (97), Raman scattering (98) or thermal detection (99).

1.3 Microparticles for diagnostic products

The world health organization (WHO) has defined the Anatomical Therapeutic Chemical (ATC) classification system, to provide a standardized tool for drug research and to improve the use of drugs. In this ATC classification system, the substances are divided into different groups according to the organ or system on which they act, and their therapeutic, pharmacological and chemical properties. There is also a category regrouping the diagnostic agents (category ATC V04), the contrast media (category ATC V08) and the diagnostic radiopharmaceuticals (category ATC V09) whose use is intended in diagnosis purposes (100). From a research point of view, diagnostic microparticles are left aside, and only few products are available on the market. Among them, a minority is formulated as solid microparticulate products that are intended to be administered by oral, rectal, or venous pathway, or by inhalation. The manufacturing process of these marketed products is either not published or protected by patents, thus only a brief description can be given.

1.3.1 Category ATC V04: diagnostic agents

1.3.1.1 Breath test for the detection of *Helicobacter pylori*

H. pylori is a bacteria that is responsible of gastric diseases and can increase the risk of developing gastric cancer (101) and can be easily detected by a urea breath test. The difference between the products comes from the formulation: a powder for drinkable solution (Helikit™, Isotechnika Inc, Canada)(102), a soluble tablet (Pylobactell®, Torbet Laboratories, UK)(103), a capsule (Helifinder® InBioNet Pharmaceutical)(104) or a tablet (UBiT®, Otsuka Pharmaceuticals, Japan)(105) (106). The patient has to ingest the diagnostic product, ^{13}C labeled urea. After few minutes, the patient exhales in a tube to analyze the breath (107). The bacterial urease coming from *H. pylori* hydrolyses the urea into ammonium and bicarbonate, the latter contains the ^{13}C isotope that is expired into CO_2, and can further be measured by mass spectrometry (108) or infrared spectrometer (109). The main advantage of this test is that it is non-invasive, non-radioactive and can be used on children (102).

1.3.1.2 Mannitol bronchial challenge test

A new bronchial test known as Osmohale® (Pharmaxis, Australia) was launched in 2010 onto the market as a mannitol challenge test to identify bronchial hyper-responsiveness (110). This test enables the diagnosis of asthma by measuring the lung function to detect any inflammation of the airways (111). The diagnostic product consists of a capsule of mannitol dry powder that is used with an inhalation delivery device (112–114). Mannitol is spray dried and milled to obtain particle sizes in the breathable range (<7µm). The dry powder is then encapsulated in hard gelatin capsules with different doses (10, 20 and 40mg) for cumulative dosage (115).

Figure 5: Osmohale® inhalation powder in hard capsule for mannitol bronchial challenge test. Different doses are available in a blister wallet for cumulative dosage (116).

1.3.2 Category ATC V08: diagnostic contrast media

An important part of diagnostic products is intended to enhance the visibility of internal body structures and fluids during imaging. The contrast agents are divided in 4 categories: Iodinated and non-iodinated media for X-ray, MRI contrast media and ultrasound contrast media (117).

1.3.2.1 Diagnostic products for X-rays

X-ray contrast products are typically iodine or barium compounds. For instance, barium sulfate commercialized under the brand name Micropaque® (Guerbet, France) is an X-ray contrast media used to explore the condition of esophagus, stomach, and intestines to diagnose digestive problems. It is formulated as a barium sulfate suspension and is used for oral or rectal administration (118).

1.3.2.2 Diagnostic products for MRI

Products for MRI must have magnetic properties to be detected by the scanner. For instance, ferumoxsil is contrast agent commercialized as Lumirem® (Guerbet, France). It is formulated as a suspension of iron oxide crystals coated with siloxane, that are arranged in a crystalline structure to provide the superparamagnetic properties that are compulsory in magnetic imaging (23). This product is administered orally or rectally for the exploration of the digestive tract (119).

1.3.2.3 Diagnostic products for ultrasounds

Echovist® is a contrast medium that was developed by Bayer Schering Pharma (Berlin, Germany) for ultrasound examinations. The echographic contrast is obtained by the dispersion of air microbubbles in the blood (120). The production of these microbubbles is due to the property of sugars to retain air in their crystalline network and absorb water on their surface. Echovist® consists of galactose granules, made of micro-particles whom size is at 99% under 12 µm. When extemporaneously suspended in appropriate medium and vigorously shaken, the granules break down into galactose microparticles, causing the production of air microbubbles between the microparticles (121). After injection, the galactose microparticles are dissolved and release the microbubbles, inducing an increase of the echo signals from the venous vascular system and the observation of the blood flow. The reproducible size of the microbubbles is linked to the granulation process of the galactose but is mainly due to the dispersion of the granules into microparticles (122).

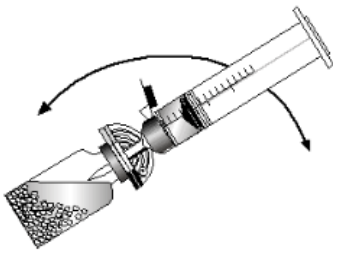

Figure 6: Schematic representation of Echovist® reconstitution from galactose granules.

Source: imedikament.de

1.3.3 Category ATC V09: diagnostic radiopharmaceuticals

Radiopharmaceuticals are diagnostic products containing radioisotopes and are used to help in the visualization of internal body structures by nuclear imaging (123). The radioactive compound is given in a very small amount by injection, *per os*, or by inhalation. The product is designed to be distributed in a defined part of the body where the disease or abnormality is located and emits radiations that are detected by a γ-camera or by positron emission tomography to diagnose patient's troubles (124).

As an example, the Schilling test is performed in 4 steps to determine an abnormal absorption of vitamin B12 indicated by low levels. The patient receives a shot of non-radioactive vitamin B12 and swallows a tablet of ^{57}Co-radiolabeled vitamin B12 (cyanocobalamin). The urine is collected during the next 24 hours to analyze its radioactivity counts. This test enables the diagnosis of pernicious anemia, that is a consequence of a decrease in red blood cells due to a poor absorption of vitamin B12 in the intestines (125,126).

1.4 A step towards personalized medicine

1.4.1 Current situation

Given the small number of diagnostic products on the market; most treatments are prescribed after a simple diagnostic from the doctor, and are supposed to be based on the sex, age, and weight of the patient. Medications are produced by pharmaceutical industries to fit the largest population and thus, are dosed for an adult of approximately 70 kg (127). However, having the same disease does not mean everyone needs the same medication or the same dose.

Figure 7 illustrates 4 patients with the same disease who were prescribed the same treatment, 1 tablet of drug X. The first patient is a young man, approximately 70 kg in good physical condition; the treatment is adapted to him. The second patient is an old woman, about 45 kg with difficulties to swallow and a slowed metabolism, the treatment is too strong for her, and not appropriated, she might develop side or even toxic effects. The third patient is an overweight person; a single tablet may be too low dose and give an incomplete therapeutic effect. The fourth patient is an Asian woman in good physical condition, but the medication might not be appropriate or toxic for her because she comes from an ethnic group that is not able to metabolize this drug due to of a lack of enzyme.

This simple example shows that only considering sex, age, weight for a prescription is not sufficient, and conventional prescriptions with fixed doses market forms can lead to a lot of low/no-therapeutic effects, overdoses, and side effects. Indeed, after a systematic review, Kongkaew et al. showed that 5.3 % of hospital admissions are associated to drug adverse effects (128). To limit these

inaccuracies and optimize drug therapies, it is important to personalize the diagnosis and the treatments to the patient.

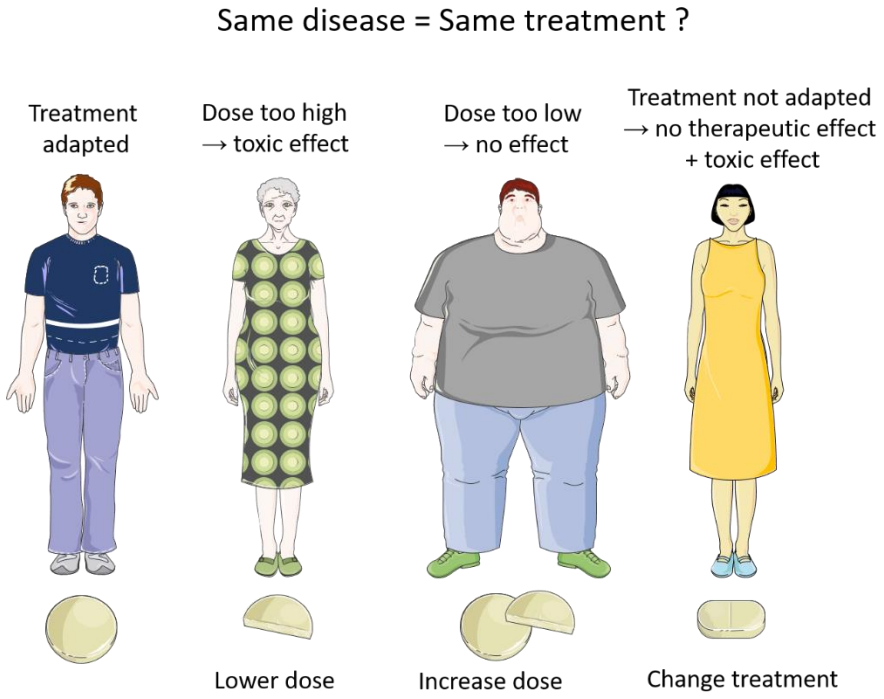

Figure 7: Illustration of personalized medicine depending on each patient.

For the same disease, the standard treatment does not fit to every patient. Depending on the phenotype of the patient, the treatment can be adapted. It can also be toxic or ineffective because of the inadequate dose, but can also be inappropriate because the patient does not respond to the molecule.

1.4.2 Companion diagnostics

In order to determine if a patient would benefit or not from a particular treatment, specific tests known as companion diagnostics were developed (129). According to the FDA, a companion diagnostic refers to an *in vitro* or *in vivo* diagnostic tool, which helps physicians to get the necessary information concerning the safe and effective use of a specific drug (130).

With the companion diagnostics, it is possible to identify the patients who can benefit from a distinct therapeutic treatment, those who have risk to develop serious side effects because of the treatment and to monitor the response to the treatment to adjust it and improve its safety and its efficiency. Regarding the result of the test, the physician can decide to prescribe or not prescribe the treatment to the patient (130). For instance, if a patient presents a mutation in the KRAS gene (involved in the synthesis of the protein K-Ras for regulation of

the cell division), the action of the target drugs (cetuximab or panitumumab) in the colorectal tumor tissue would be ineffective to treat the cancer (131).

There are 5 types of companion diagnostics: the ones for screening and detection to test familial genetic patterns, the prognosis tests to predict the future course of a disease, the thera(g)nostic[1] companions to verify the patient's response to the therapy, the monitoring tests to evaluate the effectiveness and appropriate dosing of a prescribed therapy and finally the recurrence companion diagnostics to analyze the risk of recurrence of the disease (133).

The rising of companion diagnostics started in 1998 with the approval of HecepTest™, an immunohistochemistry assay detecting the expression of the HER2 receptor involved in the growth of cancer cells and thus, determining the efficacy of trastuzumab (Herceptin®, Genentech, USA) for patients with HER2 positive breast cancers (134). Since the approval of HerecpTest™, many new companion diagnostics devices were developed together with targeted cancer drugs to bring effective and safe treatments to patients.

A list of approved companion diagnostics is published on the website of the FDA (Table 1) (130). Most of these companion diagnostics target solid tumor (135) for cancer therapies e.g. gastric cancer (136), lung cancer (137), and breast cancer (138). Several new companion diagnostic products are currently in different clinical trial phases for the diagnostic and treatment of rheumatoid arthritis (139), thrombotic disease (140), HIV (141,142), colorectal and prostate cancers, kidney insufficiency after transplant (143), and hepatitis C (144). A companion diagnostic to identify the appropriate anti-platelet therapy (clopidogrel or ticagrelor) is currently in late phase of clinical trials (Clinical trial NCT01742117). Indeed, patients presenting a polymorphic variation of CYP2C19 get a low response to clopidogrel and need to be treated by ticagrelor that is not metabolized by this cytochrome (145).

[1] *Thera(g)nostic comes from the combination of the words therapeutic and diagnostic and defines a single dosage form containing both diagnostic and therapeutic agents* (132). *It is found with 2 spellings in the literature: theranostic and theragnostic.*

Table 1: Companion diagnostics approved by the FDA.

Test	Manufacturer	Drugs	Indication
Cobas KRAS Mutation test	Roche	Cetuximab Panitumumab	Colorectal cancer
Therascreen KRAS RGQ PCR Kit	Qiagen		
Dako EGFR	Dako		
Therascreen EGFR RGQ PCR Kit	Qiagen	Afatinib Gefitinib	Non-small cell lung cancer
PD-L1 IHC 22C3	Dako	Pembrolizumab	
Cobas EGFR Mutation Test v2	Roche	Osimertinib	
Cobas EGFR Mutation Test	Roche	Erlotinib	
Ventana ALK CDx	Ventana	Crizotinib	
Vysis ALK Break Apart FISH probe kit	Abbott		
Inform Her 2/Neu	Ventana	Trastuzumab	Breast cancer
Pathway Anti Her-2/Neu			
Inform Her2 Dual ISH DNA			
InSite Her 2/Neu KIt	Biogenex		
Spot –Light Her2 CISH Kit	Life technologies		
Her2 CISH PharmDx Kit			
Her2 FISH	Dako		
HERCEPTEST			
Bond Oracle Her2 ICH System	Leica		
PATHVYSION Her-2 DNA Probe Kit	Abbott		
Dako C Kit PharmDx	Dako	Imatinib mesylate	Gastrointestinal stromal tumors
Kit D816V Mutation detection	ARUP Laboraories		Systemic mastocytosis
PDGFRB FISH			Myelodysplastic syndrome / Myeloproliferative disease
BRACAnalysis CDx	Myriad genetic	Olaparib	Ovarian cancer
THxID BRAF	bio Mérieux	Tramatenib Dabrafenib	Melanoma
BRAF V600	Roche	Vemurafenib	
FerriScan®	Resonnance Health	Deferasiox	Thalassemia

As it can be seen in Table 1, companion diagnostics are very often associated to cancer treatments and involve biological material such as antibodies. However, it is possible to develop companion diagnostics for other types of diseases with small molecule drug products. The only example that is approved by the FDA is FerriScan®. It is a diagnostic test based on MRI to measure liver iron concentration in patients suffering of β-thalassemia. As a companion diagnostic of deferasirox (Exjade®) it helps physicians to identify and

monitor patients with non-transfusion-dependent thalassemia for an effective treatment (146,147).

1.4.3 Phenotyping cocktails as companion diagnostics

The development of companion diagnostics is generally based on specific genetic mutations. The capacity of patients to respond to the treatment is directly linked to their genotype. However, the genotype does not consider other factors that are not associated to the genes, such as the patient's weight and health condition, a smoking/drinking habit or a special diet. These characteristics can influence and modify the response to a drug by increasing or slowing down its metabolism. That is why the consideration of environmental factors, in addition to the genotype, is very important to define the phenotype of the patient (148).

Phenotyping consist in the determination of the phenotype, by the administration of an appropriate probe drug, that is metabolized by a given enzyme into a known metabolite. It results in the determination of the patient's metabolism profile and the prediction of the drug activity. Phenotyping cocktails are a combination of several probe drugs that are used to in first instance to identify drug-drug interactions, leading to an induced or an inhibitory effect of one or more drugs during a combination therapy (149). Phenotyping cocktails can be considered as companion diagnostics because they help in the evaluation of the metabolism of drugs before the implementation of a medical treatment to personalize it to the patient's needs.

The Basel cocktail is a phenotyping cocktail that was developed by the University hospital of Basel (149). Until now, there was an absence of a dedicated phenotyping cocktail formulation, and thus, the 6 different probe drugs were administered as individual marketed medications. The diversity of dosage forms the cocktail can induce different release kinetics, dosage inaccuracy and excipients cross-reactions (150). To overcome these issues, it was necessary to develop a single dosage form combining the probe drugs at the needed dose, without inducing any physicochemical interactions. An attempt to fill this gap is described later in the article "CombiCap, a novel drug formulation for the Basel phenotyping cocktail".

2 AIM OF THE THESIS

The introduction part of this thesis reveals the importance of diagnostic products in helping the physicians to detect and diagnose a disease; allowing the adaption of medical treatments to each individual patient, based on more precise criteria than age, weight, and sex. Unfortunately, laboratories have the tendency to develop curative products for treating diseases and neglect the importance of developing diagnostic products for accurate diagnosis to personalize medicine. In the following chapters, we describe the development of 2 diagnostic products, the first one at the nanoparticulate level and the second one at the microparticulate level.

- **PDMS-PMOXA polymersomes containing quantum dots for cellular imaging**

During the last decades, nanoscience was increasingly developed for medical purposes but mainly for drug delivery. The most common example is Doxil®, a liposomal formulation encapsulating doxorubicin for cancer chemotherapy. In the first chapter, we describe the formulation of polymersomes for cellular imaging. Polymersomes are artificial nanovesicles made of bloc copolymers that self-assemble into a double-layered vesicle allowing the loading of hydrophilic molecules in its cavity and hydrophobic molecules in the polymeric membrane. Quantum dots are already used for medical imaging but in limited applications because of their toxicity. To overcome this constraining property, we decided to isolate some quantum dots inside PDMS-PMOXA polymersomes and study their imaging properties *in vitro*.

- **CombiCap, a novel drug formulation for the Basel phenotyping cocktail**

The second chapter is based on microparticulate products for diagnostics. The objective of this project was to create a pharmaceutical dosage form for the Basel Cocktail. The phenotyping process is important in diagnosis, for instance in the evaluation of enzymes involved in the metabolism of xenobiotics, such as drugs. Thus, with the detailed status of these enzymes, it is possible to personalize a therapeutic treatment to a patient, to deliver the right drug at the right dose, avoiding any adverse effect. We developed a formulation platform that can be adapted for any phenotyping cocktail thanks to its multiple properties.

3 ARTICLES IN PEER-REVIEWED JOURNALS

3.1 Nanoparticles as diagnostic product

Polymersomes containing quantum dots for cellular imaging

Marine Camblin[1], Pascal Detampel[1], Helene Kettiger[1], Dalin Wu[2], Vimalkumar Balasubramanian[1], Jörg Huwyler[1]

[1]Division of Pharmaceutical Technology, University of Basel, Basel, Switzerland
[2]Department of Chemistry, University of Basel, Basel, Switzerland

International Journal of Nanomedicine 2014: 9 2287-2298

International Journal of Nanomedicine

Dovepress
open access to scientific and medical research

Open Access Full Text Article

ORIGINAL RESEARCH

Polymersomes containing quantum dots for cellular imaging

This article was published in the following Dove Press journal:
International Journal of Nanomedicine
12 May 2014
Number of times this article has been viewed

Marine Camblin[1]
Pascal Detampel[1]
Helene Kettiger[1]
Dalin Wu[2]
Vimalkumar Balasubramanian[1,*]
Jörg Huwyler[1,*]

[1]Division of Pharmaceutical Technology, [2]Department of Chemistry, University of Basel, Basel, Switzerland

*These authors contributed equally to this work

Abstract: Quantum dots (QDs) are highly fluorescent and stable probes for cellular and molecular imaging. However, poor intracellular delivery, stability, and toxicity of QDs in biological compartments hamper their use in cellular imaging. To overcome these limitations, we developed a simple and effective method to load QDs into polymersomes (Ps) made of poly(dimethylsiloxane)-poly(2-methyloxazoline) (PDMS-PMOXA) diblock copolymers without compromising the characteristics of the QDs. These Ps showed no cellular toxicity and QDs were successfully incorporated into the aqueous compartment of the Ps as confirmed by transmission electron microscopy, fluorescence spectroscopy, and fluorescence correlation spectroscopy. Ps containing QDs showed colloidal stability over a period of 6 weeks if stored in phosphate-buffered saline (PBS) at physiological pH (7.4). Efficient intracellular delivery of Ps containing QDs was achieved in human liver carcinoma cells (HepG2) and was visualized by confocal laser scanning microscopy (CLSM). Ps containing QDs showed a time- and concentration-dependent uptake in HepG2 cells and exhibited better intracellular stability than liposomes. Our results suggest that Ps containing QDs can be used as nanoprobes for cellular imaging.

Keywords: quantum dots, polymersomes, cellular imaging, cellular uptake

Introduction

Development of highly sensitive and stable imaging probes is of considerable interest in many areas of biomedical research, ranging from cellular biology to molecular imaging and diagnostics. Fluorescent semiconductor quantum dots (QDs) are promising fluorescent nanoprobes offering an alternative to conventional organic fluorophores due to their unique properties.[1,2] QDs show superior optical and chemical properties, ie, broad spectral absorption with a narrow emission band, higher brightness of fluorescence despite a low quantum yield, high photostability, and resistance to photobleaching.[3,4] However, poor chemical stability, particle aggregation, and toxicity mediated by the cadmium semiconductor core limit the use of QDs in imaging.[5–7] These limitations are of major concern in applications where cellular uptake of QDs is required to visualize intracellular compartments.

In cell culture media, QDs have low stability due to particle aggregation and surface degradation, which leads to minimal cellular uptake and difficulties with respect to the interpretation of cellular images.[8] Therefore, attempts have been made to improve the stability and promote cellular uptake of QDs using surface chemistry modifications. This includes the functionalization of QDs with biomolecules such as antibodies,[9] proteins,[10] or peptides,[11] as well as their coating with polymers or amphiphilic copolymers.[12,13] However, modification of the QD surface may significantly

Correspondence: Jörg Huwyler
University of Basel, Department of Pharmaceutical Sciences, Division of Pharmaceutical Technology, Klingelbergstrasse 50, Basel, Switzerland
Tel +41 61 267 1513
Fax +41 61 267 1516
Email joerg.huwyler@unibas.ch

submit your manuscript | www.dovepress.com
Dovepress
http://dx.doi.org/10.2147/IJN.S59189

alter their fluorescence properties.[14] Once taken up by target cells, QDs often end up in the endolysosomal compartment or aggregate in intracellular regions.[15] Earlier studies showed that QDs may disintegrate under acidic conditions in these compartments, leading to intracellular release of toxic heavy metals. This leads to oxidative stress, induction of apoptosis, and eventually, cell death.[16] Recently, it was shown that polymer-coated QDs could be stabilized during cellular uptake. However, their coating dissociated in intracellular compartments such as lysosomes.[17] Thus, new strategies are needed to improve both the uptake and the intracellular stability of QDs.

Amphiphilic block copolymers are known to self-assemble into various supramolecular aggregates such as micelles, tubes, sheets, or vesicles in aqueous solutions.[18] In particular, polymersomes (Ps; so-called polymeric vesicles) have gained increasing interest in recent years for various biomedical applications, including their use as drug and gene delivery nanocarriers, nanoreactors, and even artificial organelles.[19] Ps are nanometer-sized hollow spheres with an aqueous cavity surrounded by a hydrophobic membrane and hydrophilic inner and outer surfaces. They are promising candidates for nanocarriers because many hydrophilic and hydrophobic molecules can be incorporated into their aqueous cavity or their membrane, respectively.[20,21] Additionally, chemical surface modifications can be used to tailor their physicochemical and biological properties to improve the delivery of a wide range of therapeutics.[22,23] Numerous types of Ps have been proposed as nanocarriers for encapsulating small drug molecules, larger therapeutic proteins, and other types of nanoparticles.[24–26] Reports on the use of Ps as carriers of water-soluble nanoparticles such as QDs are scarce.[27] Recently, Ps prepared from amphiphilic poly (D,L-lactide)-poly(2-methacryloyl-oxy-ethylphosphorylcholine) (PLA-PMPC) diblock copolymers have been used to encapsulate phosphorylcholine-coated QDs. This coating confers hydrophilic properties to the QDs and also creates ion-pair interactions with PMPC, binding QDs to the inner and outer surfaces of Ps.[27] However, this approach has limitations, since the presence of physiological buffer can destabilize the QDs and release them from the surface of the Ps.

The present study aimed to use a recent type of diblock copolymers composed of poly(dimethylsiloxane)-poly (2-methyloxazoline) (PDMS-PMOXA)[28] to prepare Ps and to load them with QDs. The hydrophilic fraction and molecular weight of the PDMS-PMOXA were chosen to meet the prerequisites for diblock amphiphilic copolymers to form vesicles.[29] The neutral hydrophilic PMOXA outside the Ps thereby acts as a protein repellent, similar to conventional polyethylene glycol (PEG), to minimize interactions with phagocytic cells such as macrophages and monocytes.[30,31] In this way, colloidal stability, cellular delivery, and intracellular stability needed for cellular imaging were improved. QDs were loaded into the aqueous cavity of Ps made of PDMS-PMOXA without altering the surface properties of Ps. Loading efficiency and colloidal stability in suspension were characterized by transmission electron microscopy (TEM), fluorescence spectroscopy (FS), zeta potential, and fluorescence correlation spectroscopy (FCS). The cellular toxicity of PDMS-PMOXA Ps was excluded by the 3-(4,5-dimethylthiazol-2-yl)-2,5-diphenyltetrazolium bromide (MTT) assay. Intracellular delivery of Ps containing QDs was investigated in human liver carcinoma (HepG2) cells. Concentration- and time-dependent cellular uptake of Ps containing QDs in HepG2 cells was analyzed using confocal laser scanning microscopy (CLSM). Results were compared to those obtained for liposomes containing QDs.

Materials and methods

Amphiphilic block copolymers

Poly (dimethylsiloxane)-poly (2-methyloxazoline) ($PDMS_{65}$-$PMOXA_{14}$) was kindly provided by Prof Wolfgang Meier (Department of Chemistry, University of Basel, Basel, Switzerland). This amphiphilic diblock copolymer was synthesized as described elsewhere.[28,31] An excess of pre-activated PDMS was used to induce the polymerization of the hydrophilic PMOXA blocks. Unreacted PDMS was removed from the diblock copolymer by centrifugation.

Preparation of Ps

Ps were prepared using a film rehydration method.[32] PDMS-PMOXA diblock copolymer (5 mg) was first dissolved in pure ethanol (1 mL). The polymeric solution was evaporated to dryness using a rotary evaporator (Rotavapor; BÜCHI Labortechnik AG, Flawil, Switzerland; 174 mbar, 40°C, 80 rpm) to obtain a thin film. Residual humidity was removed in a vacuum oven (Vacutherm; Thermo Scientific, Wohlen, Switzerland) in high vacuum (0.3 mbar, 40°C, 4 hours). Phosphate buffer solution (PBS; 1 mL, 0.1 mM) was added to the film for rehydration under vigorous stirring at room temperature for 6 hours. The resulting suspension was extruded (Mini extruder; Avanti Polar Lipids, Alabaster, AL, USA) eleven times through a polycarbonate filter with an average pore diameter of 0.4 µm, followed by eleven extrusions through a filter with an average pore diameter of

0.2 µm (Nucleopores; Whatman, VWR International AG, Dietikon, Switzerland).

Loading of QDs

An aliquot (100 µL) of QDs solution (8 µM solution in 50 mM borate, pH 9) with a maximum red fluorescence emission of 625 nm (Qdot® ITK™ carboxyl quantum dots, cadmium–selenium core; Invitrogen, Life technologies, Lucerne, Switzerland) was mixed with PBS (900 µL, 1 mM) to obtain a final QDs concentration of 200 nM. The photoluminescence yield of CdSe QDs was previously reported to be negligible for emission wavelengths in the red spectral range.[33] This suspension was added to a dry polymer film and stirred for 6 hours at room temperature and protected from light. QDs were encapsulated in Ps during the self-assembly process. After extrusion (as described in paragraph Preparation of PS), non-encapsulated QDs were removed by size-exclusion chromatography using a Sepharose 2B column (Sigma Aldrich, Buchs, Switzerland) eluted with PBS (0.1 mM). The first fraction corresponding to the Ps-containing QDs was detected by UV absorption at 280 nm. It should be noted that free QDs cannot be separated from the suspension by dialysis due to their big molecular size.

Dynamic light scattering

Suspensions of empty Ps and Ps-containing QDs were measured for average size and size distribution using dynamic light scattering (DLS) with a Delsa™ Nano C (Beckman Coulter, Inc., Nyon, Switzerland) equipped with Dual 30 mW laser diodes (wavelength lambda: 632.8 nm). Data were analyzed using the CONTIN program[34] (DelsaNano UI software version 3.73/2.30, Beckman Coulter, Inc.).

Surface charge – zeta potential

Suspensions of free QDs, empty Ps, and Ps-containing QDs were measured for zeta potential determination using electrophoretic light scattering in a Delsa™ Nano C. Suspensions were measured in a flow cell using PBS as buffer. Data were converted with the Smoluchowski equation (DelsaNano UI software, Beckman Coulter, Inc.).

Transmission electron microscopy

Samples for transmission electron microscopy (TEM) were prepared using an aliquot (5 µL) of suspension of empty Ps and Ps-containing QDs on a carbon-coated grid. Samples were negatively stained with freshly prepared 2% uranyl acetate. The grids were air-dried overnight before TEM analysis (CM-100; Philips, Eindhoven, the Netherlands).

Fluorescence spectroscopy

A microplate fluorescence spectrometer (SpectraMax M2e, Molecular Device, Biberach an der Riss, Germany) was used to analyze the efficiency of loading QDs into Ps. All samples (free QDs, empty Ps, and Ps-containing QDs) were excited at 405 nm, and continuous emission spectra were recorded from 500 to 700 nm. All measurements were performed in a polystyrene 96-well microplate (Greiner-bio one, Frickenhausen, Germany). Fluorescence intensity of QDs changes over time. Therefore, fluorescence signals are represented in relative fluorescent units.

FCS

FCS measurements were performed on the surface of a cover glass using a Zeiss 510-META/Confocor2 laser-scanning microscope (Carl Zeiss AG, Feldbach, Switzerland) equipped with an argon laser (477 nm) in the FCS mode. Fluctuations of fluorescence intensity were processed by means of an autocorrelation function. FCS was used to analyze the loading of QDs into Ps and to determine quantitatively the number of QDs in each polymersome.[35] Diffusion times of free QDs determined independently were included in the fitting procedure. All results represent the average of ten measurements. For stability determinations, Ps-containing QDs were analyzed regularly over a period of 6 weeks.

Cell culture

HepG2 cells (ATCC HB-8065) were kindly provided by Prof Dietrich von Schweinitz (University Hospital Basel, Basel, Switzerland). Cells were cultured in Dulbecco's Modified Eagle Medium (DMEM) supplemented with low glucose (1 g/L), 10% fetal bovine serum (FBS), 0.1 mM non-essential amino acids (NEAA), 2 mM GlutaMAX™, and 10 mM HEPES (all obtained from Gibco, Life Technologies, Lucerne, Switzerland) at 37°C under 5% CO_2 and saturated humidity. Cells were confirmed to be free of mycoplasma (MycoAlert™; Lonza, Visp, Switzerland).

MTT cellular toxicity assay

The 3-(4,5-dimethylthiazol-2-yl)-2,5-diphenyltetrazolium bromide (MTT) assay was used with some modifications as described elsewhere.[36] The MTT stock solution (Roth AG, Arlesheim, Switzerland) was prepared by dissolving 5 mg MTT/mL PBS, sterile-filtered, and stored at 4°C. Briefly, HepG2 cells were seeded at a density of 2.5×10^4 cells/well in a 96-well plate. After 24 hours, the medium was removed and 100 µL aliquots containing the corresponding concentration of Ps were added. A blank medium served as a negative

control. After 24 hours, the medium was replaced by blank medium containing 10% MTT solution. The plates were incubated for 2 hours at 37°C, and the resultant formazan crystals were dissolved by adding 3% soduim dodecyl sulfate (20 µL) and 40 mM HCl (100 µL) in isopropanol. Optical density was measured at 550 nm using a spectrophotometer (SpectraMax M2e; Molecular Device). Test substances showed no absorbance overlapping with the signal of MTT. Unspecific background signal was determined at 680 nm and subtracted to reduce artifacts.

Cellular uptake of Ps-containing QDs

We analyzed the cellular uptake of Ps-containing QDs in HepG2 liver cancer cells using CLSM. HepG2 cells were cultured on poly-D-lysine–coated cover slips (#1.5; Menzel Glasbearbeitungswerk GmbH & Co, KG, Braunschweig, Germany). Cells were incubated at 37°C with Ps (100–500 µg/mL) or liposomes (0.14 mM of phospholipids) loaded with QDs. Nucleus counterstaining was performed by adding Hoechst 33342 dye (1 µg/mL) to the cells 5 minutes before the completion of the uptake assay. Cells were washed three times with cold D-PBS (Dulbecco's PBS) and fixed for 15 minutes with 2% paraformaldehyde at 4°C. After an additional wash, slides were embedded in Prolong Gold antifade reagent (Gibco) and sealed with nail polish after drying. Samples were analyzed with an Olympus FV-1000 inverted confocal laser scanning microscope (Olympus, Le Mont-sur-Lausanne, Switzerland), using a 60× Plan Apo N oil-immersion objective (numerical aperture 1.40), and images were processed using either the Olympus FluoView software (v3.1, Olympus) or Gimp software (v2.8; GNU image manipulation program, http://www.gimp.org). Intracellular QDs were activated by light-emitting diodes (LEDs) with a wavelength of 400 nm (210 mW/cm^2) or 490 nm (190 mW/cm^2),[37] using a pE-2 LED (CoolLED Limited, Andover, UK) excitation system. For activation, samples were exposed to a wavelength of 490 nm for 1 minute prior to analysis.

Results and discussion

Characterization of Ps

These last years, the development of Ps for technical or pharmaceutical applications is increasing. In this study, we have formulated Ps with a PDMS-PMOXA diblock copolymer, composed of 65 siloxane and 14 2-methyloxazoline units (Figure 1B),[28,31] as nanosized carriers for QDs.

Size and morphology of extruded PDMS-PMOXA Ps were determined by DLS and TEM (Figure 1). The mean hydrodynamic diameter was approximately 205 nm for empty Ps and 223 nm for Ps-containing QDs (Figure 1A). Table 1 shows the polydispersity index (PDI) of free QDs, empty Ps, and Ps-containing QDs. The very low PDI values for both Ps preparations indicated a homogeneous population with a very narrow size distribution range.

However, the absence of a significant difference in average diameters of the two Ps preparations suggests that encapsulation of high-molecular weight QD nanoparticles did not affect the molecular self-assembly of PDMS-PMOXA copolymers into Ps. In TEM investigations, we observed spherical vesicles with a diameter of approximately 200 nm, confirming the formation of Ps. Collapsed Ps revealed a hollow vesicular structure (Figure 1C). A recent report on self-assembly of a similar molecular composition of PDMS-PMOXA into vesicular structures supports our findings.[28]

Loading of QDs into Ps

TEM investigations showed the presence of monodispersed QDs inside the Ps. QDs incorporated into Ps had the same appearance as free QDs in suspension, confirming that QDs were located in the aqueous compartment of the Ps without any aggregations. The morphology of empty Ps and Ps loaded with QDs remained the same (Figure 1D), confirming that encapsulation of QDs did not affect the formation of Ps. The number of QDs per Ps ranged from a single QD to tens of QDs, according to the statistical probability of available QDs in close proximity (for loading) during Ps formation. The stabilizing effect of the Ps provides indirect evidence

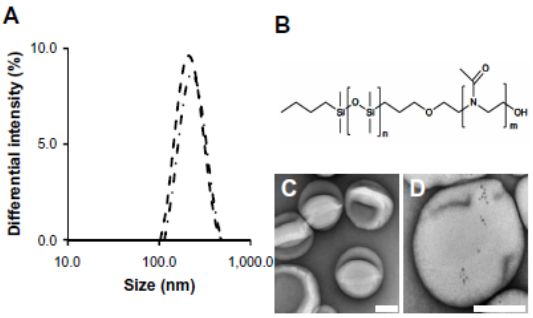

Figure 1 Chemical composition, size, and morphology of PDMS-PMOXA Ps-containing QDs. (**A**) Size distribution of Ps determined by DLS. Average diameter of Ps was 200 nm (dashed line: empty Ps, dot-dashed line: Ps-containing QDs); (**B**) chemical structure of PDMS-PMOXA amphiphilic block copolymers; (**C**) TEM analysis of Ps; (**D**) TEM analysis of Ps-containing QDs.
Note: The scale bars represent 100 nm.
Abbreviations: DLS, dynamic light scattering; PDMS-PMOXA, poly(dimethylsiloxane)-poly(2-methyloxazoline); Ps, polymersomes; QDs, quantum dots; TEM, transmission electron microscopy.

Table 1 Size, PDI, and surface charge of QDs and Ps

Sample	Diameter (nm)	PDI	Zeta potential (mV)
Free QDs	7–10[a]	nd	–24.18
Empty Ps	205±7	0.075	5.62
Ps-containing QDs	223.9±9	0.053	9.69

Note: [a]Size according to data provided by the manufacturer for ITK™ carboxyl quantum dots (Invitrogen, Life Technologies, Lucerne, Switzerland).
Abbreviations: nd, no data; PDI, polydispersity index; Ps, polymersomes; QDs, quantum dots.

that the QDs are contained inside the Ps, and are not just loosely attached to the outer surface of the Ps membrane. Figure 2A shows characteristic emission spectra of free QDs, empty Ps, and Ps-containing QDs at the excitation wavelength of 405 nm. The appearance of the characteristic emission of QDs without any shift in the Em_{max} (625 nm) in Ps-containing QDs and the absence of this emission peak in empty Ps demonstrated the loading of QDs in Ps without alteration of the fluorescent properties of QDs. Thus, QDs can be incorporated into Ps without aggregation and without affecting the fluorescence properties of QDs. The main advantage of QDs is not their high quantum yield, which is often lower than that of many organic dyes. However, their high absorption rate and increased photostability finally result in a brighter fluorescence signal. Moreover, the Stokes shift leads to a very low background signal. In Figure 2A, fluorescence signals obtained from Ps-containing QDs are lower than from free QDs. This can be explained by the fact that QDs are encapsulated within Ps, which absorbs some of the excitation light. In addition, not all QDs were entrapped within the Ps during their preparation and were thus lost during the consecutive purification steps. However, this reduced fluorescence intensity of encapsulated QDs can be easily compensated by an increased excitation light intensity since there is no risk of photobleaching.

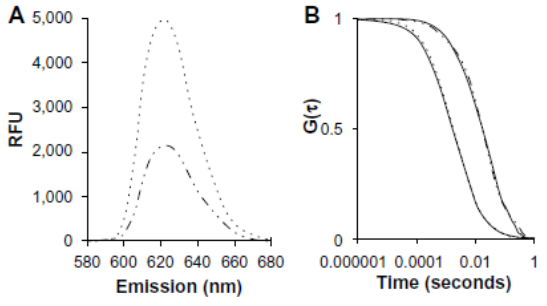

Figure 2 Analysis of QDs loading efficacy by fluorescence spectroscopy and FCS. (**A**) Emission fluorescence spectra of free QDs (dotted-lines), Ps-containing QDs (dot-dashed lines), and empty Ps (dashed lines), excitation wavelength 405 nm; (**B**) FCS auto-correlation curves, experimental (solid lines) and fitted (dashed-lines) of free QDs (dotted-lines) and Ps-containing QDs (dot-dashed lines).
Abbreviations: FCS, fluorescence correlation spectroscopy; Ps, polymersomes; QDs, quantum dots; RFU, relative fluorescent units.

Free QDs are characterized by a negative surface charge (zeta potential: –25 mV; Table 1). After loading into Ps, the zeta potential increases to 9 mV. This positive value is very similar to the zeta potential of empty Ps. Thus, masking of the surface charge of QDs after loading into Ps is an indication of their presence within the Ps as opposed to a mere binding to the outer surface of the Ps.

FCS analyzes the intensity fluctuations of molecules in a defined confocal volume. These signals can be correlated to the diffusion time of molecules (τ_D). We determined that τ_D=4,000 µs for freely diffusing QDs and τ_D=15,000–17,000 µs for QDs loaded into Ps (Figure 2B). This is in agreement with the reported diffusion time of Ps of a similar size based on the PDMS-PMOXA block copolymer.[28]

Molecular brightness measurements have been used to calculate the number of fluorescent molecules encapsulated inside each polymersome.[25,38] We estimated the average number of QDs per polymersome based on brightness obtained from the count rate per molecule (cpm, kHz). We calculated an average of four QDs/polymersome based on the brightness of free QDs and QDs encapsulated in Ps. The loading efficiency of Ps in our study was comparable with the reported loading efficiency of liposomes (ie, three QDs/liposome on average).[39,40] However, we aimed to improve the loading efficiency by introducing 5% amine-functionalized PDMS-PMOXA copolymers in hydroxyl-functionalized PDMS-PMOXA copolymers to generate charges in the copolymer system (Figures S1–S4 in supplementary material). We calculated an average of eight QDs/Ps based on brightness measurements. This was clearly superior to the loading of purely hydroxyl-functionalized copolymers (neutral charge). Our results suggest that introducing a small amount of amine-functionalized monomers to the copolymer system causes favorable electrostatic interactions leading to improved loading efficiency. Geometric considerations and analysis of TEM images suggest that much higher loading efficiency can be achieved up to a theoretical maximal up-loading content of 4,900 QDs per polymersome. However, the achieved accumulation of QDs at picomolar concentrations within individual Ps is sufficient to induce a bright fluorescence signal suitable for cellular imaging (see below).

Stability of Ps-containing QDs

The stability of Ps-containing QDs was investigated using size measurements by DLS, morphology analysis by TEM,

and FCS analysis yielding release profiles of QDs from Ps. These tests were carried out over a period of 6 weeks at regular intervals (Figure 3). We did not observe any significant changes in size (~200 nm) or size distribution, suggesting that Ps were highly stable and remained intact (Figure 3D). In addition, TEM showed the presence of QDs inside the Ps (~200 nm), with no free QDs outside the Ps between day 1 and week 6 (Figure 3B and C).

For stability analysis, auto-correlation curves obtained with FCS were fitted with a two components model. Diffusion times of free QDs were determined independently and were included in the fitting procedure. The majority of the particle population (99.9%) represented QDs encapsulated in Ps, as confirmed by corresponding diffusion times (τ_D=15,000–17,000 µs), that were similar to those of freshly prepared Ps loaded with QDs (Figure 3A). This finding confirms that QDs were not released from the Ps even after 6 weeks, due to the robust impermeable membrane of the Ps (~15 nm).[28] In addition, passive transmembrane diffusion is unlikely due to the high molecular weight of the QDs. Thus, DLS, TEM, and FCS experiments clearly indicated that Ps were highly stable. They retained their size and shape and entrapped the QDs for a long period of time.

Cellular viability (MTT) assay

Various types of PMOXA-PDMS-PMOXA tri-block copolymers were previously suggested to be non-toxic and non-immunogenic.[30,31] The PDMS-PMOXA diblock copolymer used in the present study showed no cellular toxicity in a HepG2 human liver carcinoma cell line (Figure 4). There was no loss of viability in HepG2 cells after 24 hours of incubation with PDMS-PMOXA Ps at concentrations up to 300 µg/mL.

Cellular uptake of Ps-containing QDs

Time-and dose-dependent uptake kinetics of Ps-containing QDs were studied using incubation times of 1, 7, and 24 hours and different polymer concentrations

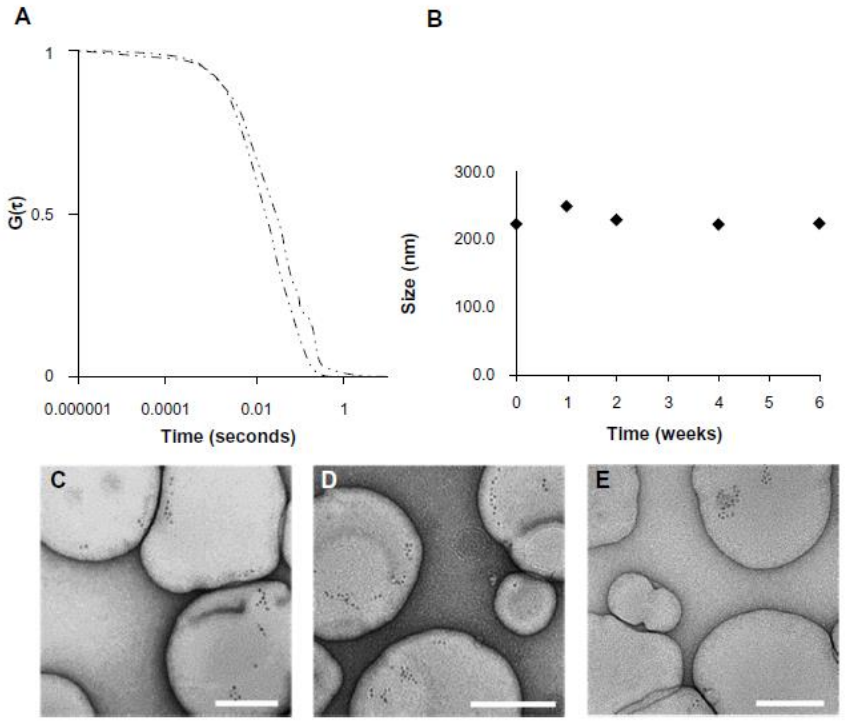

Figure 3 Long-term stability of Ps-containing QDs.

Notes: (**A**) FCS auto-correlation curve of Ps-containing QDs at day 1 (dot-dashed lines) and Ps-containing QDs at week 6 (double dot-long dashed lines); (**B**) average particle size determined by DLS over 6 weeks (**C**) TEM analysis of Ps-containing QDs at day 1 (week 0); (**D**) TEM micrograph analysis of Ps-containing QDs at week 6; (**E**) TEM micrograph analysis of Ps-containing QDs after 1 year of storage at 4°C. Average size determined by DLS for the Ps-containing QDs after of 1 year storage was 221.1 nm (PDI =0.068). Scale bar represents 100 nm.

Abbreviations: DLS, dynamic light scattering; FCS, fluorescence correlation spectroscopy; PDI, polydispersity index; Ps, polymersomes; QDs, quantum dots; TEM, transmission electron microscopy.

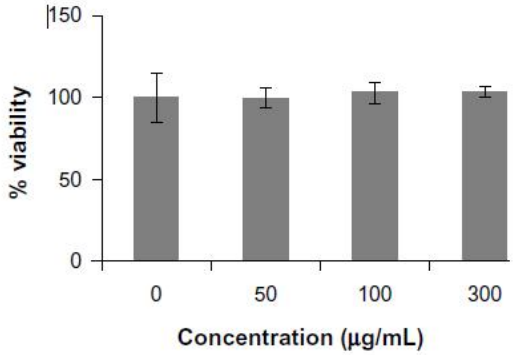

Figure 4 Viability of HepG2 cells incubated with Ps (MTT assay). HepG2 cells showed no loss of viability after 24 hours of incubation with different concentrations of Ps (50–300 µg/mL).
Note: Data are means ± SD, n=3.
Abbreviations: Ps, polymersomes; HepG2, human liver carcinoma cells.

(100 µg/mL, 300 µg/mL, 500 µg/mL). While no uptake was observed for any concentrations after 1 hour of incubation, the uptake rate increased linearly from 7 hours to 24 hours, indicating the time-dependent uptake of Ps-containing QDs. Simultaneously, we observed a gradual increase in the uptake rate between the low concentration (100 µg/mL) to higher concentration (300 µg/mL), suggesting dose-dependent uptake (Figure 5). The appearance of red fluorescent signals, mainly in the perinuclear regions, was indicative of the intracellular accumulation of Ps-containing QDs in HepG2 cells. Concentrations of Ps used for imaging purposes rarely exceed 100 µg/mL. Under these conditions, cellular uptake is minimal. Free QDs are rapidly taken up by living cells. However, this process is not specific, and therefore QDs cannot be used to label defined tissues or sub-populations of cells within tissues. In addition, free Cd/Se QDs are cytotoxic because of their heavy metal core. In contrast, Ps-containing QDs were demonstrated in our work to be non-cytotoxic. Their cellular uptake is negligible. This absence of unspecific cellular interactions is a mandatory prerequisite for their use to implement specific targeting strategies. For this latter purpose (ie, to promote cellular targeting and uptake), Ps can be modified by covalent modification of their surfaces using, for example, receptor-specific targeting ligands. Thus, surface-modified, polymer-based nanoparticles can be conveniently labeled with stabilized QDs to study and visualize their cellular interactions.[41] The low uptake between 1 hour and 7 hours suggests that the PMOXA block acts as a protein repellent, reducing cellular interactions of Ps. This property has previously been described for other types of nanoparticles such as PEGylated liposomes,[41] and is a prerequisite for in vivo implementation of targeting strategies. Thus, prolonged incubation (24 hours) was needed to induce forced uptake by HepG2 cells. We presume that cellular

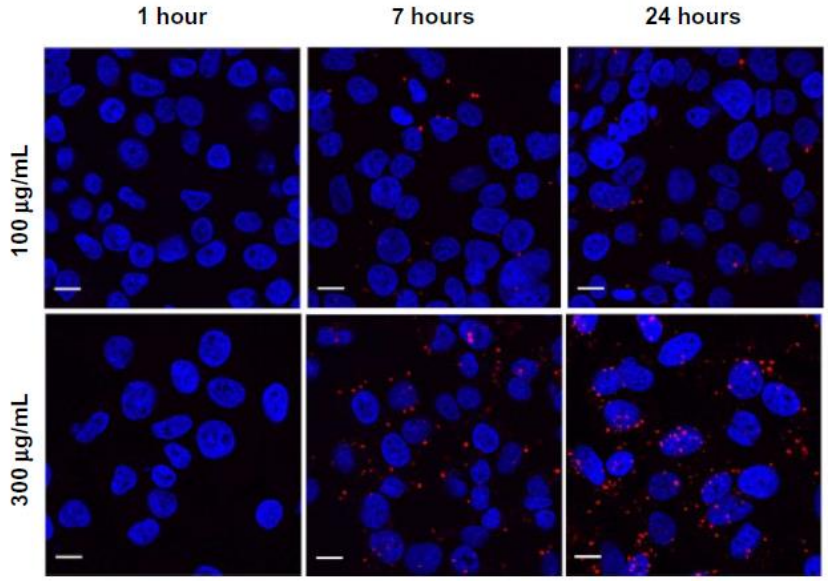

Figure 5 Dose- and time-dependent uptake of Ps-containing QDs in HepG2 cells. Ps concentrations incubated with HepG2 cells were 100 µg/mL (upper row, recommended concentration) to 300 µg/mL (lower row). Incubation times were 1 hour (left column), 7 hours (center column), and 24 hours (right column, condition of forced uptake). QDs were photo-activated at a wavelength of 490 nm for 1 minute. Red fluorescence: Ps-containing QDs, blue fluorescence: nuclei stained with Hoechst 33342.
Note: Scale bars represent 10 µm.
Abbreviations: Ps, polymersomes; QDs, quantum dots; HepG2, human liver carcinoma cells.

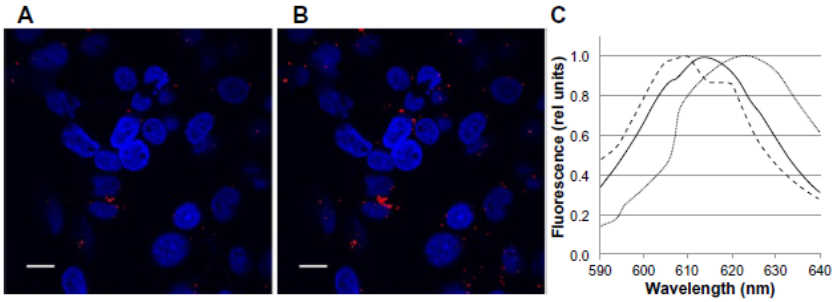

Figure 6 Fluorescence activities of QDs loaded into Ps under intracellular conditions.
Notes: HepG2 cells were incubated with Ps-containing QDs (red signal) and were analyzed before (**A**) and after (**B**) photo-activation at a wavelength of 400 nm for 15 seconds. (**C**) Emission peak of a lambda scan of intracellular QDs in Ps (solid lines) and in liposomes (dashed-lines) compared with free QDs (dotted-lines). Nuclei were stained with Hoechst 33342 (blue signal).
Abbreviations: Ps, polymersomes; QDs, quantum dots; HepG2, human liver carcinoma cells.

uptake can be further increased by surface modifications of the Ps, such as, for example, cationization or coupling of specific receptor ligands.[41] Previous publications suggest that cellular uptake of nanoparticles is a prerequisite to induce cellular toxicity.[42] In order to explore the potential toxic effect of the Ps, the concentration in medium was increased to 300 µg/mL. A long incubation time (24 hours) under these conditions led to cellular uptake. However, the MTT assay demonstrated an absence of toxicity under these conditions of forced uptake. Therefore, we recommend to limit incubation times with Ps-containing QDs to 24 hours and not to exceed a polymer concentration of 100 µg/mL.

Intracellular stability of Ps-containing QDs

QDs encapsulated in Ps or liposomes can be photoactivated by UV irradiation at 405 nm. This is a widely used technique to enhanced fluorescence signals of QDs in suspension or cells.[43] Photoactivation was made evident by a blue-shift of cellular emission fluorescence signals by 10 nm (Ps) or 15 nm (liposomes), as compared to free QDs (Figure 6C). This is indicative of the slow degradation of the QD core under these conditions. In liposomes, photoactivation of encapsulated QDs resulted in a blurred and unspecific staining of the whole cell cytoplasm (data not shown, preparation of liposomes containing QDs can be found in supplementary material). However, photoactivation of QDs in Ps resulted in a sharp and punctuated intracellular staining pattern (Figure 6A and B). These results suggest that QDs encapsulated in Ps were retained in the intact polymer vesicles, whereas QDs encapsulated in liposomes were released into the cytoplasm due to degradation of the liposomal carrier.

In living cells, photoactivation of QDs is caused by the generation of reactive oxygen species (ROS) within the target cell.[43] In view of the pronounced intracellular stability of Ps, the question arises how oxidation of QDs within Ps can be induced by cellular ROS. It was recently proposed that the membranes of Ps are permeable to ROS, such as superoxide or singlet oxygen, which are major contributors to the degradation of the QD surface.[43,44]

For a similar type of Ps made of PMOXA-PDMS-PMOXA, ROS were reported to permeate the polymer membrane. Ps remained stable inside cells after having escaped from endosomes without releasing the encapsulated compounds.[24,25,45] Therefore, it is possible that in our experiments, QDs were partially degraded inside the Ps without being released. Due to the stability of Ps in cellular conditions, degradation of QDs and background signals were dramatically lower in Ps than in liposomes. Similarly, increased photo-enhancement of QDs embedded in silica colloids have been reported in living cells, due to partial degradation mediated by oxidation with minimal aggregation.[46] Results suggested that Ps protect QDs from biological interactions in cell compartments, thus improving the quality of cellular imaging.

Conclusion

QDs are a promising tool for a variety of bio-imaging applications. However, their use in biological systems is limited by their chemical instability and toxicity. We demonstrated that loading of QDs into Ps made of the diblock copolymer PDMS-PMOXA may overcome these problems. In particular, Ps-containing QDs were stable for a prolonged time upon storage and had improved optical properties after cellular uptake.

The implications of these findings are two-fold. First, stabilization of QDs by a protective shell of diblock copolymers may facilitate their preparation, storage, and use in biological systems. Second, chemical modification of the

Ps surface may improve their recognition and uptake by target cells. Therefore, design of such targeted Ps offers the possibility to deliver QDs to specific cellular targets within the organism for diagnostic purposes or imaging applications.

Acknowledgments

We would like to thank Professor Dr Wolfgang Meier for providing the PDMS-PMOXA diblock copolymers. We thank Dr Silvia Rogers for editorial assistance.

Disclosure

The authors report no conflicts of interest in this work.

References

1. Bruchez M, Moronne M, Gin P, Weiss S, Alivisatos AP. Semiconductor nanocrystals as fluorescent biological labels. *Science*. 1998;281(5385):2013–2016.
2. Chan WC. Quantum dot bioconjugates for ultrasensitive nonisotopic detection. *Science*. 1998;281(5385):2016–2018.
3. Resch-Genger U, Grabolle M, Cavaliere-Jaricot S, Nitschke R, Nann T. Quantum dots versus organic dyes as fluorescent labels. *Nat Methods*. 2008;5(9):763–775.
4. Alivisatos AP, Gu W, Larabell C. Quantum dots as cellular probes. *Annu Rev Biomed Eng*. 2005;7:55–76.
5. Derfus AM, Chan WCW, Bhatia SN. Probing the cytotoxicity of semiconductor quantum dots. *Nano Lett*. 2004;4(1):11–18.
6. Michalet X, Pinaud FF, Bentolila LA, et al. Quantum dots for live cells, in vivo imaging, and diagnostics. *Science*. 2005;307(5709):538–544.
7. Hardman R. A toxicologic review of quantum dots: toxicity depends on physicochemical and environmental factors. *Environ Health Perspect*. 2006;114(2):165–172.
8. Hu X, Gao X. Silica-polymer dual layer-encapsulated quantum dots with remarkable stability. *ACS Nano*. 2010;4(10):6080–6086.
9. Zhang H, Zeng X, Li Q, Gaillard-Kelly M, Wagner CR, Yee D. Fluorescent tumour imaging of type I IGF receptor in vivo: comparison of antibody-conjugated quantum dots and small-molecule fluorophore. *Br J Cancer*. 2009;101(1):71–79.
10. Selvan ST, Tan TTY, Yi DK, Jana NR. Functional and multifunctional nanoparticles for bioimaging and biosensing. *Langmuir*. 2010;26(14):11631–11641.
11. Derfus AM, Chan WCW, Bhatia SN. Intracellular delivery of quantum dots for live cell labeling and organelle tracking. *Adv Mater*. 2004;16(12):961–966.
12. Jańczewski D, Tomczak N, Han MY, Vancso GJ. Synthesis of functionalized amphiphilic polymers for coating quantum dots. *Nat Protoc*. 2011;6(10):1546–1553.
13. Gao X, Cui Y, Levenson RM, Chung LWK, Nie S. In vivo cancer targeting and imaging with semiconductor quantum dots. *Nat Biotechnol*. 2004;22(8):969–976.
14. Gerion D, Pinaud F, Williams SC, et al. Synthesis and properties of biocompatible water-soluble silica-coated CdSe/ZnS semiconductor quantum dots. *J Phys Chem B*. 2001;105(37):8861–8871.
15. Bayles AR, Chahal HS, Chahal DS, Goldbeck CP, Cohen BE, Helms BA. Rapid cytosolic delivery of luminescent nanocrystals in live cells with endosome-disrupting polymer colloids. *Nano Lett*. 2010;10(10):4086–4092.
16. Kong L, Zhang T, Tang M, Pu Y. Apoptosis induced by cadmium selenide quantum dots in JB6 cells. *J Nanosci Nanotechnol*. 2012;12(11):8258–8265.
17. Chen H, Zou P, Connarn J, Paholak H, Sun D. Intracellular dissociation of a polymer coating from nanoparticles. *Nano Res*. 2012;5(11):815–825.v
18. Balasubramanian V, Onaca O, Enea R, Hughes DW, Palivan CG. Protein delivery: from conventional drug delivery carriers to polymeric nanoreactors. *Expert Opin Drug Deliv*. 2010;7(1):63–78.
19. Battaglia G. Polymersomes and Their Biomedical Applications. In: *Nanotechnologies for the Life Sciences*. Weinheim, Germany: Wiley-VCH Verlag; 2007. Available at: http://onlinelibrary.wiley.com/doi/10.1002/9783527610419.ntls0250/abstract. Accessed June 3, 2013.
20. Lee JS, Feijen J. Polymersomes for drug delivery: design, formation and characterization. *J Controlled Release*. 2012;161(2):473–483.
21. Ahmed F, Pakunlu RI, Brannan A, Bates F, Minko T, Discher DE. Biodegradable polymersomes loaded with both paclitaxel and doxorubicin permeate and shrink tumors, inducing apoptosis in proportion to accumulated drug. *J Controlled Release*. 2006;116(2):150–158.
22. Sanson C, Schatz C, Le Meins J-F, et al. A simple method to achieve high doxorubicin loading in biodegradable polymersomes. *J Controlled Release*. 2010;147(3):428–435.
23. Lomas H, Canton I, MacNeil S, et al. Biomimetic pH sensitive polymersomes for efficient DNA encapsulation and delivery. *Adv Mater*. 2007;19(23):4238–4243.
24. Balasubramanian V, Onaca O, Ezhevskaya M, Doorslaer SV, Sivasankaran B, Palivan CG. A surprising system: polymeric nanoreactors containing a mimic with dual-enzyme activity. *Soft Matter*. 2011;7(12):5595–5603.
25. Tanner P, Onaca O, Balasubramanian V, Meier W, Palivan CG. Enzymatic cascade reactions inside polymeric nanocontainers: a means to combat oxidative stress. *Chemistry*. 2011;17(16):4552–4560.
26. Jaskiewicz K, Larsen A, Schaeffel D, et al. Incorporation of nanoparticles into polymersomes: size and concentration effects. *ACS Nano*. 2012;6(8):7254–7262.
27. Liu GY, Liu XS, Wang SS, Chen CJ, Ji J. Biomimetic polymersomes as carriers for hydrophilic quantum dots. *Langmuir*. 2012;28(1): 557–562.
28. Egli S, Nussbaumer MG, Balasubramanian V, et al. Biocompatible functionalization of polymersome surfaces: a new approach to surface immobilization and cell targeting using polymersomes. *J Am Chem Soc*. 2011;133(12):4476–4483.
29. Mai Y, Eisenberg A. Self-assembly of block copolymers. *Chem Soc Rev*. 2012;41(18):5969.
30. De Vocht C, Ranquin A, Van Ginderachter J, et al. Polymeric nanoreactors for enzyme replacement therapy of MNGIE. *J Control Release*. 2010;148(1):e19–e20.
31. Nardin C, Hirt T, Leukel J, Meier W. Polymerized ABA triblock copolymer vesicles. *Langmuir*. 2000;16(3):1035–1041.
32. Lee JC-M, Bermudez H, Discher BM, et al. Preparation, stability, and in vitro performance of vesicles made with diblock copolymers. *Biotechnol Bioeng*. 2001;73(2):135–145.
33. Qu L, Peng X. Control of photoluminescence properties of CdSe nanocrystals in growth. *J Am Chem Soc*. 2002;124(9):2049–2055.
34. Williams G, Watts DC, Dev SB, North AM. Further considerations of non symmetrical dielectric relaxation behaviour arising from a simple empirical decay function. *Trans Faraday Soc*. 1971;67(0):1323–1335.
35. Rigler P, Meier W. Encapsulation of fluorescent molecules by functionalized polymeric nanocontainers: investigation by confocal fluorescence imaging and fluorescence correlation spectroscopy. *J Am Chem Soc*. 2006;128(1):367–373.
36. Seeland S, Török M, Kettiger H, Treiber A, Hafner M, Huwyler J. A cell-based, multiparametric sensor approach characterises drug-induced cytotoxicity in human liver HepG2 cells. *Toxicol In Vitro*. 2013;27(3):1109–1120.
37. CoolLED. LED Intensity – CoolLED. 2012. Available at: http://www.coolled.com/Life-Sciences-Analytical/Products/pE-2/. Accessed October 17, 2012.
38. Onaca O, Hughes DW, Balasubramanian V, Grzelakowski M, Meier W, Palivan CG. SOD antioxidant nanoreactors: influence of block copolymer composition on the nanoreactor efficiency. *Macromol Biosci*. 2010;10(5):531–538.

39. Sigot V, Arndt-Jovin DJ, Jovin TM. Targeted cellular delivery of quantum dots loaded on and in biotinylated liposomes. *Bioconjug Chem*. 2010;21(8):1465–1472.
40. Chen C-S, Yao J, Durst R. Liposome encapsulation of fluorescent nanoparticles: quantum dots and silica nanoparticles. *J Nanoparticle Res*. 2006;8(6):1033–1038.
41. Huwyler J, Drewe J, Krähenbuhl S. Tumor targeting using liposomal antineoplastic drugs. *Int J Nanomedicine*. 2008;3(1):21–29.
42. Kettiger H, Schipanski A, Wick P, Huwyler J. Engineered nanomaterial uptake and tissue distribution: from cell to organism. *Int J Nanomedicine*. 2013;8:3255–3269.
43. Zhang Y, He J, Wang P-N, et al. Time-dependent photoluminescence blue shift of the quantum dots in living cells: effect of oxidation by singlet oxygen. *J Am Chem Soc*. 2006;128(41):13396–13401.
44. Carrillo-Carrión C, Cárdenas S, Simonet BM, Valcárcel M. Quantum dots luminescence enhancement due to illumination with UV/Vis light. *Chem Commun (Camb)*. 2009;(35):5214–5226.
45. Baumann P, Balasubramanian V, Onaca-Fischer O, Sienkiewicz A, Palivan CG. Light-responsive polymer nanoreactors: a source of reactive oxygen species on demand. *Nanoscale*. 2013;5(1):217–224.
46. Dembski S, Graf C, Krüger T, et al. Photoactivation of CdSe/ZnS quantum dots embedded in silica colloids. *Small*. 2008;4(9):1516–1526.

Supplementary material

Materials and methods

Preparation of liposomes containing QDs

A mixture of lipids of disuccinatocisplatin (DSPC; 5.5 µmol), cholesterol (4.5 µmol), and 1,2-distearoyl-sn-glycero-3-phosphoethanolamine-N-poly(ethylene glycol) (DSPE-PEG; 0.27 µmol), were dissolved in chloroform/methanol (2:1, volume/volume). The solution was evaporated by vacuum in a water bath at 60°C for 1 hour to form a homogenous lipid film using a rotary evaporator (Rotavapor, BÜCHI Labortechnik AG, Flawil, Switzerland). The lipid film was hydrated for 10 minutes in 1 mL in a 100 nM solution of QDs (Qdot® ITK™ carboxyl quantum dots; Invitrogen, Life Technologies, Lucerne, Switzerland) in 0.1 M phosphate buffer solution (PBS) containing 1 mM EDTA, pH 7.2; extrusion was performed five times through a polycarbonate filter with an average pore diameter of 0.2 µm, followed by nine extrusions through a filter with an average pore diameter of 0.08 µm (Nucleopores, Whatman, VWR International AG, Dietikon, Switzerland).

Liposomes containing QDs were purified by size exclusion chromatography using a Superose 6 prep column (1.6 × 20 cm), (GE Healthcare, Cleveland, OH, USA) eluting with 0.01 M PBS, pH 7.2.

Results

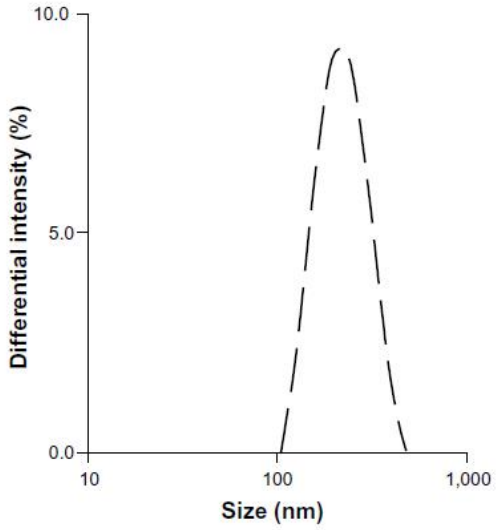

Figure S1 Size of Ps made of PDMS-PMOXA with 5% amine function (long-dashed lines), loaded with QDs. Average diameter of Ps was 210 nm.
Abbreviations: PDMS-PMOXA, poly(dimethylsiloxane)-poly(2-methyloxazoline); Ps, polymersomes; QDs, quantum dots.

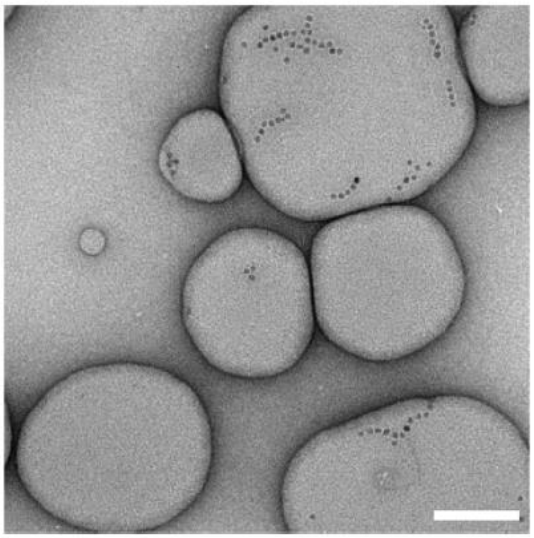

Figure S2 TEM morphology analysis of Ps made of PDMS-PMOXA with 5% amine function, loaded with QDs.
Note: Scale bar represents 100 nm.
Abbreviations: PDMS-PMOXA, poly(dimethylsiloxane)-poly(2-methyloxazoline); Ps, polymersomes; QDs, quantum dots; TEM, transmission electron microscopy.

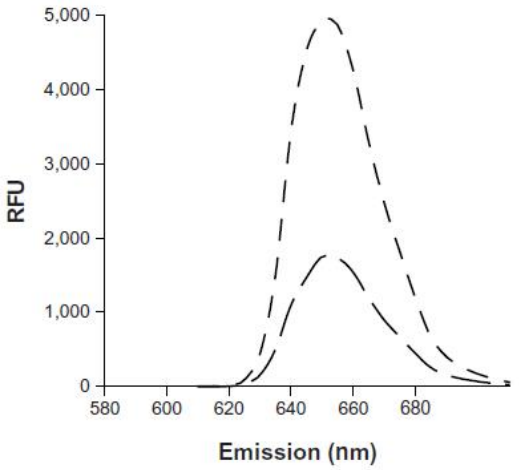

Figure S3 Analysis of QDs loading efficacy by fluorescence spectroscopy. Emission fluorescence spectra of free QDs (dotted-lines), Ps with 5% amine function containing QDs (long-dashed lines), and empty Ps (dashed lines), excitation wavelength 405 nm.
Abbreviations: Ps, polymersomes; QDs, quantum dots; RFU, relative fluorescent units.

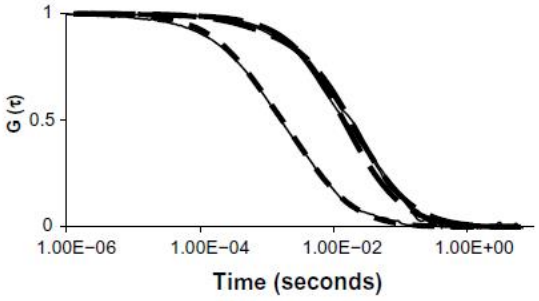

Figure S4 Analysis of QDs loading efficacy by FCS. FCS auto-correlation curves, experimental (solid lines) and fitted (dashed-lines) of free QDs (dotted-lines), Ps-containing QDs (dot-dashed lines), and Ps with 5% amine function containing QDs (long-dashed lines).
Abbreviations: FCS, fluorescence correlation spectroscopy; Ps, polymersomes; QDs, quantum dots.

3.2 Microparticles as diagnostic product

CombiCap: A novel drug formulation for the Basel phenotyping cocktail

Marine Camblin[1], Benjamin Berger[2], Manuel Haschke[2], Stephan Krähenbühl[2], Jörg Huwyler[1], Maxim Puchkov[1]

[1]Division of Pharmaceutical Technology, Department of Pharmaceutical Sciences, University of Basel, Basel, Switzerland

[2]Division of Clinical Pharmacology and Toxicology, Department of Biomedicine, University of Basel, Basel, Switzerland

International Journal of Pharmaceutics 512 (2016) 253-261

International Journal of Pharmaceutics 512 (2016) 253–261

Contents lists available at ScienceDirect

International Journal of Pharmaceutics

journal homepage: www.elsevier.com/locate/ijpharm

CombiCap: A novel drug formulation for the basel phenotyping cocktail

Marine Camblin[a], Benjamin Berger[b], Manuel Haschke[b], Stephan Krähenbühl[b], Jörg Huwyler, Prof. Dr.[a,*], Maxim Puchkov[a]

[a] Division of Pharmaceutical Technology, Department of Pharmaceutical Sciences, University of Basel, Basel, Switzerland
[b] Division of Clinical Pharmacology and Toxicology, Department of Biomedicine, University of Basel, Basel, Switzerland

ARTICLE INFO

Article history:
Received 20 June 2016
Received in revised form 19 August 2016
Accepted 23 August 2016
Available online 24 August 2016

Keywords:
CYP450 phenotyping
Drug loading
Drug formulation
Mini tablets
Basel Cocktail
Fujicalin

ABSTRACT

Phenotyping of cytochrome P450 isoenzymes is used for metabolic profiling. Phenotyping cocktails are usually administered as individual marketed products, which are not designed for diagnostic applications. Therefore, a formulation strategy was developed, which can be applied to any phenotyping cocktail. The formulation was validated *in vitro* and *in vivo* in human volunteers using caffeine, efavirenz, flurbiprofen, metoprolol, midazolam, and omeprazole (Basel Cocktail). Spray dried di-calcium phosphate particles (Fujicalin) were used as an inert drug carrier for probe drugs. All drugs were successfully loaded into Fujicalin by a solvent evaporation method. Mini-tablets were produced and demonstrated good physical characteristics, expected drug content and immediate release profiles for all drug formulations. Mini-tablets were introduced into a capsule (CombiCap) and used for a pilot study in human volunteers. Plasma samples were collected and analyzed by liquid chromatography and mass spectrometry. Plasma concentration ratios between the parent drugs and the respective metabolites were equivalent for the novel CombiCap formulation and individually dosed Basel Cocktail drugs. We conclude that the CombiCap formulation platform can be easily adopted for different types of phenotyping cocktails due to its scalable and modular design, which allows a simple and convenient combination of variable doses of different probe drugs.

1. Introduction

1.1. Phenotyping

Phenotyping is used to determine the enzymatic activity of enzymes that are involved in drug metabolism (Tracy et al., 2016). Of special interest are thereby cytochrome P450 (CYP) isoenzymes, which are responsible for more than 50% of the phase I dependent metabolism of commonly used drugs (Ingelman-Sundberg, 2004). Inter-individual activity of these mixed-function oxidases is often highly variable due to genetic variants and the influence of endogenous or environmental factors. This variability is of clinical importance because it can affect plasma concentrations (and thus pharmacological effect) of metabolized drugs. Activity of different CYPs can be assessed simultaneously by administration of a cocktail made of selected drugs that are substrates of the respective enzymes, followed by collection of plasma samples in order to quantify the plasma concentration ratio between the parent drugs and their metabolites (Nguyen et al., 2016). The principles of phenotyping procedures and a selection of used probe drugs and probe drug mixtures have been comprehensively reviewed by Fuhr et al. (2007). Thus, metabolic profiles of individuals (*e.g.* volunteers in clinical trials or patients) can be determined (Wilkinson, 2005). The phenotyping strategy is valuable for the detection of CYP-mediated drug–drug interactions (DDI) (Murray, 2006), the stratification of cohorts in clinical trials (Spaggiari et al., 2014) and in personalized medicine to adjust patient's treatments (Preissner et al., 2013). The Basel cocktail contains mixture of 6 commercially used drugs. This drug cocktail was developed at the University Hospital Basel (Donzelli et al., 2014). The cocktail consists of 10 mg caffeine (CAF), 50 mg efavirenz (EFA), 12.5 mg flurbiprofen (FLU), 10 mg of metoprolol tartrate (MET), 2 mg midazolam (MID), and 10 mg omeprazole (OME), (Derungs et al., 2015; Donzelli et al., 2014) used as probe drugs for CYP1A2, CYP2B6, CYP2C9, CYP2D6, CYP3A4, and CYP2C19, respectively.

Abbreviations: CYP, cytochrome P450; DDI, drug–drug interactions; BCS, biopharmaceutical classification system; CAF, caffeine; EFA, efavirenz; FLU, flurbiprofen; MET, metoprolol tartrate; MID, midazolam; OME, omeprazole; DMSO, dimethyl sulfoxide; SEM, scanning electron microscopy.

* Corresponding author at: Division of Pharmaceutical Technology, Department of Pharmaceutical Sciences, Klingelbergstrasse 50, 4056 Basel, Switzerland.
E-mail address: joerg.huwyler@unibas.ch (J. Huwyler).

http://dx.doi.org/10.1016/j.ijpharm.2016.08.043
0378-5173/

There are several phenotyping cocktails described in the literature (including the Basel Cocktail), in which drugs or other commercial products such as, *e.g.* Nescafé® single-serve sachet (Bosilkovska et al., 2014) have been administered. In all of these cocktails, drug formulations were not designed to serve the purpose of diagnostics and phenotyping and can therefore be considered to be suboptimal (Adedoyin et al., 1998; Blakey et al., 2004; Bosilkovska et al., 2014; Bruce et al., 2001; Brynne et al., 1999; Chainuvati et al., 2003; de Andrés et al., 2013; Frye et al., 1997; Ghassabian et al., 2009; Ghassabian and Murray, 2013; Kakuda et al., 2014; Kashuba et al., 1998; Krösser et al., 2006; Nguyen et al., 2016; Pedersen et al., 2013; Ryu et al., 2007; Sharma et al., 2004; Tanaka et al., 2003; Tennezé et al., 1999; Tomalik-Scharte et al., 2005; Zgheib et al., 2006; Zhu et al., 2001). Problems include limited availability of immediate release formulations leading to delays between drug administration and plasma sampling; imprecise dosing despite the use of scored tablets (Habib et al., 2014) and the use of pharmacologically active excipients in commercial formulations, which can influence the activity of different CYPs (Engel et al., 2012).

1.2. Aim

In order to overcome these problems, a standardized formulation platform is needed. This formulation should have unified release kinetics and should be scalable, allowing adjustment of doses prior to administration (*i.e.* use of multi-unit proportional formulations). Used excipients should be inert and present in constant proportions. Manufacturing should be achieved at competitive costs. Finally, the used formulation should be convenient and well accepted by patients. Based on these considerations, new standard requirements for a solid dosage formulation for diagnostic cocktails should be defined as follows:

1) Drug substance requirements include a sufficiently high drug load, separation of drugs from each other to exclude potential chemical degradation, the use of the same excipients in identical proportions for all drugs and applicability of the formulation to all BCS classes ("The Biopharmaceutics Classification System (BCS) Guidance," 2016).
2) Patient requirements include age appropriate administration for children ("Guideline on pharmaceutical development of medicine for paediatric use," 2013; Liu et al., 2014; van Riet-Nales et al., 2014) and elderly (Aleksovski et al., 2015; Liu et al., 2014; Stegemann et al., 2010) including persons with dysphagia (Stegemann et al., 2012; Thomson et al., 2009).
3) Biopharmaceutical requirements include identical release kinetics for all probe drugs and the possibility to use release modifiers such as a gastro-resistant coating of the dosage form.
4) Technical requirements include scalability to enable industrial production and the possibility of dose change or dose adaptation prior to application (multi-unit system).

Based on these four considerations, the aim of the present study was to develop and validate a formulation strategy for different types of phenotyping cocktails. The Basel Cocktail was thereby selected as a well characterized reference cocktail.

2. Material and methods

2.1. Materials

Spherically granulated dibasic calcium phosphate (Fujicalin®) was provided by Fuji Chemical Industries (Toyama, Japan), Dimethyl sulfoxide (Rotipuran® 99.8% p.a.) was purchased from Roth AG (Switzerland), Fumed silica (Aerosil 200®) came from Evonik industries (Germany), Croscarmellose sodium (AcDiSol®) was provided by FMC Bio Polymer (USA), and Sodium stearyl fumarate (LubriSanaq®) was provided by Pharmatrans-Sanaq AG Pharmaceuticals (Switzerland). Caffeine (PubChem CID: 2519) originated from BASF (Switzerland), Efavirenz (PubChem CID: 64139) was supplied by Hetero (India), Flurbiprofen (PubChem CID: 3394) from Sun Pharma (India), Metoprolol tartrate (PubChem CID: 4171) from Pfannenschmidt (Germany), Midazolam hydrochlorate (PubChem CID: 43032) was purchased from Hänseler AG (Switzerland) and Omeprazole (PubChem CID: 4594) 10 mg gastro resistant capsules (Sandoz, France) was bought in a pharmacy. Sodium lauryl sulfate and hydrochloric acid were both bought from Roth AG (Switzerland), acetonitrile Chromanorm® was purchased from VWR (Switzerland), glacial acetic acid comes from Hänsler AG (Switzerland), sodium acetate, sodium hydroxide and sodium phosphate monobasic dihydrate were supplied by Sigma Aldrich (Switzerland).

Table 1
Composition of drug-loaded Fujicalin mixtures.

Formulation	API		Fujicalin		DMSO		Water	
	% (w/w)	g	% (w/w)	g	% (w/w)	g	% (w/w)	g
Caffeine	3.6	1.5	59.5	25	33.3	13.6	3.6	1.5
Efavirenz	27	15	45	25	25.3	13.6	2.7	1.5
Flurbiprofen	16.5	8	51.5	25	28.9	13.6	3.1	1.5
Metoprolol	14.7	7	52.7	25	32.6	15.1	0	0
Midazolam	3.6	1.5	59.5	25	36.9	15.1	0	0

2.2. Methods

2.2.1. Solvent loading method of Fujicalin

A calculated amount of each drug was introduced in a 250 mL round bottom flask and dissolved in a solvent mixture of DMSO/water (Table 1). It was important to not exceed a total liquid volume (*i.e.* drug solubilized in the solvent mixture) of 25 mL due to the maximum Fujicalin loading capacity of 1.1 mL/g ("Fujicalin. The unique DCPA," 2009). Gentle heating (up to 70 °C) was required to help the dissolution of CAF, FLU and MID. The resulting solutions were frozen in liquid nitrogen before 25 g Fujicalin powder was added (Table 1). The round bottom flask was immediately connected to a vacuum pump for 5 min to evacuate air from the Fujicalin particle pores. The mixture was subsequently heated to 80 °C (under vacuum) to melt the frozen drug solution and to promote its penetration into the pores of the Fujicalin particles (Fig. 1). After loading, the drug-loaded particles were dried in a vacuum oven at 50 °C at a reduced pressure of 200 mbars with a supply of N_2 for 48 h to remove DMSO from the final product. This loading protocol was used for all drug formulations with the exception of OME, which is commercially available in the form of pellets.

2.2.2. Scanning electron microscopy (SEM)

To verify the absence of extra-particulate drug crystallization, SEM pictures were made with an FEI/Philips XL30 FEG instrument (Philips, Netherlands) (Preisig et al., 2014). Each sample was placed in a sputter coating apparatus (MED 020, BalTec AG, Liechtenstein) and was sputtered with a 10 nm gold layer prior to imaging.

2.2.3. Preparation of mini-tablets

Each batch of drug-loaded Fujicalin particles prepared as described in Section 2.2.1 was separately mixed with 2% (w/w) croscarmellose sodium, 0.5% (w/w) sodium stearyl fumarate, and 0.5% (w/w) fumed silica.

Tablets were produced on the Styl'one tablet press (Medelpharm, France) with a 12 mini multi-tips punch (concave, diameter

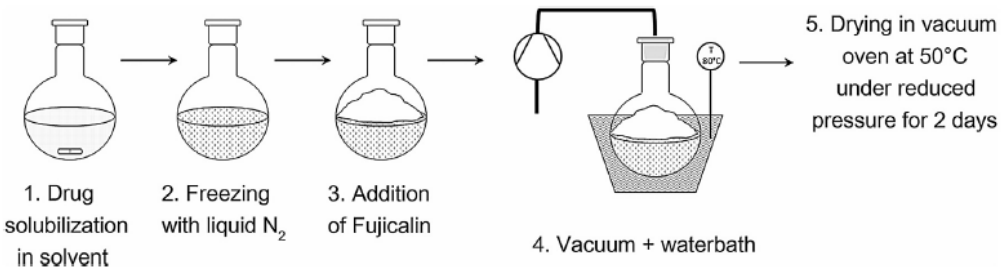

Fig. 1. Drug loading of Fujicalin particles.

2 mm, Notter, Germany). Filling depth of the punch was fixed at 8 mm and the compression force was set to 4 kN. The same parameters were applied for every drug formulation. The resulting tablets (containing each a separate individual drug) were combined and packed together into a hard gelatin capsule size 0 according to the required doses. OME pellets (10 mg) were removed from their original capsule and added to the final product. This final dosage form is named CombiCap.

2.3. Characterization of mini-tablets

2.3.1. Mini-tablets dimension and weight

Mini-tablets height and diameter (n = 10) were measured with a digital slide caliper gauge (Matrix-Handels, Germany). Individual mass (n = 10) was measured on an electronic balance (AX 204 Delta Range, Mettler Toledo, Switzerland). Measurements were done for every probe drug formulation (except OME).

2.3.2. Uniformity of mass

The weight and mass uniformity of every mini-tablet formulation were determined following the method described in Ph. Eur (EDQM, 2012). In brief, 20 tablets were individually weighed on an electronic balance (AX 204 Delta Range, Mettler Toledo, Switzerland) and the average mass was calculated.

2.3.3. Drug content and uniformity of content

Drug content of the mini-tablets (n = 10) was determined using HPLC-UV (Agilent 1100 Series HPLC Value System, Agilent, Switzerland). Ten mini-tablets were independently dissolved in a defined volume of mobile phase (Table 2), followed by the filtration of the solutions (0.22 μm PTFE syringe filters, VWR, USA). The chromatographic measurement was carried out according to Table 2. The area under the curve (AUC) of the chromatogram was then correlated to the drug concentration, according to the calibration curve that was prepared with 5 defined concentrations. The same C18 column (XTerra RP18, 5 μm particle size, 2.1 × 150 mm, Waters, Switzerland) was used for every drug; the column temperature was set to 40 °C.

Drug content uniformity was determined on 10 mini-tablets, according to Ph. Eur (EDQM, 2012).

2.3.4. Hardness and tensile strength

A texture analyzer (FMT-310, Force Tester, Alluris GmbH&Co KG, Germany) was used in order to evaluate the hardness (n = 10) of the mini-tablets. The sensor travelled at a speed of 0.5 mm/s towards the mini-tablet until breakage occurred. The value corresponding to the breakage force was considered to be the hardness of the mini-tablet (Eberle et al., 2015). The tensile strength was then calculated using Eq. (1) for convex-faced tablets (EDQM, 2012):

$$\sigma_x = \frac{10F}{\pi D^2}\left[\frac{2.84H}{D} - \frac{0.126H}{W} - \frac{3.15W}{D} + 0.01\right]^{-1} \quad (1)$$

where σ_x is the tensile strength (MPa), F is the breaking force (N), D is the tablet diameter (mm), H is the tablet height (mm) and W is the wall height (mm).

2.3.5. Friability

A single friability test was carried out on uncoated 20 mini-tablets at 25 rpm to get 100 revolutions (TA200, Erweka, Germany) as specified in European Pharmacopeia (EDQM, 2012). Friability was calculated for CAF, EFA, FLU, MET and MID mini-tablets with Eq. (2):

$$F = \frac{W_i - W_f}{W_t} \quad (2)$$

where W_t is the initial weight (mg) and W_f is the final weight after the friability testing.

2.3.6. Disintegration of mini-tablets

The disintegration test was carried out in DT2 (Sotax, Switzerland). One mini-tablet was introduced in each of the 6 tubes with a disc to prevent flotation (EDQM, 2012). Time was registered manually with a stopwatch.

Table 2
HPLC parameters for determination of Basel Cocktail drug content.

Drug	Wavelength (nm)	Mobile phase	Flow rate (μL/min)	Injection volume (μL)	Retention time (min)	Calibration curve parameters		
						Slope	Intercept	R^2
CAF	273	Acetonitrile/Water (15:85)	400	10	1.88	70.706	155.22	0.999
EFA	252	Acetonitrile/Water (60:40)	500	5	1.97	28.146	87.743	0.999
FLU	247	Acetonitile/Water/Acetic acid (35:60:5)	500	10	2.05	99.216	−9.800	0.999
MET	221	Acetonitrile/Phosphate buffer (0.02 M) pH 3.5 (40:60)	400	10	1.28	38.161	94.033	0.999
MID	227	Acetonitrile/Sodium acetate buffer (0.01 M) pH 3.14 (35:65)	500	10	3.75	97.157	391.87	0.999

Table 3
Dissolution assay conditions ("Dissolution Methods", 2015) for caffeine (CAF), efavirenz (EFA) (United States Pharmacopeia Convention, 2007), flurbiprofen (FLU), metoprolol (MET), midazolam (MID).

Drug	UV wavelength	Medium	Calibration curve parameters		
			Slope	Intercept	R^2
CAF	273 nm	900 mL water	0.0547	−0.0042	0.999
EFA	252 nm	2% SLS in 1L water	0.004	0.0045	0.999
FLU	247 nm	900 mL phosphate buffer pH 7	0.0488	0.0076	0.999
MET	221 nm	900 mL SGF	0.0084	−0.0001	0.999
MID	227 nm	900 mL SGF	0.029	0.0137	0.999

2.3.7. Dissolution studies

The drug release from each formulation was performed using an USP II apparatus (AT7, Sotax, Switzerland) at 37.0 ± 0.5 °C and according to dissolution conditions listed in Table 3. The dissolution buffers were: distilled water, 2% sodium lauryl sulfate (SLS) in water, phosphate buffer (0.05 M) pH 7 and simple simulated gastric fluid (SGF, 0.1 N HCl). The number of mini-tablets in a dissolution vessel comprised the final dose of each drug. Samples were taken at one minute time intervals and were analyzed with UV–vis spectrophotometer (Ultrospec 3100 pro, Amersham Biosciences, UK).

2.3.8. In vivo study

The *in vivo* evaluation of the Combicap formulation was done in a pilot study with 3 healthy volunteers. The procedure was brought to the attention of the Ethics Committee northwest/central Switzerland (EKNZ) (notification No. EKNZ UBE-15/17). The study was based on the protocol described by Derungs et al. (2015) for the Basel Cocktail with marketed products. Results from this pilot experiment were compared to results from a previous clinical trial done in 16 healthy volunteers (ClinicalTrials.gov ID: NCT01386593). The 3 participants had to fast for 10 h prior to the intake of the CombiCap and to fast an additional 4 h after the administration of the capsule. They were not allowed to consume any caffeine for 48 h before the administration of drugs and until the end of the study period. The capsule containing mini-tablets (CAF: 20, EFA: 11, FLU: 4, MET: 3, MID: 3) and pellets of OME (10 mg) was administered *per os* with a glass of water. Venous blood samples for pharmacokinetic analysis were collected into 2.7 mL EDTA tubes at 0, 1, 2, 4, 6 and 8 h following the CombiCap administration.

Blood samples were analyzed using a previously developed liquid chromatography tandem mass spectrometry (LC–MS/MS) method (Donzelli et al., 2014) in order to determine the concentrations of probe drugs and their respective phase I metabolites. The method was modified to include flurbiprofen, 4′-OH-flurbiprofen, and flurbiprofen-d3 (IS). Chromatographic separation was performed on a Shimadzu HPLC system (Shimadzu AG, Reinach, Switzerland) coupled to a triple quadrupole tandem mass spectrometer (API4000, AB/MDS Sciex, Concord, Canada) operating in positive electrospray ionization mode, except for efavirenz, 8′-hydroxyefavirenz, flurbiprofen, 4′-hydroxyflurbiprofen, and their respective internal standards, which were detected in negative mode. Total run time was 2.9 min. Inter-assay accuracy (determined as the% bias) ranged from −8.5 to 6.8 and inter-assay precision (determined as the CV%) was lower than 13.9 for all analytes.

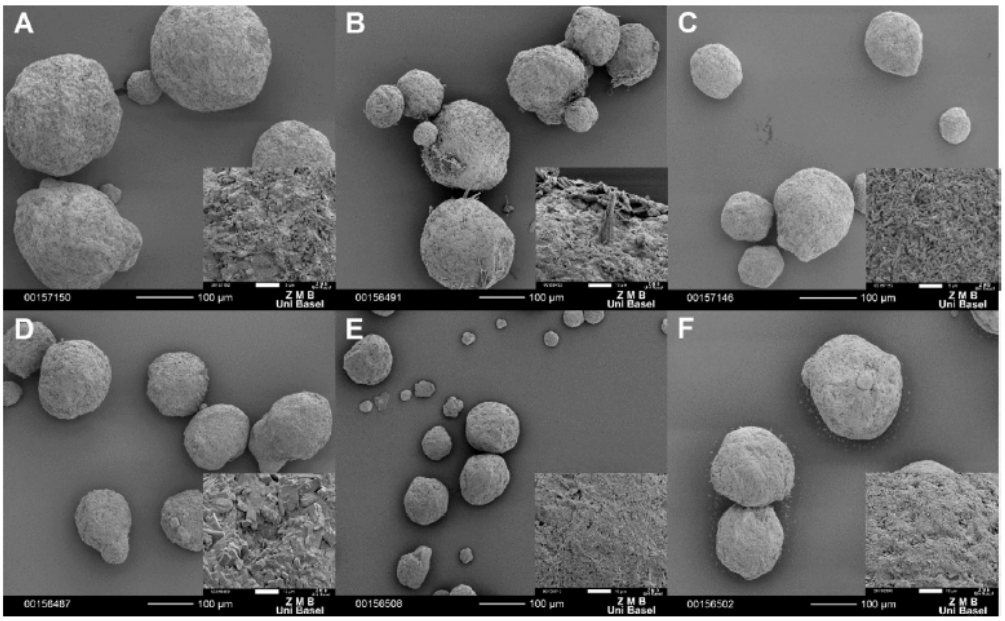

Fig. 2. SEM visualization of Fujicalin particles. (A) Fujicalin particles were loaded with (B) caffeine, (C) efavirenz, (D) flurbiprofen, (E) metoprolol, and (F) midazolam. Scale bars: 100 µm (A–F), 10 µm (inserts B and D–F), and 5 µm (inserts A and C).

3. Results

3.1. Qualitative loading of drugs into Fujicalin particles

Fig. 2 shows SEM pictures of Fujicalin before and after loading with CAF, EFA, FLU, MET and MID. Pictures B–F depict different surfaces compared to porous pure Fujicalin (A), demonstrating qualitative loading of Basel Cocktail probe drugs (except OME) into Fujicalin particles. As it can be seen from the low magnification images there is no extra-particulate crystallization. This indicates that the drug substances were loaded into Fujicalin particles only. After visual inspection, dried drug-loaded particles have similar flowability as pure Fujicalin particles.

3.2. Preparation and characterization of mini-tablets

3.2.1. Drug content and content uniformity

The measured doses (Table 4) show an average drug loading efficiency of 94% with the expected doses. Based on these results, the effective dose in the CombiCap was within 85–115% (w/w) as specified by the Ph.Eur (EDQM, 2012).

3.3. Characterization of mini-tablets

The data obtained from post-compression parameters for the mini-tablets of all formulations such as weight, diameter, height, hardness and tensile strength, friability, and disintegration time are summarized in Table 5. The dimensions of mini-tablets show a maximal height difference of 0.8 mm between drug formulations but reveal very small variations within probe drug formulations. The diameter of the mini-tablets remains constant.

The weight of the mini-tablets differs from one drug formulation to another *i.e.* 10.74 mg for CAF mini-tablets and 14.40 mg for MET mini-tablets. The uniformity of mass requirements (EDQM, 2012) are fulfilled for each probe drug formulation with a maximum deviation of 4.3% in the case of EFA mini-tablets.

The hardness determined with the texture analyzer gave results between 8.2 N for FLU mini-tablets and 35 N for MET mini-tablets. Despite the apparent low hardness, the tensile strength indicated sufficient tablet stability.

The friability of the Basel Cocktail mini-tablets showed values below 0.4% with a maximum weight loss for EFA mini-tablets.

The full disintegration of 6 mini-tablets for every formulation was achieved in less than 4 min and was thus in accordance with the disintegration requirements for uncoated tablets (inferior to 15 min) (EDQM, 2012).

3.4. Dissolution and release studies

Fig. 3 illustrates the data obtained from dissolution tests for mini-tablets and commercial products. The FLU, MET and MID mini-tablets release profiles were faster than those for the commercial products Froben® 50 mg (Abbott, Switzerland), Lopressor® 100 mg (Daiichi-Sankyo, France) and Dormicum® 7.5 mg (Roche, Switzerland) respectively. In all these cases the complete release of a drug from the mini-tablets is within 10 min. Despite the differences in release profiles, commercial products and mini-tablets are considered equivalent as their complete release is within 15 min time ("Dissolution Methods," 2015; "Guidance for industry Dissolution testing if immediate release solid oral dosage forms," 1997; "Guideline on the investigation of bioequivalence," 2010).

3.5. In vivo studies

Fig. 4 displays the concentration ratios of the 6 probe drugs and corresponding metabolites obtained with the CombiCap and the marketed products (A). The data for marketed products, except from the FLU data that were published from the Geneva Cocktail by Bosilkovska et al. (2016), were obtained from the clinical trial (n = 16) described by Derungs et al. (2015). The comparison was done for specific time points defined in the article that are 2 h for MID, 4 h for CAF and OME and 6 h for EFA and MET. In the case of MET mini-tablets, the time point was set to 4 h as a result of the mini-tablets having an immediate release whereas Beloc ZOK® is a retarded dosage form. Fig. 4 also present the plasma concentrations of the probe drugs CAF (B), EFA (C), FLU (D), MET (E), MID (F), and OME (G) with their respective metabolites in the 3 health volunteers.

4. Discussion

4.1. Loading of Fujicalin particles

Porous Fujicalin di-calcium phosphate particles were used as an inert drug carrier for probe drugs and as the basis for a simple formulation amendable to direct compression. A solvent evaporation method was developed applicable to drug loading of five

Table 4
Drug content in mini-tablets and in a CombiCap capsule size 0.

Drug	Expected dose (mg)/mini-tablet	Average measured dose (mg)/ mini-tablet n = 10	Required dose in whole CombiCap capsule (mg)	Number of mini-tablets needed in CombiCap capsule	Effective calculated average dose in CombiCap capsule (mg)
CAF	0.54	0.47 ± 0.02	10	22	9.87 ± 0.44
EFA	4.5	4.20 ± 0.09	50	12	50.4 ± 1.08
FLU	3	3.02 ± 0.02	12.5	4	12.10 ± 0.08
MET	3.2	3.16 ± 0.08	10	3	9.48 ± 0.24
MID	0.65	0.60 ± 0.01	2	3	1.80 ± 0.03

Table 5
Characteristics of Basel Cocktail mini-tablets (average ± standard deviation).

Drug	Height (mm) n = 10	Diameter (mm) n = 10	Weight (mg) n = 10	Hardness (N) n = 10	Tensile strength (MPa) n = 10	Friability[a] (%)	Disintegration time (s) n = 6
CAF	2.61 ± 0.01	2.06 ± 0.01	10.74 ± 0.115	14.85 ± 1.55	1.69 ± 0.18	0.23	<2
EFA	3.07 ± 0.03	2.03 ± 0.01	12.16 ± 0.156	13.51 ± 3.26	1.26 ± 0.30	0.33	71 ± 61
FLU	3.41 ± 0.01	2.05 ± 0.01	13.71 ± 0.139	8.24 ± 0.56	0.70 ± 0.05	0.14	22 ± 7
MET	2.94 ± 0.02	2.04 ± 0.01	14.40 ± 0.173	35.0 ± 2.26	3.38 ± 0.22	0.21	67 ± 18
MID	2.82 ± 0.01	2.06 ± 0.01	11.48 ± 0.138	8.65 ± 1.67	0.92 ± 0.18	0.04	<10

[a] Single measurement with 20 mini-tablets.

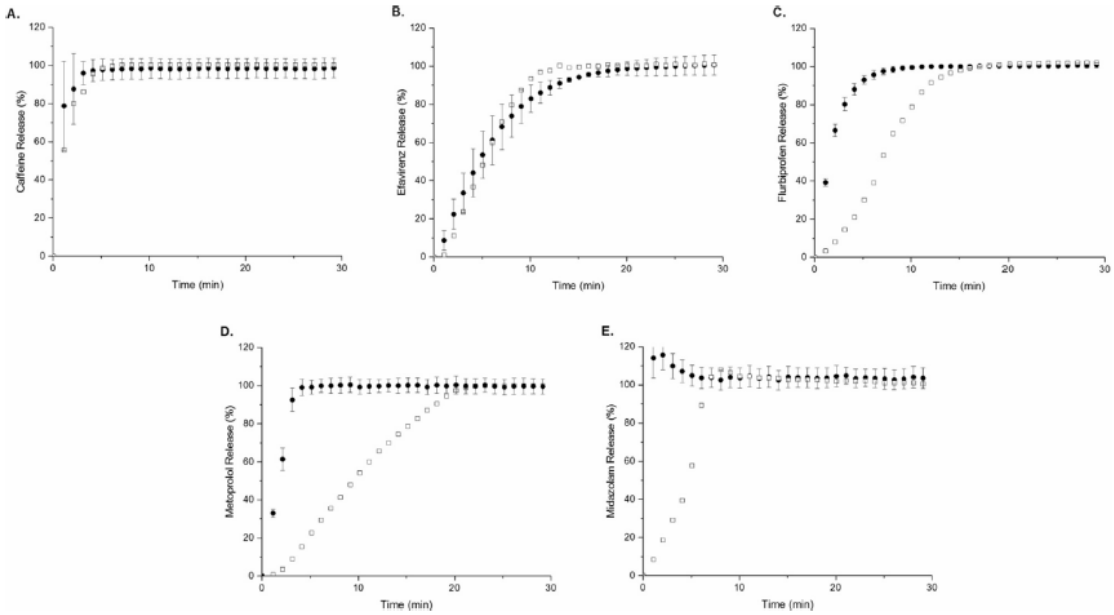

Fig. 3. Release profiles of mini-tablets and marketed product formulations. Dissolution was determined for (A) caffeine, (B) efavirenz, (C) flurbiprofen, (D) metoprolol, and (E) midazolam. Solid squares: Basel Cocktail formulations. Open squares: Reference formulations of marketed products. Values are means ± standard deviation, n = 9.

probe drugs of the Basel Cocktail. According to the results, it was possible to formulate all drugs independently from each other. For this purpose, the used components, namely Fujicalin, DMSO and water, have shown excellent applicability. DMSO is essentially nontoxic when ingested, with a reported oral single-dose LD50 value of 17.4–28.3 g/kg (rat) (Robert and McKim, 2008). The European and US Pharmacopeias are referencing DMSO as Class 3 solvent with low toxic potential to man. Therefore, no health-based exposure limit is needed (EDQM, 2012). Class 3 solvents have permitted daily exposures (PDE) of 50 mg or more per day. The residual amounts of DMSO in the tested mini-tablets (as based on weight loss during drying) represent a negligible fraction of the PDE of 50 mg/day. It was possible to apply the same adsorption process to every drug, while taking care to not exceed the maximum adsorption capacity defined in the specifications of Fujicalin (1.1 mL/g). The uniformity within the five different formulations was thus assured and the potential risk of enzyme-excipient interactions with the targeted CYPs was minimized. The main advantage of this simple formulation is the speed of processing in a single vessel. Thus, there is no limitation factor in the lab scale that would impact the scale up for industrial production. Larger batches can be formulated by proportionally increasing amounts of drug, solvent and Fujicalin and by adapting the size of the formulation vessel. In this study the excess DMSO was removed under vacuum conditions and therefore can be difficult to scale-up for industrial large volume demands. In this respect, an alternative solvent removal process such as reduced-pressure fluidized bed process can be used (Leuenberger et al., 2006).

Basel Cocktail probe drugs belong to different BCS classes. For instance, caffeine and metoprolol tartrate belong to BCS class I whereas efavirenz, flurbiprofen and midazolam belong to class II (Wu and Benet, 2005). The obtained results show that DMSO/water mixtures could be used in the loading of all probe drugs. All five drug substances had a sufficient solubility in DMSO/water despite their different BCS classes. Visual analysis of loaded Fujicalin particles by SEM revealed drug deposition either on or within the Fujicalin particles. The absence of visible drug crystals after loading (Fig. 2, high magnification pictures) indicates no extra-particulate crystallization of caffeine, efavirenz, flurbiprofen, metoprolol and midazolam with average loading efficiency value of 94%. This finding and the inspection of surface morphology of loaded particles or pure Fujicalin suggest an efficient retention of Basel Cocktail probe drugs by carrier particles.

The sixth drug used in the Basel Cocktail is Omeprazole, which was not formulated according to the proposed strategy. Instead a commercial pellet-formulation was used. In case a pH-sensitive drug substance such as Omeprazole has to be formulated in a similar way as the rest of the drugs, an enteric coating can be applied on the capsule or the mini-tablets to ensure simultaneous dissolution of the cocktail components.

4.2. Preparation and characterization of mini-tablets

Drug loaded Fujicalin particles mixed with the external phase were compressed into mini-tablets having a maximum diameter of 2 mm and a maximum height of 3.4 mm. The mechanical properties of the obtained compacts suggest sufficient stability and, hence, an applicability for further processing. This offers the possibility to coat mini-tablets with a protective colored film for drug differentiation or with a release modifier coating. The weight of mini-tablets is uniform, in agreement with requirements defined by the Ph. Eur., indicating a good repeatability of the compression process and a good flowability of the powder mixtures in the die of the tablet press. This indirectly supports the findings from drug loading SEM picture analysis. With the absence of external deposition or crystallization the carrier particles retain excellent flowability.

The small tablet size makes this formulation suitable for children or elderly persons with dysphagia, which fulfills the patient compliance goal for cocktail formulations.

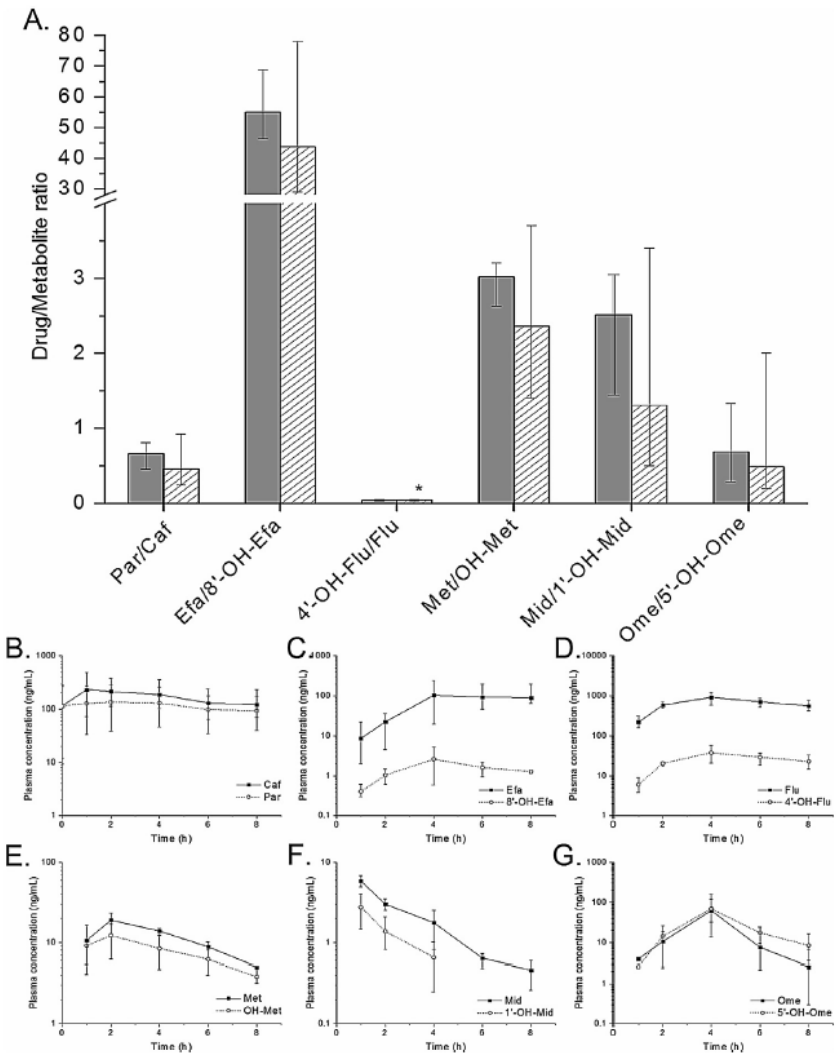

Fig. 4. Metabolic ratios and plasma concentrations of Basel Cocktail probe drugs in human volunteers. Panel A: Metabolic ratios between caffeine (Caf), efavirenz (Efa), flurbiprofen (Flu), metoprolol (Met), midazolam (Mid) and the corresponding metabolites paraxenthine (Par), 8-hydroxyefavirenz (8′OH-Efa), α-hydroxymetoprolol (OH-Met), 4′-hydroxyflurbiprofen (4′-OH-Flu), 1′-hydroxymidazolam (1′-OH-Mid), 5-hydroxyomeprazole (5′-OH-Ome) were determined. Comparison between CombiCap (grey bars, n = 3) and marketed products (white bars, n = 16). *: Clinical data for a commercial flurbiprofen formulation as published previously for the Geneva Cocktail (Bosilkovska et al., 2014). Panel B–G: Average plasma concentration (n = 3) of caffeine and paraxenthine (B), efavirenz and 8-hydroxyefavirenz (C), flurbiprofen and 4′-hydroxyflurbiprofen (D), metoprolol and α-hydroxymetoprolol (E), midazolam (Mid) and 1′-hydroxymidazolam (F), omeprazole and 5′-hydroxyomeprazole (G). Values are means ± standard deviation.

4.3. Disintegration and dissolution

In accordance with the regulations for uncoated tablets, all mini-tablets disintegrated in less than four minutes, fulfilling the requirement for immediate release as intended for the Basel Cocktail phenotyping studies. The results of dissolution studies of each probe drug formulation confirm this statement. As it is seen in Fig. 3, drugs were fully released from mini-tablets in less than 15 min supporting the immediate release. As compared with marketed dosage forms that were previously used in the Basel Cocktail studies, the dissolution of the mini-tablets shows identical curves for CAF and EFA whereas mini-tablets of FLU, MET and MID have a faster release than the commercial products. However, complete release of these three drugs from the mini-tablets within 15 min can be considered to be equivalent to the performance of commercial products. Thus, the goal of obtaining identical release kinetics between all drug formulations is achieved. This allows for simultaneous dosage and plasma sampling for all probe drugs, and therefore simultaneous determination of enzymatic activity for all CYPs.

The final form consists of a hard gelatin capsule containing the number of mini-tablets indicated in Table 4, corresponding to the required doses of the phenotyping cocktail. It should be emphasized that the multi-unit formulation allows for an adaptation of each probe drug dose by simply varying the number of mini-tablets contained within a capsule. Prior to administration, capsules can be opened to facilitate administration of mini-tablets to children or persons experiencing difficulties with swallowing.

4.4. In vivo study

The comparison of *in vivo* drug/metabolite ratios and the corresponding plasma concentration profiles (Fig. 4) shows similar ranges between the data obtained from the CombiCap trial and the data of the Basel Cocktail clinical studies. Despite the limited number of human volunteers (n = 3) participating in this pilot experiment and the resulting statistical variability, results are considered to be similar. Interestingly, the total error of the CombiCap formulation, despite significant difference in population size, is less in comparison with the commercial products. This can be explained by a uniform immediate release pattern of the CombiCap formulation; therefore, the time to C_{max} is more uniform and allows more precise assessment of the metabolic ratios. Such results indicate that the CombiCap can be implemented for future clinical studies, while allowing for a simplification of the clinical procedure and increased patient compliance, especially if the venous sampling can be substituted by dried blood spot or similar technologies (Donzelli et al., 2014).

5. Conclusion

New standards were defined for the design of cocktail formulations. The results of the experimental work suggest full coverage of the initially set study goals and fulfillment of the requirements on contemporary phenotyping formulations for different BCS classes of the Basel Cocktail drugs such as: sufficiently high drug load, separation of drugs from each other to exclude potential chemical degradation, the use of the same excipients in identical proportions for all drugs and applicability of the formulation to all BCS classes, age appropriate formulations, including persons with dysphagia, with identical release kinetics for all probe drugs, scalability to enable industrial production and the possibility of dose change or dose adaptation prior to application (multi-unit system).

The CombiCap formulation platform for phenotyping cocktails was developed and successfully validated using the Basel Cocktail composition. The performance of this formulation is confirmed by both *in vitro* and *in vivo* studies. The novel formulation concept is versatile, scalable and compatible with identified requirements for such formulations. This approach is novel and has, to our knowledge, never been proposed before. We therefore believe that our formulation strategy will be instrumental to facilitate and promote the use of patient phenotyping and the development of personalized medicines.

Conflict of interest

The authors have no conflict of interest that is directly relevant to the content of this article.

Acknowledgments

The authors thank Darryl Borland for editorial assistance, Carola Alampi for SEM pictures and Claudia Blasi for her assistance with *in vivo* studies.

References

Adedoyin, A., Frye, R.F., Mauro, K., Branch, R.A., 1998. Chloroquine modulation of specific metabolizing enzymes activities: investigation with selective five drug cocktail. Br. J. Clin. Pharmacol. 46, 215–219.

Aleksovski, A., Dreu, R., Gašperlin, M., Planinšek, O., 2015. Mini-tablets: a contemporary system for oral drug delivery in targeted patient groups. Expert Opin. Drug Deliv. 12, 65–84. doi:http://dx.doi.org/10.1517/17425247.2014.951633.

The Biopharmaceutics Classification System (BCS), 2016. Guidance [WWW Document]. URL http://www.fda.gov/AboutFDA/CentersOffices/OfficeofMedicalProductsandTobacco/CDER/ucm128219 (accessed 3.14.16.).

Blakey, G.E., Lockton, J.A., Perrett, J., Norwood, P., Russell, M., Aherne, Z., Plume, J., 2004. Pharmacokinetic and pharmacodynamic assessment of a five-probe metabolic cocktail for CYPs 1A2 3A4, 2C9, 2D6 and 2E1. Br. J. Clin. Pharmacol. 57, 162–169.

Bosilkovska, M., Clément, M., Dayer, P., Desmeules, J., Daali, Y., 2014. Incorporation of flurbiprofen in a 4-drug cytochrome P450 phenotyping cocktail. Basic Clin. Pharmacol. Toxicol. 115, 465–466. doi:http://dx.doi.org/10.1111/bcpt.12231.

Bosilkovska, M., Samer, C., Déglon, J., Thomas, A., Walder, B., Desmeules, J., Daali, Y., 2016. Evaluation of mutual drug–drug interaction within Geneva cocktail for cytochrome P450 phenotyping using innovative dried blood sampling method. Basic Clin. Pharmacol. Toxicol. doi:http://dx.doi.org/10.1111/bcpt.12586.

Bruce, M.A., Hall, S.D., Haehner-Daniels, B.D., Gorski, J.C., 2001. In vivo effect of clarithromycin on multiple cytochrome P450s. Drug Metab. Dispos. 29, 1023–1028.

Brynne, N., Böttiger, Y., Hallén, B., Bertilsson, L., 1999. Tolterodine does not affect the human in vivo metabolism of the probe drugs caffeine, debrisoquine and omeprazole. Br. J. Clin. Pharmacol. 47, 145–150.

Chainuvati, S., Nafziger, A.N., Leeder, J.S., Gaedigk, A., Kearns, G.L., Sellers, E., Zhang, Y., Kashuba, A.D.M., Rowland, E., Bertino, J.S., 2003. Combined phenotypic assessment of cytochrome p450 1A2, 2C9, 2C19, 2D6, and 3A, *N*-acetyltransferase-2, and xanthine oxidase activities with the "Cooperstown 5+1 cocktail. Clin. Pharmacol. Ther. 74, 437–447. doi:http://dx.doi.org/10.1016/S0009-9236(03)00229-7.

de Andrés, F., Sosa-Macías, M., Lazalde-Ramos, B.P., Naranjo, M.E.G., Tarazona-Santos, E., Llerena, A., 2013. CEIBA.FP Consortium of the Ibero-American Network of Pharmacogenetics and Pharmacogenomics RIBEFa, 2013. Evaluation of drug-metabolizing enzyme hydroxylation phenotypes in Hispanic populations: the CEIBA cocktail. Drug Metabol. Drug Interact. 28 (135) doi:http://dx.doi.org/10.1515/dmdi-2013-0020.

Derungs, A., Donzelli, M., Berger, B., Noppen, C., Krähenbühl, S., Haschke, M., 2015. Effects of cytochrome P450 inhibition and induction on the phenotyping metrics of the basel cocktail: a randomized crossover study. Clin. Pharmacokinet. 55 (1), 79–91. doi:http://dx.doi.org/10.1007/s40262-015-0294-y.

Dissolution Methods [WWW Document], 2015. US Food Drug Adm. Prot. Promot. Your Health. URL http://www.accessdata.fda.gov/scripts/cder/dissolution/dsp_getallData.cfm (accessed 2.24.16.).

Donzelli, M., Derungs, A., Serratore, M.-G., Noppen, C., Nezic, L., Krähenbühl, S., Haschke, M., 2014. The basel cocktail for simultaneous phenotyping of human cytochrome P450 isoforms in plasma, saliva and dried blood spots. Clin. Pharmacokinet. 53, 271–282. doi:http://dx.doi.org/10.1007/s40262-013-0115-0.

EDQM, 2012. European Pharmacopoeia, 7.6. ed. Council of Europe Strasbourg.

Eberle, V.A., Häring, A., Schoelkopf, J., Gane, P.A.C., Huwyler, J., Puchkov, M., 2015. In silico and in vitro methods to optimize the performance of experimental gastroretentive floating mini-tablets. Drug Dev. Ind. Pharm. 1–10. doi:http://dx.doi.org/10.3109/03639045.2015.1078350.

Engel, A., Oswald, S., Siegmund, W., Keiser, M., 2012. Pharmaceutical excipients influence the function of human uptake transporting proteins. Mol. Pharm. 9, 2577–2581. doi:http://dx.doi.org/10.1021/mp3001815.

Frye, R.F., Matzke, G.R., Adedoyin, A., Porter, J.A., Branch, R.A., 1997. Validation of the five-drug "Pittsburgh cocktail" approach for assessment of selective regulation of drug-metabolizing enzymes. Clin. Pharmacol. Ther. 62, 365–376. doi:http://dx.doi.org/10.1016/S0009-9236(97)90114-4.

Fuhr, U., Jetter, A., Kirchheiner, J., 2007. Appropriate phenotyping procedures for drug metabolizing enzymes and transporters in humans and their simultaneous use in the "cocktail" approach. Clin. Pharmacol. Ther. 81, 270–283. doi:http://dx.doi.org/10.1038/sj.clpt.6100050.

Fujicalin, 2009. The unique DCPA [WWW Document]The Unique DCPA [WWW Document]. URL http://www.fujicalin.com (accessed 2.22.16.).

Ghassabian, S., Murray, M., 2013. Simultaneous in vivo phenotyping of CYP enzymes. Methods Mol. Biol. Clifton NJ 987, 261–267. doi:http://dx.doi.org/10.1007/978-1-62703-321-3_22.

Ghassabian, S., Chetty, M., Tattam, B.N., Chem, M.C., Glen, J., Rahme, J., Stankovic, Z., Ramzan, I., Murray, M., McLachlan, A.J., 2009. A high-throughput assay using liquid chromatography-tandem mass spectrometry for simultaneous in vivo phenotyping of 5 major cytochrome p450 enzymes in patients. Ther. Drug Monit. 31, 239–246. doi:http://dx.doi.org/10.1097/FTD.0b013e318197e1bf.

Guidance for industry Dissolution testing if immediate release solid oral dosage forms, 1997.

Guideline on the investigation of bioequivalence, 2010

Guideline on pharmaceutical development of medicine for paediatric use, 2013

Habib, W.A., Alanizi, A.S., Abdelhamid, M.M., Alanizi, F.K., 2014. Accuracy of tablet splitting: comparison study between hand splitting and tablet cutter. Saudi Pharm. J. 22, 454–459. doi:http://dx.doi.org/10.1016/j.jsps.2013.12.014.

Ingelman-Sundberg, M., 2004. Human drug metabolising cytochrome P450 enzymes: properties and polymorphisms. Naunyn Schmiedebergs Arch. Pharmacol. 369, 89–104. doi:http://dx.doi.org/10.1007/s00210-003-0819-z.

Kakuda, T.N., Van Solingen-Ristea, R.M., Onkelinx, J., Stevens, T., Aharchi, F., De Smedt, G., Peeters, M., Leopold, L., Hoetelmans, R.M.W., 2014. The effect of single- and multiple-dose etravirine on a drug cocktail of representative cytochrome P450 probes and digoxin in healthy subjects. J. Clin. Pharmacol. 54, 422–431. doi:http://dx.doi.org/10.1002/jcph.214.

Kashuba, A.D., Nafziger, A.N., Kearns, G.L., Leeder, J.S., Gotschall, R., Rocci, M.L., Kulawy, R.W., Beck, D.J., Bertino, J.S., 1998. Effect of fluvoxamine therapy on the activities of CYP1A2, CYP2D6, and CYP3A as determined by phenotyping. Clin. Pharmacol. Ther. 64, 257–268. doi:http://dx.doi.org/10.1016/S0009-9236(98)90174-6.

Krösser, S., Neugebauer, R., Dolgos, H., Fluck, M., Rost, K.-L., Kovar, A., 2006. Investigation of sarizotan's impact on the pharmacokinetics of probe drugs for major cytochrome P450 isoenzymes: a combined cocktail trial. Eur. J. Clin. Pharmacol. 62, 277–284. doi:http://dx.doi.org/10.1007/s00228-006-0101-7.

Leuenberger, H., Plitzko, M., Puchkov, M., 2006. Spray freeze drying in a fluidized bed at normal and low pressure. Dry. Technol. 24, 711–719. doi:http://dx.doi.org/10.1080/07373930600684932.

Liu, F., Ranmal, S., Batchelor, H.K., Orlu-Gul, M., Ernest, T.B., Thomas, I.W., Flanagan, T., Tuleu, C., 2014. Patient-centred pharmaceutical design to improve acceptability of medicines: similarities and differences in paediatric and geriatric populations. Drugs 74, 1871–1889. doi:http://dx.doi.org/10.1007/s40265-014-0297-2.

Murray, M., 2006. Role of CYP pharmacogenetics and drug–drug interactions in the efficacy and safety of atypical and other antipsychotic agents. J. Pharm. Pharmacol. 58, 871–885. doi:http://dx.doi.org/10.1211/jpp.58.7.0001.

Nguyen, T.T., Bénech, H., Delaforge, M., Lenuzza, N., 2016. Design optimisation for pharmacokinetic modeling of a cocktail of phenotyping drugs. Pharm. Stat. 15, 165–177. doi:http://dx.doi.org/10.1002/pst.1731.

Pedersen, R.S., Damkier, P., Christensen, M.M.H., Brosen, K., 2013. A cytochrome P450 phenotyping cocktail causing unexpected adverse reactions in female volunteers. Eur. J. Clin. Pharmacol. 69, 1997–1999. doi:http://dx.doi.org/10.1007/s00228-013-1561-1.

Preisig, D., Haid, D., Varum, F.J.O., Bravo, R., Alles, R., Huwyler, J., Puchkov, M., 2014. Drug loading into porous calcium carbonate microparticles by solvent evaporation. Eur. J. Pharm. Biopharm. 87, 548–558. doi:http://dx.doi.org/10.1016/j.ejpb.2014.02.009.

Preissner, S.C., Hoffmann, M.F., Preissner, R., Dunkel, M., Gewiess, A., Preissner, S., 2013. Polymorphic cytochrome P450 enzymes (CYPs) and their role in personalized therapy. PLoS One 8, e82562. doi:http://dx.doi.org/10.1371/journal.pone.0082562.

Strub, Robert, McKim, A.S., 2008. Dimethyl sulfoxide USP, PhEur in approved pharmaceutical products and medical devices. Pharm. Technol. 32.

Ryu, J.Y., Song, I.S., Sunwoo, Y.E., Shon, J.H., Liu, K.H., Cha, I.J., Shin, J.G., 2007. Development of the "Inje cocktail" for high-throughput evaluation of five human cytochrome P450 isoforms in vivo. Clin. Pharmacol. Ther. 82, 531–540. doi:http://dx.doi.org/10.1038/sj.clpt.6100187.

Sharma, A., Pilote, S., Bélanger, P.M., Arsenault, M., Hamelin, B.A., 2004. A convenient five-drug cocktail for the assessment of major drug metabolizing enzymes: a pilot study. Br. J. Clin. Pharmacol. 58, 288–297. doi:http://dx.doi.org/10.1111/j.1365-2125.2004.02162.x.

Spaggiari, D., Geiser, L., Daali, Y., Rudaz, S., 2014. A cocktail approach for assessing the in vitro activity of human cytochrome P450s: an overview of current methodologies. J. Pharm. Biomed. Anal. JPBA Reviews 2014 (101), 221–237. doi:http://dx.doi.org/10.1016/j.jpba.2014.03.018.

Stegemann, S., Ecker, F., Maio, M., Kraahs, P., Wohlfart, R., Breitkreutz, J., Zimmer, A., Bar-Shalom, D., Hettrich, P., Broegmann, B., 2010. Geriatric drug therapy: neglecting the inevitable majority. Ageing Res. Rev. 9, 384–398. doi:http://dx.doi.org/10.1016/j.arr.2010.04.005.

Stegemann, S., Gosch, M., Breitkreutz, J., 2012. Swallowing dysfunction and dysphagia is an unrecognized challenge for oral drug therapy. Int. J. Pharm. 430, 197–206. doi:http://dx.doi.org/10.1016/j.ijpharm.2012.04.022.

Tanaka, E., Kurata, N., Yasuhara, H., 2003. How useful is the "cocktail approach" for evaluating human hepatic drug metabolizing capacity using cytochrome P450 phenotyping probes in vivo? J. Clin. Pharm. Ther. 28, 157–165. doi:http://dx.doi.org/10.1046/j.1365-2710.2003.00486.x.

Tennezé, L., Verstuyft, C., Becquemont, L., Poirier, M., Wilkinson, G.R., Funck-Brentano, C., 1999. Assessment of CYP2D6 and CYP2C19 activity in vivo in humans: a cocktail study with dextromethorphan and chloroguanide alone and in combination. Clin. Pharmacol. Ther. 66, 582–588. doi:http://dx.doi.org/10.1053/cp.1999.v66.103401001.

Thomson, S.A., Tuleu, C., Wong, I.C.K., Keady, S., Pitt, K.G., Sutcliffe, A.G., 2009. Minitablets: new modality to deliver medicines to preschool-aged children. Pediatrics 123, e235–e238. doi:http://dx.doi.org/10.1542/peds.2008-2059.

Tomalik-Scharte, D., Jetter, A., Kinzig-Schippers, M., Skott, A., Sörgel, F., Klaassen, T., Kasel, D., Harlfinger, S., Doroshyenko, O., Frank, D., Kirchheiner, J., Bräter, M., Richter, K., Gramatté, T., Fuhr, U., 2005. Effect of propiverine on cytochrome P450 enzymes: a cocktail interaction study in healthy volunteers. Drug Metab. Dispos. 33, 1859–1866. doi:http://dx.doi.org/10.1124/dmd.105.005272.

Tracy, T.S., Chaudhry, A.S., Prasad, B., Thummel, K.E., Schuetz, E.G., Zhong, X., Tien, Y.-C., Jeong, H., Pan, X., Shireman, L.M., Tay-Sontheimer, J., Lin, Y.S., 2016. Interindividual variability in cytochrome P450-mediated drug metabolism. Drug Metab. Dispos. 44, 343–351. doi:http://dx.doi.org/10.1124/dmd.115.067900.

United States Pharmacopeia Convention, 2007. United States Pharmacopeia nd National Formulary (USP 30-NF 25). United States Pharmacopeia Convention Rockville, MD.

van Riet-Nales, D.A., Römkens, E.G.A.W., Saint-Raymond, A., Kozarewicz, P., Schobben, A.F.A.M., Egberts, T.C.G., Rademaker, C.M.A., 2014. Oral medicines for children in the European paediatric investigation plans. PLoS One 9 doi:http://dx.doi.org/10.1371/journal.pone.0098348.

Wilkinson, G.R., 2005. Drug metabolism and variability among patients in drug response. N. Engl. J. Med. 352, 2211–2221. doi:http://dx.doi.org/10.1056/NEJMra032424.

Wu, C.-Y., Benet, L.Z., 2005. Predicting drug disposition via application of BCS: transport/absorption/elimination interplay and development of a biopharmaceutics drug disposition classification system. Pharm. Res. 22, 11–23.

Zgheib, N.K., Frye, R.F., Tracy, T.S., Romkes, M., Branch, R.A., 2006. Validation of incorporating flurbiprofen into the Pittsburgh cocktail. Clin. Pharmacol. Ther. 80, 257–263. doi:http://dx.doi.org/10.1016/j.clpt.2006.06.005.

Zhu, B., Ou-Yang, D.S., Chen, X.P., Huang, S.L., Tan, Z.R., He, N., Zhou, H.H., 2001. Assessment of cytochrome P450 activity by a five-drug cocktail approach. Clin. Pharmacol. Ther. 70, 455–461.

4 DISCUSSION

4.1 Importance of diagnosis and diagnostic products

Diagnostic products are powerful tools that are used to reveal a particular health condition and help physicians in their diagnosis, in order to personalize the treatment to the patient. Diagnosis is often generalized and tends to standardize the diseases and the patients, which may lead to adverse effects that can be fatal in some cases. Despite their added value, only a few diagnostic products are commercialized. The development of *in vitro* or *in vivo* diagnostic products is left aside at the expense of therapeutic products. In chapter 3, we attempted to overcome this lack with the formulation of 2 types of diagnostic products; the nanoparticles for cellular imaging and the microparticles for phenotyping.

The development of a diagnostic product must combine several features to lead to a good quality product. It should be safe, reliable, specific, customizable, easy to formulate, and easy to use. In this chapter, we will discuss how our 2 diagnostic products fulfill these conditions and how they can be used in the objective of personalized medicine.

4.2 Input of nanoparticles in diagnosis

Nanodiagnostic products are mostly used for imaging purposes. In the introduction, we gave an overview of nanoparticles that can be used either for MRI, X-rays, fluorescence microscopy, SPECT, or PET. Among these nanoparticles, the QDs are valuable as highly fluorescent nanocrystals. Their optical properties are interesting and present many advantages such as a very low photobleaching, a tunable color depending on the size of the QD, and a long and bright fluorescent lifetime. However, the toxicity of the semiconductor core limits the use of QDs in cellular imaging.

In chapter 3, we described how we formulated PDMS-PMOXA polymersomes to isolate the QDs from the cells to prevent any risk of toxicity. The challenge was to encapsulate the QDs in the core of the polymersome without altering their imaging properties. The product is now safe and non-toxic as shown by the result of the MTT assay (Figure 4 in part 3.1). The stability data over weeks, months and even year demonstrated the cohesion of the polymer double layer, preventing the escape of the QDs from the core of the polymersomes, and proving the reliability

of the product. The advantage of the polymersomes is their synthetic aspect and the possibility to tune their membrane by diversifying the polymers and their assembling process, to modify the properties of the vesicles and improve their biocompatibility as well as their circulation time *in vivo*. Polymersomes are easy to formulate and do not need long and complicated procedures to be prepared. A simple film rehydration method followed by several extrusions to homogenize the size of the vesicles are the only needed steps. The loading of imaging probes is as simple because they can be added directly in the rehydration medium. Depending on their affinity to water, the probes can be included either inside the hydrophobic membrane, or in the hydrophilic core of the PDMA-PMOXA polymersomes.

The polymersomes containing QDs are easy to use. A fluorescence microscope is sufficient for their visualization during *in vitro* cellular imaging. Concerning *in vivo* imaging, Michalet et al., demonstrated that the QDs are still visible through the skin of mice. The visualization of the QDs was done by microPET and fluorescence (151). In our case, the PDMS-PMOXA polymersomes were visualized by fluorescence microscopy. They could be internalized by HepG2 cells by passive targeting and forced intake. However, to get a more precise image of the cells of interest, it is possible to functionalize the bloc copolymers with several ligands and achieve a specific and active targeting (152–154).

The vesicular structure of the polymersomes offers further opportunities in the view of personalized medicine. Indeed, the polymeric composition of the vesicle gives the possibility to include hydrophobic molecules within the membrane, as well as hydrophilic molecules in the polymersome cavity. Thus, it is possible to load a drug and an imaging probe in a single polymersome. Alibolandi et al. developed a folate receptor-targeted polymersome containing QDs and doxorubicin for the simultaneous imaging and treatment of breast adenocarcinoma. They studied the effect *in vitro* and *in vivo* on mice and could visualize the cancer cells by fluorescence microscopy. They were able to prove the inhibitory effect of the folate on the tumor besides the good therapeutic efficiency of the targeted polymersomes over the non-targeted ones and over the free doxorubicin (155). This combination of diagnostic and therapeutic applications is called thera(g)nostics, and will be increasingly developed in the

future, for personalized medicine (132). The novelty of this topic has not yet enable the scientists to decide between the 2 spellings: theranostics and theragnostics. Both words can be find in search engines.

As mentioned in the introduction, nanoparticules can also be used as labels in immunoassays to display the result of the test. The example of lateral flow assays is interesting because they are very easy to use as they just need to be soaked with a liquid sample. The nanolabels that are immobilized on the test migrate by capillarity, react with the test sample, and produce a visible signal to indicate the result. Only few drops of urine, saliva or tears are enough to give a fast and reliable result. The lecture of the test can be done without requiring any analysis equipment and thus can be performed at a point of care. These types of tests can be adapted for the diagnosis of various health conditions like pregnancy, infections, or diabetes. They can be improved with a digital lecture window to eliminate any doubt as to the result of the test. They can even be connected to a smartphone application, allowing a better monitoring of the results in the case of a disease requiring a regular follow-up (15). For now, the results remain only qualitative but research is done on other types of labeling nanoparticles and other detection methods to improve LFAs to provide quantitative results. The characteristics of the LFAs let us imagine many ways to use these diagnostics products in the future. For instance, in the detection of molecules like the biomarkers that are used in cancer diagnosis.

4.3 Input of microparticulate diagnostic products

Microparticulate diagnostic products are more well-known than nanodiagnostics because they are commonly used in diagnostic tests, contrast imaging, and radiopharmaceutics, to get a more accurate diagnosis. But a precise diagnosis is pointless if the patient does not respond correctly to the treatment.

Indeed, there is a big inter-individual variability of the different CYP isoforms and thus a difference in the capacity on the patients to metabolize certain drugs. To predict the behavior of the patient towards a drug and personalize his treatment, it is important to determine the activity of his CYPs. This determination is called phenotyping, and is performed with a cocktail of probe drugs that are metabolized by defined CYPs. Even that many research

groups tried to develop their own phenotyping cocktail, there is a lack of clinically tested examples to phenotype the patients prior to the assignment of a therapy. The Basel cocktail was developed in this intention at the University hospital of Basel, and is composed of 6 different drugs: caffeine, efavirenz, flurbiprofen, metoprolol, midazolam, and omeprazole.

Among all phenotyping cocktails described in the literature, none of them has a dedicated formulation. The CombiCap, that is presented in chapter 3, fulfills this gap for the Basel cocktail, with a formulation platform presenting many advantages compared to the actual way of dispensing cocktails.

The CombiCap can be considered as a diagnostic product because it is used to deepen the knowledge on the patient health condition by the determination of his phenotype. It is a safe product because we used the minimum detectable dose of each drug, enabling to achieve the diagnostic objectives while limiting the therapeutic effects. It is reliable since the standardized formulation reduces the interaction of the excipients. The reliability of the product also rests on the comparative *in vitro* and *in vivo* results that showed the equivalence of the CombiCap to the 6 individual marketed drugs. The stability of the product is also guaranteed by the multiparticulate formulation (mini-tablets) that permits the physicochemical separation of the 6 different active ingredients. The CombiCap is easy to formulate because the active ingredients are simply dissolved in an adequate solvent and loaded in the pores of the excipient (Fujicalin®). The critical step is the drying of the blend under vacuum, to evaporate the remaining solvent. An insufficient drying can lead to poor flowability of the blend and difficulties to press the mini-tablets. It is possible to customize the CombiCap for the needs of a phenotyping study, by specifically adapting the dosage and the composition of the cocktail simply, by adding or removing some mini-tablets. And finally, the CombiCap is easy to use because it is an oral medication. It improves the compliance of the patient with a single dosage form (compared to 6 in the first studies on the Basel cocktail). The small size of the mini-tablets give the possibility for children and elderly to swallow the content of the capsule in several intakes if they have difficulties with the hard gelatin capsule.

Unlike the genotype that remains the same throughout life, the phenotype can vary depending on the living conditions. Therefore, it would be necessary to

re-determine the phenotype several times during the patient's life. The Combi Cap could be given at every hospital admission, or in the case of a disease involving a complex medical care with multiple medications leading to drug-drug interactions. Thus, the physician would be able to personalize a medical treatment by prescribing drugs and doses adapted to the metabolism of the patient, at every stage of his life.

4.4 Companion diagnostics

Companion diagnostics are *in vitro* diagnostic tests that are developed in parallel of the therapeutic molecule to provide essential information in order to optimize the safety of a treatment and determine its applicability to the patient (129). They are powerful tools in the domain of diagnosis and are essentially based on the detection of specific mutations that are found in some cancers.

As presented in paragraph 1.4.2, only a limited number of companion diagnostics are approved by the FDA, mainly in the domain of oncology, and they rely on biomarkers as diagnostic products, but new therapeutic areas are emerging. With the increasing number of drugs that specifically target cells or tissues, pharmaceutical companies realized that companion diagnostics can boost the success of their medications. Companion diagnostics can also be a great help in the selection of the candidates for clinical trials, which decreases the costs of research, and achieve a faster time to market of the drug (157). In this context, it is probable that more companion diagnostics will be developed in the coming years. Table 2 shows some current facts about companion diagnostics and let figure the trend for the future. It is obvious that the need of new companion diagnostics is important and that they should be increasingly developed in the years to come.

Table 2: Current facts about companion diagnostics. Source: www.genengnews.com

Diagnostic facts	
1 %	of marketed drugs have a companion diagnostic
10 %	of marketed drugs recommend genetic testing for optimal treatment
30 %	of all treatments in late clinical development rely on biomarker data
60 %	of all treatments in preclinical development rely on biomarker data
50 %	of clinical trials collect DNA from patients to aid in biomarker development

As mentioned above, the companion diagnostics are developed in combination with therapeutic molecules to ensure a safe and optimized treatment based on the information obtained on the patient's genetic profile. A parallel can be made with phenotyping cocktails, that are used to determine the patient's metabolism regarding drugs and therefore personalize and optimize the medical treatments. In this circumstances, we can consider the phenotyping as a companion diagnostic test that requires phenotyping cocktails as diagnostic products.

Generally speaking, diagnostic products can be assimilated to companion diagnostics because they fit to the description that is given in 1.4.2. Indeed, they can be used either for the screening or the identification of genetic and phenotypic markers; and they can monitor the effectiveness and the dosing of a therapy.

4.5 Personalized medicine, the future of medical practice

Diagnosis and diagnostic products that have been discussed previously are unavoidable in the instigation of personalized medicine. This relatively new discipline gives the potential to customize medical care in order to obtain the best response to a drug treatment, while increasing the safety of the patient. Indeed, personalized therapy implies the specific design of a medical treatment that is compatible with the phenotype of each individual patient.

However, it should be noted that personalized medicine is not intended to produce unique medications for every patient. The idea is rather based on the classification of the patients suffering from a specific disease, into sub-populations, depending on their phenotype and their predisposition to respond to the treatment. In the end, the objective is to optimize the effectiveness of the treatment by adjusting the dose, and to minimize the drug toxicity by selecting the appropriate therapeutic molecules (158).

Personalized medicine has many advantages and is a great advance in the therapeutic field. In-depth knowledge of the patient health condition reduces the prescriptions errors and the prescription of ineffective medications. Thus, owing

to less drug side effects, the adherence of the patient to the treatment is increased, and his life quality is improved. From a financial point of view, the development costs of a drug can be reduced with the possibility to pre-select the volunteers and the patients for the clinical trials. Personalized medicine can also optimize the overall cost of health care due to the individualization of the treatments that limits the prescription of unnecessary drugs and thereby, their reimbursement by health insurance.

The research interest on personalized medicine has exponentially increased as shown in Figure 8. Within 30 years, the number of articles dealing with personalized medicine rose from 12 to over 6000 references, representing a 500-fold increase. Based on this results, we can predict an escalation of the research on the topic of personalized medicine, and consequently an increased interest on the development of diagnostic products to precise the diagnosis. The 21st century brought us in a new medical era, where the trend is on personalization of therapies to provide the right drug, at the right dose to the right patient.

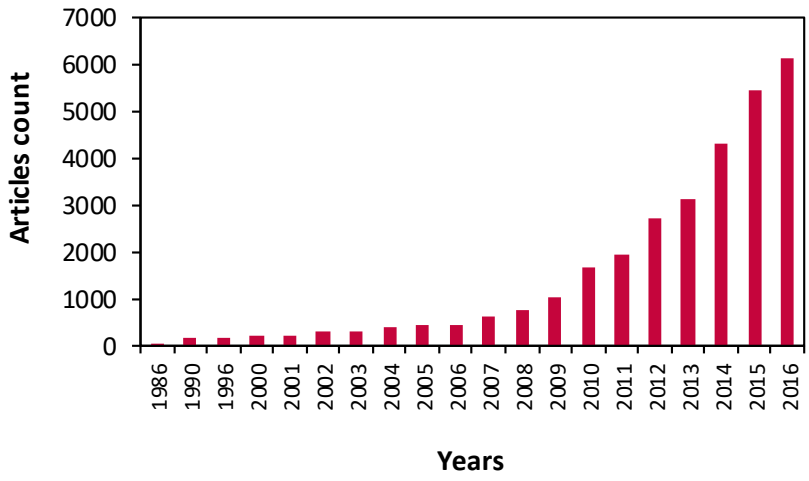

Figure 8: Number of articles referencing the personalized medicine from 1986 to 2016.

Source PubMed.

5 CONCLUSION AND OUTLOOK

Diagnosis is an ancestral medical practice that has undergone a very sharp evolution from the ancient Egypt to the present day. Huge advances have been done in this filed since the 20th century. Particularly, the progress in technology and the development of diagnostic products brought an additional source of information to help determine the health condition of a person, and prescribe the indicated medical treatment.

Diagnostics products are used in the sampling and the analysis of body elements to assist the early diagnosis of a disease or a disorder. The precision of the diagnosis is essential for the personalization of the therapies and for an improved medical care. Personalized medicine brings a safe and optimal therapy to patients, while preventing potential drugs side effects. It also reduces the time and costs of clinical trials with the possibility to better select the candidates. It helps to manage a disease from early detection to a response-guided medication. For this application, proper and accurate diagnostic tools are indispensable. However, the supply of diagnostic products is rather low and does not meet the growing demand for a more accurate diagnosis. We attempted to satisfy this lack with the 2 diagnostic products that are presented in the chapter 3.

5.1 Particulate material in diagnostics

The first diagnostic product we described is the PDMS-PMOXA polymersome. Polymersomes are very interesting tools for diagnosis because their tunable properties and their loading capacities, make them ideal tools for isolating QDs or other imaging probes, from the external environment. The strong stability of the polymeric membrane does not allow the release of the polymersome content over weeks. Thus, the encapsulation inside the core of the vesicle limits the toxic effect of the QDs towards the cells.

We assert that polymersomes containing QDs can be used in imaging for diagnostic purpose because they meet all the previously defined requirements for the diagnostic products. The physicochemical characteristics of the polymersomes are also interesting for thera(g)nostics. The polymersomes could be used as carriers, incorporating a drug and a screening agent, to monitor the delivery of the drug at the right site. To achieve this goal, 2 modifications of the PDMS-PMOXA di-bloc copolymer would be necessary. First, the addition of a

linker with a targeting agent to spot the receptors. Second, the insertion of a channel or a spacer is necessary to allow the diffusion of the drug trough the polymeric vesicle, because of the superior stability of the PDMS-PMOXA membrane.

The second diagnostic product we formulated is the CombiCap. This unique formulation concept simplifies the phenotyping procedures. Indeed, all 6 probe drugs of the phenotyping cocktail are formulated according to a standardized formula, leading to identical pharmacokinetic profiles of the drugs. The dose of each drug was carefully selected and minimized to stick to the diagnostic purpose, without inducing therapeutic effects. The phenotyping data obtained with the CombiCap were equivalent to those obtained with the individual probe drugs, proving the reliability of our formulation. The formulation platform we developed for the Basel cocktail can also be applied to other phenotyping cocktails, due to the versatility of the formula and of the manufacturing process of the CombiCap. Hence, it is possible to increase the knowledge about CYP activity and the metabolizer type of each person, to determine the best therapeutic option in case of a therapy. Other types of cocktails could also be developed for other metabolic enzymes like the glucuronyl-transferase that is involved in the metabolism of deferasirox, the companion diagnostic of FerriScan® (159).

The polymersomes and the CombiCap are 2 different particulate products that are safe, reliable, specific, customizable, easy to formulate and easy to use. We formulated them in the objective of developing new diagnostic tools, to make personalized medicine accessible to everyone.

5.2 What is the future of medicine?

The concept of “one drug fits all”, taking account of large patient populations belongs to the past. The personalized medicine represents the future and holds promise for improving health care, by enabling each patient to receive earlier diagnosis, risk assessment and optimal treatment. The clear increase of the research articles involving personalized medicine confirms the importance of the individualization of diagnostic procedures with the help of diagnostic products to achieve a better treatment of the patient.

Phenotyping cocktails and companion diagnostics deserve to be more considered and developed by pharmaceutical industries because they provide essential information on the use and on the utility of drugs. They are particularly useful in the case of serious diseases such as cancer, but also HIV, rheumatoid arthritis, or hepatitis C. The input they provide is huge and increases the knowledge about the disease and the patient. But such diagnostic products remain an exception and only a few drugs have a companion diagnostic product. The expectation for the future is to provide a companion diagnostic for every drug therapy. Phenotyping is as well of a great interest because it allows to anticipate the behavior of a patient regarding certain drugs, and thus, favors the prescription of a medical treatment while avoiding side effects.

In few decades, personalized diagnosis and treatment will be a common practice in the field of medicine. The determination of the phenotype will become a standard procedure integrated to every diagnosis. It could be performed upon the admission of a patient at the hospital and in case of a treatment involving a multi-therapy. The phenotyping could also be performed at a point of care, using LFAs for the detection of the metabolic ratios. Some attempts were done to facilitate the analysis procedure of phenotyping with breath tests, but no evidence was pointed out for the usefulness of this method (156).

Furthermore, nanoparticles and microparticles might be combined in a single diagnosis process. For instance; in parallel of writing the medical prescription, the doctor would add a phenotyping cocktail dosage form, as the companion diagnostic of the treatment. One hour after the ingestion of the cocktail, the patient uses a lateral flow assay that indicates his metabolizer type within minutes. He brings this diagnostic test to the pharmacist, who will be able to deliver the appropriate treatment based on the phenotyping results. The monitoring of the therapy would be then done by targeted thera(g)nostic nanoparticles containing an imaging probe, to control the drug release to the appropriate cellular tissue.

6 BIBLIOGRAPHY

1. Definition of diagnosis. In: Oxford dictionary [Internet]. [cited 2016 Jun 22]. Available from: http://www.oxforddictionaries.com/definition/english/diagnosis

2. Summerton N. Making a diagnosis in primary care: symptoms and context. Br J Gen Pract. 2004 Aug 1;54(505):570–1.

3. GUIDELINE FOR THE MANUFACTURE OF IN VITRO DIAGNOSTIC PRODUCTS [Internet]. 1994 [cited 2016 Apr 14]. Available from: http://fda.complianceexpert.com/agency-documents/medical-device-guidance/fda-guidelines/guideline-for-the-manufacture-of-in-vitro-diagnostic-products-1.94060

4. van Middendorp JJ, Sanchez GM, Burridge AL. The Edwin Smith papyrus: a clinical reappraisal of the oldest known document on spinal injuries. Eur Spine J Off Publ Eur Spine Soc Eur Spinal Deform Soc Eur Sect Cerv Spine Res Soc. 2010 Nov;19(11):1815–23.

5. Fournier A. Diagnosing Diabetes. J Gen Intern Med. 2000 Aug;15(8):603–4.

6. Berger D. A brief history of medical diagnosis and the birth of the clinical laboratory. Part 1--Ancient times through the 19th century. MLO Med Lab Obs. 1999 Jul;31(7):28–30, 32, 34–40.

7. Luiggi C. The Pee-in-a-Cup Test, circa 1500. The Scientist Magazine® [Internet]. 2010 Nov [cited 2016 Jun 30];24(11). Available from: http://www.the-scientist.com/?articles.view/articleNo/29345/title/The-Pee-in-a-Cup-Test--circa-1500/

8. Magiorkinis E, Diamantis A. The fascinating story of urine examination: From uroscopy to the era of microscopy and beyond. Diagn Cytopathol. 2015 Dec;43(12):1020–36.

9. Henry's clinical diagnosis and management by laboratory methods - NLM Catalog - NCBI [Internet]. [cited 2016 Jun 22]. Available from: http://www.ncbi.nlm.nih.gov/nlmcatalog/101674690

10. Technology and medicine [Internet]. [cited 2016 Nov 6]. Available from: http://www.sciencemuseum.org.uk/broughttolife/themes/technologies

11. Opacic T, Paefgen V, Lammers T, Kiessling F. Status and trends in the development of clinical diagnostic agents. Wiley Interdiscip Rev Nanomed Nanobiotechnol. :n/a-n/a.

12. Personalized Medicine Coalition - Precision Medicine Advocacy and Education [Internet]. [cited 2016 Nov 6]. Available from: http://www.personalizedmedicinecoalition.org/

13. Jain KK. Nanodiagnostics: application of nanotechnology in molecular diagnostics. Expert Rev Mol Diagn. 2003 Mar;3(2):153–61.

14. Nune SK, Gunda P, Thallapally PK, Lin Y-Y, Forrest ML, Berkland CJ. Nanoparticles for biomedical imaging. Expert Opin Drug Deliv. 2009 Nov;6(11):1175–94.

15. Quesada-González D, Merkoçi A. Nanoparticle-based lateral flow biosensors. Biosens Bioelectron. 2015 Nov 15;73:47–63.

16. Jain KK. Nanotechnology in clinical laboratory diagnostics. Clin Chim Acta. 2005 Aug;358(1–2):37–54.

17. Key J, Leary JF. Nanoparticles for multimodal in vivo imaging in

nanomedicine. Int J Nanomedicine. 2014;9:711–26.

18. Cormode DP, Skajaa T, Fayad ZA, Mulder WJM. Nanotechnology in medical imaging: probe design and applications. Arterioscler Thromb Vasc Biol. 2009 Jul;29(7):992–1000.

19. Baetke SC, Lammers T, Kiessling F. Applications of nanoparticles for diagnosis and therapy of cancer. Br J Radiol. 2015 Oct;88(1054):20150207.

20. Bernsen MR, Guenoun J, van Tiel ST, Krestin GP. Nanoparticles and clinically applicable cell tracking. Br J Radiol. 2015 Oct;88(1054):20150375.

21. Kiessling F, Mertens ME, Grimm J, Lammers T. Nanoparticles for Imaging: Top or Flop? Radiology. 2014 Oct;273(1):10–28.

22. Bashir MR, Bhatti L, Marin D, Nelson RC. Emerging applications for ferumoxytol as a contrast agent in MRI. J Magn Reson Imaging JMRI. 2015 Apr;41(4):884–98.

23. Scheidler J, Heuck AF, Meier W, Reiser MF. MRI of pelvic masses: efficacy of the rectal superparamagnetic contrast agent Ferumoxsil. J Magn Reson Imaging JMRI. 1997 Dec;7(6):1027–32.

24. Rosen JE, Chan L, Shieh D-B, Gu FX. Iron oxide nanoparticles for targeted cancer imaging and diagnostics. Nanomedicine Nanotechnol Biol Med. 2012 Apr;8(3):275–90.

25. Hernandez-Pedro NY, Pineda B, Rangel-Lopez E, Magana-Maldonado R, Perez de la Cruz V, Santamaia del Angel A, et al. Application of Nanoparticles on Diagnosis and Therapy in Gliomas, Application of Nanoparticles on Diagnosis and Therapy in Gliomas. BioMed Res Int BioMed Res Int. 2013 Apr 18;2013, 2013:e351031.

26. Boraschi P, Braccini G, Gigoni R, Cartei F, Perri G. MR enteroclysis using iron oxide particles (ferristene) as an endoluminal contrast agent: an open phase III trial. Magn Reson Imaging. 2004 Oct;22(8):1085–95.

27. Reimer P, Balzer T. Ferucarbotran (Resovist): a new clinically approved RES-specific contrast agent for contrast-enhanced MRI of the liver: properties, clinical development, and applications. Eur Radiol. 2003 Jun;13(6):1266–76.

28. Fu T, Kong Q, Sheng H, Gao L. Value of Functionalized Superparamagnetic Iron Oxide Nanoparticles in the Diagnosis and Treatment of Acute Temporal Lobe Epilepsy on MRI. Neural Plast. 2016;2016:2412958.

29. Wan X, Song Y, Song N, Li J, Yang L, Li Y, et al. The preliminary study of immune superparamagnetic iron oxide nanoparticles for the detection of lung cancer in magnetic resonance imaging. Carbohydr Res. 2016 Jan;419:33–40.

30. Resch-Genger U, Grabolle M, Cavaliere-Jaricot S, Nitschke R, Nann T. Quantum dots versus organic dyes as fluorescent labels. Nat Methods. 2008 Sep;5(9):763–75.

31. Bilan R, Nabiev I, Sukhanova A. Quantum Dot-Based Nanotools for Bioimaging, Diagnostics, and Drug Delivery. Chembiochem Eur J Chem Biol. 2016 Aug 18;

32. Panagiotopoulou M, Salinas Y, Beyazit S, Kunath S, Duma L, Prost E, et al. Molecularly Imprinted Polymer Coated Quantum Dots for Multiplexed Cell Targeting and Imaging. Angew Chem Int Ed Engl. 2016 May 30;

33. Hardman R. A toxicologic review of quantum dots: toxicity depends on physicochemical and environmental factors. Environ Health Perspect. 2006 Feb;114(2):165–72.

34. Camblin M, Detampel P, Kettiger H, Wu D, Balasubramanian V, Huwyler J. Polymersomes containing quantum dots for cellular imaging. Int J Nanomedicine. 2014;9:2287–98.

35. Hainfeld JF, Slatkin DN, Focella TM, Smilowitz HM. Gold nanoparticles: a new X-ray contrast agent. Br J Radiol. 2006 Mar 1;79(939):248–53.

36. Kim D, Park S, Lee JH, Jeong YY, Jon S. Antibiofouling polymer-coated gold nanoparticles as a contrast agent for in vivo X-ray computed tomography imaging. J Am Chem Soc. 2007 Jun 20;129(24):7661–5.

37. Botchway SW, Coulter JA, Currell FJ. Imaging intracellular and systemic in vivo gold nanoparticles to enhance radiotherapy. Br J Radiol. 2015 Oct;88(1054):20150170.

38. Petersen AL, Hansen AE, Gabizon A, Andresen TL. Liposome imaging agents in personalized medicine. Adv Drug Deliv Rev. 2012 Oct;64(13):1417–35.

39. Jensen GM, Bunch TH. Conventional liposome performance and evaluation: lessons from the development of Vescan. J Liposome Res. 2007;17(3–4):121–37.

40. Ito K, Hamamichi S, Asano M, Hori Y, Matsui J, Iwata M, et al. Radiolabeled liposome imaging determines an indication for liposomal anticancer agent in ovarian cancer mouse xenograft models. Cancer Sci. 2016 Jan;107(1):60–7.

41. Tanifum EA, Ghaghada K, Vollert C, Head E, Eriksen JL, Annapragada A. A Novel Liposomal Nanoparticle for the Imaging of Amyloid Plaque by Magnetic Resonance Imaging. J Alzheimers Dis JAD. 2016 Mar 25;52(2):731–45.

42. Richardson VJ, Jeyasingh K, Jewkes RF, Ryman BE, Tattersall MH. Properties of [99mTc] technetium-labelled liposomes in normal and tumour-bearing rats. Biochem Soc Trans. 1977;5(1):290–1.

43. Proffitt RT, Williams LE, Presant CA, Tin GW, Uliana JA, Gamble RC, et al. Tumor-imaging potential of liposomes loaded with In-111-NTA: biodistribution in mice. J Nucl Med Off Publ Soc Nucl Med. 1983 Jan;24(1):45–51.

44. Henderson K, Stewart J. A dipstick immunoassay to rapidly measure serum oestrone sulfate concentrations in horses. Reprod Fertil Dev. 2000;12(3–4):183–9.

45. Tanaka R, Yuhi T, Nagatani N, Endo T, Kerman K, Takamura Y, et al. A novel enhancement assay for immunochromatographic test strips using gold nanoparticles. Anal Bioanal Chem. 2006 Aug;385(8):1414–20.

46. Ahn JS, Choi S, Jang SH, Chang HJ, Kim JH, Nahm KB, et al. Development of a point-of-care assay system for high-sensitivity C-reactive protein in whole blood. Clin Chim Acta Int J Clin Chem. 2003 Jun;332(1–2):51–9.

47. Lou SC, Patel C, Ching S, Gordon J. One-step competitive immunochromatographic assay for semiquantitative determination of lipoprotein(a) in plasma. Clin Chem. 1993 Apr;39(4):619–24.

48. Wittfooth S, Qin Q-P, Lund J, Tierala I, Pulkki K, Takalo H, et al. Immunofluorometric point-of-care assays for the detection of acute coronary

syndrome-related noncomplexed pregnancy-associated plasma protein A. Clin Chem. 2006 Sep;52(9):1794–801.

49. Abitbol CL, Chandar J, Onder AM, Nwobi O, Montané B, Zilleruelo G. Profiling proteinuria in pediatric patients. Pediatr Nephrol Berl Ger. 2006 Jul;21(7):995–1002.

50. Cho JH, Paek SH. Semiquantitative, bar code version of immunochromatographic assay system for human serum albumin as model analyte. Biotechnol Bioeng. 2001 Dec 20;75(6):725–32.

51. Choi S, Choi EY, Kim DJ, Kim JH, Kim TS, Oh SW. A rapid, simple measurement of human albumin in whole blood using a fluorescence immunoassay (I). Clin Chim Acta Int J Clin Chem. 2004 Jan;339(1–2):147–56.

52. Ang SH, Thevarajah TM, Woi PM, Alias YB, Khor SM. A lateral flow immunosensor for direct, sensitive, and highly selective detection of hemoglobin A1c in whole blood. J Chromatogr B Analyt Technol Biomed Life Sci. 2016 Mar 15;1015–1016:157–65.

53. Kikkas I, Mallone R, Larger E, Volland H, Morel N. A rapid lateral flow immunoassay for the detection of tyrosine phosphatase-like protein IA-2 autoantibodies in human serum. PloS One. 2014;9(7):e103088.

54. Kalogianni DP, Goura S, Aletras AJ, Christopoulos TK, Chanos MG, Christofidou M, et al. Dry reagent dipstick test combined with 23S rRNA PCR for molecular diagnosis of bacterial infection in arthroplasty. Anal Biochem. 2007 Feb 15;361(2):169–75.

55. Gussenhoven GC, van der Hoorn MA, Goris MG, Terpstra WJ, Hartskeerl RA, Mol BW, et al. LEPTO dipstick, a dipstick assay for detection of Leptospira-specific immunoglobulin M antibodies in human sera. J Clin Microbiol. 1997 Jan;35(1):92–7.

56. Al-Yousif Y, Anderson J, Chard-Bergstrom C, Kapil S. Development, evaluation, and application of lateral-flow immunoassay (immunochromatography) for detection of rotavirus in bovine fecal samples. Clin Diagn Lab Immunol. 2002 May;9(3):723–5.

57. Zhu Y, He W, Liang Y, Xu M, Yu C, Hua W, et al. Development of a rapid, simple dipstick dye immunoassay for schistosomiasis diagnosis. J Immunol Methods. 2002 Aug 1;266(1–2):1–5.

58. van Dam GJ, Wichers JH, Ferreira TMF, Ghati D, van Amerongen A, Deelder AM. Diagnosis of schistosomiasis by reagent strip test for detection of circulating cathodic antigen. J Clin Microbiol. 2004 Dec;42(12):5458–61.

59. Zhang G-P, Guo J-Q, Wang X-N, Yang J-X, Yang Y-Y, Li Q-M, et al. Development and evaluation of an immunochromatographic strip for trichinellosis detection. Vet Parasitol. 2006 Apr 30;137(3–4):286–93.

60. Oku Y, Kamiya K, Kamiya H, Shibahara Y, Ii T, Uesaka Y. Development of oligonucleotide lateral-flow immunoassay for multi-parameter detection. J Immunol Methods. 2001 Dec 1;258(1–2):73–84.

61. Carter DJ, Cary RB. Lateral flow microarrays: a novel platform for rapid nucleic acid detection based on miniaturized lateral flow chromatography. Nucleic Acids Res. 2007 May;35(10):e74.

62. Clavijo E, Díaz R, Anguita A, García A, Pinedo A, Smits HL. Comparison of a dipstick assay for detection of Brucella-specific immunoglobulin M antibodies with

other tests for serodiagnosis of human brucellosis. Clin Diagn Lab Immunol. 2003 Jul;10(4):612–5.

63. Ho J-AA, Wauchope RD. A Strip Liposome Immunoassay for Aflatoxin B1. Anal Chem. 2002 Apr 1;74(7):1493–6.

64. Tang D, Sauceda JC, Lin Z, Ott S, Basova E, Goryacheva I, et al. Magnetic nanogold microspheres-based lateral-flow immunodipstick for rapid detection of aflatoxin B2 in food. Biosens Bioelectron. 2009 Oct 15;25(2):514–8.

65. Zhang C, Zhang Y, Wang S. Development of multianalyte flow-through and lateral-flow assays using gold particles and horseradish peroxidase as tracers for the rapid determination of carbaryl and endosulfan in agricultural products. J Agric Food Chem. 2006 Apr 5;54(7):2502–7.

66. Wang S, Quan Y, Lee N, Kennedy IR. Rapid determination of fumonisin B1 in food samples by enzyme-linked immunosorbent assay and colloidal gold immunoassay. J Agric Food Chem. 2006 Apr 5;54(7):2491–5.

67. Verheijen R, Stouten P, Cazemier G, Haasnoot W. Development of a one step strip test for the detection of sulfadimidine residues. The Analyst. 1998 Dec;123(12):2437–41.

68. Aldus CF, Van Amerongen A, Ariëns RMC, Peck MW, Wichers JH, Wyatt GM. Principles of some novel rapid dipstick methods for detection and characterization of verotoxigenic Escherichia coli. J Appl Microbiol. 2003;95(2):380–9.

69. Carrio A, Sampedro C, Sanchez-Lopez JL, Pimienta M, Campoy P. Automated Low-Cost Smartphone-Based Lateral Flow Saliva Test Reader for Drugs-of-Abuse Detection. Sensors. 2015;15(11):29569–93.

70. Bowen RAR, George DT, Hortin GL. False-negative result for cocaine metabolites on a lateral-flow drug test slide corrected by dilution. Clin Chem. 2005 Apr;51(4):790–1.

71. Pappas MG, Schantz PM, Cannon LT, Wahlquist SP. Dot-ELISA for the rapid serodiagnosis of human hydatid disease. Diagn Immunol. 1986;4(6):271–6.

72. Mark D, Haeberle S, Roth G, Stetten F von, Zengerle R. Microfluidic lab-on-a-chip platforms: requirements, characteristics and applications. Chem Soc Rev. 2010 Feb 24;39(3):1153–82.

73. Salieb-Beugelaar GB, Hunziker PR. Towards nano-diagnostics for rapid diagnosis of infectious diseases – current technological state. Eur J Nanomedicine. 2014;6(1):11–28.

74. Wang Y, Xu H, Wei M, Gu H, Xu Q, Zhu W. Study of superparamagnetic nanoparticles as labels in the quantitative lateral flow immunoassay. Mater Sci Eng C. 2009 Apr 30;29(3):714–8.

75. Posthuma-Trumpie GA, Korf J, van Amerongen A. Lateral flow (immuno)assay: its strengths, weaknesses, opportunities and threats. A literature survey. Anal Bioanal Chem. 2009 Jan;393(2):569–82.

76. Tang D, Cui Y, Chen G. Nanoparticle-based immunoassays in the biomedical field. Analyst. 2013 Jan 22;138(4):981–90.

77. Juntunen E, Myyryläinen T, Salminen T, Soukka T, Pettersson K. Performance of fluorescent europium(III) nanoparticles and colloidal gold reporters in lateral flow

bioaffinity assay. Anal Biochem. 2012 Sep 1;428(1):31–8.

78. Hui W, Zhang S, Zhang C, Wan Y, Zhu J, Zhao G, et al. A novel lateral flow assay based on GoldMag nanoparticles and its clinical applications for genotyping of MTHFR C677T polymorphisms. Nanoscale. 2016 Feb 14;8(6):3579–87.

79. Nurul Najian AB, Engku Nur Syafirah E a. R, Ismail N, Mohamed M, Yean CY. Development of multiplex loop mediated isothermal amplification (m-LAMP) label-based gold nanoparticles lateral flow dipstick biosensor for detection of pathogenic Leptospira. Anal Chim Acta. 2016 Jan 15;903:142–8.

80. Hwang J, Lee S, Choo J. Application of a SERS-based lateral flow immunoassay strip for the rapid and sensitive detection of staphylococcal enterotoxin B. Nanoscale. 2016 Jun 2;8(22):11418–25.

81. Toubanaki DK, Athanasiou E, Karagouni E. Gold nanoparticle-based lateral flow biosensor for rapid visual detection of Leishmania-specific DNA amplification products. J Microbiol Methods. 2016 May 30;127:51–8.

82. Greenwald R, Esfandiari J, Lesellier S, Houghton R, Pollock J, Aagaard C, et al. Improved serodetection of Mycobacterium bovis infection in badgers (Meles meles) using multiantigen test formats. Diagn Microbiol Infect Dis. 2003 Jul;46(3):197–203.

83. Noguera P, Posthuma-Trumpie GA, van Tuil M, van der Wal FJ, de Boer A, Moers APHA, et al. Carbon nanoparticles in lateral flow methods to detect genes encoding virulence factors of Shiga toxin-producing Escherichia coli. Anal Bioanal Chem. 2011 Jan;399(2):831–8.

84. Posthuma-Trumpie GA, Wichers JH, Koets M, Berendsen LBJM, van Amerongen A. Amorphous carbon nanoparticles: a versatile label for rapid diagnostic (immuno)assays. Anal Bioanal Chem. 2012 Jan;402(2):593–600.

85. Vannoy CH, Tavares AJ, Noor MO, Uddayasankar U, Krull UJ. Biosensing with Quantum Dots: A Microfluidic Approach. Sensors. 2011 Oct 18;11(10):9732–63.

86. Goldman ER, Clapp AR, Anderson GP, Uyeda HT, Mauro JM, Medintz IL, et al. Multiplexed Toxin Analysis Using Four Colors of Quantum Dot Fluororeagents. Anal Chem. 2004 Feb 1;76(3):684–8.

87. Edwards KA, Baeumner AJ. Liposome-enhanced lateral-flow assays for the sandwich-hybridization detection of RNA. Methods Mol Biol Clifton NJ. 2009;504:185–215.

88. Wen H-W, Borejsza-Wysocki W, DeCory TR, Durst RA. Development of a competitive liposome-based lateral flow assay for the rapid detection of the allergenic peanut protein Ara h1. Anal Bioanal Chem. 2005 Jul;382(5):1217–26.

89. Edwards KA, Baeumner AJ. Optimization of DNA-tagged dye-encapsulating liposomes for lateral-flow assays based on sandwich hybridization. Anal Bioanal Chem. 2006 Nov;386(5):1335–43.

90. Mak WC, Sin KK, Chan CPY, Wong LW, Renneberg R. Biofunctionalized indigo-nanoparticles as biolabels for the generation of precipitated visible signal in immunodipsticks. Biosens Bioelectron. 2011 Mar 15;26(7):3148–53.

91. Park J-M, Jung H-W, Chang YW, Kim H-S, Kang M-J, Pyun J-C. Chemiluminescence lateral flow immunoassay based on Pt nanoparticle with peroxidase activity. Anal Chim Acta. 2015 Jan 1;853:360–7.

92. Parolo C, Medina-Sánchez M, Escosura-Muñiz A de la, Merkoçi A. Simple paper architecture modifications lead to enhanced sensitivity in nanoparticle based lateral flow immunoassays. Lab Chip. 2013 Jan 2;13(3):386–90.

93. Xu H, Chen J, Birrenkott J, Zhao JX, Takalkar S, Baryeh K, et al. Gold-nanoparticle-decorated silica nanorods for sensitive visual detection of proteins. Anal Chem. 2014 Aug 5;86(15):7351–9.

94. Ge C, Yu L, Fang Z, Zeng L. An enhanced strip biosensor for rapid and sensitive detection of histone methylation. Anal Chem. 2013 Oct 1;85(19):9343–9.

95. Zhu X, Shah P, Stoff S, Liu H, Li C. A paper electrode integrated lateral flow immunosensor for quantitative analysis of oxidative stress induced DNA damage. The Analyst. 2014 Jun 7;139(11):2850–7.

96. Akanda MR, Joung H-A, Tamilavan V, Park S, Kim S, Hyun MH, et al. An interference-free and rapid electrochemical lateral-flow immunoassay for one-step ultrasensitive detection with serum. The Analyst. 2014 Mar 21;139(6):1420–5.

97. Liu C, Jia Q, Yang C, Qiao R, Jing L, Wang L, et al. Lateral flow immunochromatographic assay for sensitive pesticide detection by using Fe3O4 nanoparticle aggregates as color reagents. Anal Chem. 2011 Sep 1;83(17):6778–84.

98. Li M, Yang H, Li S, Zhao K, Li J, Jiang D, et al. Ultrasensitive and quantitative detection of a new β-agonist phenylethanolamine A by a novel immunochromatographic assay based on surface-enhanced Raman scattering (SERS). J Agric Food Chem. 2014 Nov 12;62(45):10896–902.

99. Qin Z, Chan WCW, Boulware DR, Akkin T, Butler EK, Bischof JC. Significantly improved analytical sensitivity of lateral flow immunoassays by using thermal contrast. Angew Chem Int Ed Engl. 2012 Apr 27;51(18):4358–61.

100. Guidelines for ATC classification and DDD assignement [Internet]. 2016 [cited 2016 Jun 24]. Available from: http://www.whocc.no/atc_ddd_publications/guidelines/

101. Foegeding NJ, Caston RR, McClain MS, Ohi MD, Cover TL. An Overview of Helicobacter pylori VacA Toxin Biology. Toxins. 2016;8(6).

102. Helikit - Urea Breath Test [Internet]. [cited 2016 May 13]. Available from: http://www.helikit.com/en/helikit-urea-breath-test/

103. Pylobactell EMEA report [Internet]. [cited 2016 May 18]. Available from: http://www.ema.europa.eu/docs/en_GB/document_library/EPAR_-_Summary_for_the_public/human/000151/WC500045751.pdf

104. Park SJ, Park YH, Lee SI, Lee DC, Yong D, Kim JH. Comparison Between a New Low Dose Urea Capsule Test and the Conventional UBiT(R) Tablet Test for the Detection of Helicobacter pylori Infection. Korean J Lab Med. 2006 Apr;26(2):81–5.

105. Helicobacter pylori Urea Breath Test, Infra-red (UBiT) [Internet]. [cited 2016 May 13]. Available from:

http://www.questdiagnostics.com/testcenter/testguide.action?dc=TS_Hpylori_UBiT

106. PT. Otsuka Indonesia [Internet]. [cited 2016 Oct 23]. Available from: http://www.otsuka.co.id/en/product/detail/53/40//yes

107. Mock T, Yatscoff R, Foster R, Hyun JH, Chung IS, Shim CS, et al. Clinical validation of the Helikit: a 13C urea breath test used for the diagnosis of Helicobacter pylori infection. Clin Biochem. 1999 Feb;32(1):59–63.

108. Helikit - Patient Information [Internet]. [cited 2016 May 13]. Available from: http://www.helikit.com/fr/information-pour-patients/

109. Gisbert JP, Gomollón F, Domínguez-Muñoz JE, Borda F, Jiménez I, Vázquez MA, et al. [Comparison between two 13C-urea breath tests for the diagnosis of Helicobacter pylori infection: isotope ratio mass spectrometer versus infrared spectrometer]. Gastroenterol Hepatol. 2003 Mar;26(3):141–6.

110. Aridol Homepage [Internet]. Aridol. [cited 2016 May 13]. Available from: http://www.aridol.info/

111. Pharmaxis. Aridol® [Internet]. Pharmaxis. [cited 2016 May 13]. Available from: http://www.pharmaxis.com.au/approved-products/aridol/

112. Barben J, Strippoli M-PF, Trachsel D, Schiller B, Hammer J, Kuehni CE. Effect of mannitol dry powder challenge on exhaled nitric oxide in children. PloS One. 2013;8(1):e54521.

113. Barben J, Kuehni CE, Strippoli M-PF, Schiller B, Hammer J, Trachsel D, et al. Mannitol dry powder challenge in comparison with exercise testing in children. Pediatr Pulmonol. 2011 Sep;46(9):842–8.

114. Brannan JD, Porsbjerg C, Anderson SD. Inhaled mannitol as a test for bronchial hyper-responsiveness. Expert Rev Respir Med. 2009 Oct;3(5):457–68.

115. Anderson SD. Method and device for the provocation of air passage narrowing and/or the induction of septum. [Internet]. 1996 [cited 2016 May 13]. Available from: https://docs.google.com/viewer?url=patentimages.storage.googleapis.com/pdfs/US5817028.pdf

116. Osmohale ® [Internet]. Aridol. [cited 2016 Oct 23]. Available from: http://www.aridol.info/united-kingdom

117. WHOCC - ATC/DDD Index [Internet]. [cited 2016 Jun 27]. Available from: http://www.whocc.no/atc_ddd_index/?code=V08&showdescription=yes

118. Notice patient - MICROPAQUE, suspension buvable ou rectale - Base de données publique des médicaments [Internet]. [cited 2016 Jun 27]. Available from: http://base-donnees-publique.medicaments.gouv.fr/affichageDoc.php?specid=61522753&typedoc=N

119. Notice patient - LUMIREM 175 mg/l, suspension buvable et rectale - Base de données publique des médicaments [Internet]. [cited 2016 Jun 24]. Available from: http://base-donnees-publique.medicaments.gouv.fr/affichageDoc.php?specid=60581542&typedoc=N

120. Qin S, Caskey CF, Ferrara KW. Ultrasound contrast microbubbles in

imaging and therapy: physical principles and engineering. Phys Med Biol. 2009 Mar 21;54(6):R27.

121. Nanda NC, Schlief R, Goldberg BB. Advances in Echo Imaging Using Contrast Enhancement. Springer Science & Business Media; 2012. 688 p.

122. Tamási F, Weidner A, Domokos N, Bedros RJ, Bagdány S. ECHOVIST-200 enhanced hystero-sonography: A new technique in the assessment of infertility. Eur J Obstet Gynecol Reprod Biol. 2005 Aug 1;121(2):186–90.

123. Radiopharmaceuticals [Internet]. [cited 2016 May 18]. Available from: http://www.who.int/medicines/publications/pharmacopoeia/Radgenmono.pdf

124. What is nuclear medicine ? [Internet]. [cited 2016 May 18]. Available from: http://interactive.snm.org/docs/whatisnucmed2.pdf

125. Schilling test: MedlinePlus Medical Encyclopedia [Internet]. [cited 2016 Jun 27]. Available from: https://www.nlm.nih.gov/medlineplus/ency/article/003572.htm

126. Vitamin B12 Deficiency - American Family Physician [Internet]. [cited 2016 Jun 27]. Available from: http://www.aafp.org/afp/2003/0301/p979.html

127. P S S, PROMILA M. Human Body Measurements: Concepts And Applications. PHI Learning Pvt. Ltd.; 2009. 265 p.

128. Kongkaew C, Noyce PR, Ashcroft DM. Hospital admissions associated with adverse drug reactions: a systematic review of prospective observational studies. Ann Pharmacother. 2008 Jul;42(7):1017–25.

129. Jørgensen JT. Companion diagnostics: the key to personalized medicine. Foreword. Expert Rev Mol Diagn. 2015 Feb;15(2):153–6.

130. Health C for D and R. In Vitro Diagnostics - Companion Diagnostics [Internet]. [cited 2016 Jul 31]. Available from: http://www.fda.gov/MedicalDevices/ProductsandMedicalProcedures/InVitroDiagnostics/ucm407297.htm

131. Sharma A, Zhang G, Aslam S, Yu K, Chee M, Palma JF. Novel Approach for Clinical Validation of the cobas KRAS Mutation Test in Advanced Colorectal Cancer. Mol Diagn Ther. 2016 Mar 16;

132. Pene F, Courtine E, Cariou A, Mira J-P. Toward theragnostics. Crit Care Med. 2009 Jan;37(1 Suppl):S50-58.

133. Agarwal A, Ressler D, Snyder G. The current and future state of companion diagnostics. Pharmacogenomics Pers Med. 2015 Mar 31;8:99–110.

134. Vergara-Lluri ME, Moatamed NA, Hong E, Apple SK. High concordance between HercepTest immunohistochemistry and ERBB2 fluorescence in situ hybridization before and after implementation of American Society of Clinical Oncology/College of American Pathology 2007 guidelines. Mod Pathol. 2012 Oct;25(10):1326–32.

135. Watanabe A. [Companion Diagnostics for Solid Tumors]. Rinsho Byori. 2015 Nov;63(11):1310–5.

136. Yoo C, Park YS. Companion diagnostics for the targeted therapy of gastric cancer. World J Gastroenterol. 2015 Oct 21;21(39):10948–55.

137. Conde E, Hernandez S, Prieto M, Martinez R, Lopez-Rios F. Profile of Ventana ALK (D5F3) companion diagnostic assay for non-small-cell lung carcinomas. Expert Rev Mol Diagn. 2016 Jun;16(6):707–13.

138. Tamura G, Osakabe M, Yanagawa N, Ogata S, Nomura T, Fukushima N, et al. Comparison of HER2 immunohistochemical results using a monoclonal antibody (SV2-61γ) and a polyclonal antibody (for Dako HercepTest) in advanced gastric cancer. Pathol Int. 2012 Aug;62(8):513–7.

139. Kumagai S. [Optimal Treatment for Rheumatoid Arthritis with Companion Diagnostics]. Rinsho Byori. 2015 Nov;63(11):1328–35.

140. Masuda Y, Matsuno K, Shimizu C. [Companion Diagnostics for Thrombotic Disease]. Rinsho Byori. 2015 Nov;63(11):1316–22.

141. Fukutake K. [Companion Diagnostics for Selecting Antiretroviral Drugs against HIV-1]. Rinsho Byori. 2015 Nov;63(11):1323–7.

142. Valenti WM. Companion diagnostic tests in HIV medicine: the road to personalized medicine. AIDS Read. 2007 Nov;17(11):546–9.

143. Roche companion diagnostics [Internet]. [cited 2016 Jun 30]. Available from: http://roche.nsp-reports.ch/10/ar/diagnostics_en/roche_companion_diagnostics.htm

144. Colucci G. Molecular diagnostic and predictive tests in the evolution of chronic hepatitis C anti-viral therapies. BMC Infect Dis. 2012 Nov 12;12(Suppl 2):S8.

145. Zhang L, Cui G, Li Z, Wang H, Ding H, Wang DW. Comparison of High-Resolution Melting Analysis, TaqMan Allelic Discrimination Assay, and Sanger Sequencing for Clopidogrel Efficacy Genotyping in Routine Molecular Diagnostics. J Mol Diagn. 2013 Sep;15(5):600–6.

146. Savani BN. Ferritin and FerriScan in HCT recipients. Blood. 2013 Aug 29;122(9):1539–41.

147. Meerpohl JJ, Antes G, Rücker G, Fleeman N, Motschall E, Niemeyer CM, et al. Deferasirox for managing iron overload in people with thalassaemia. Cochrane Database Syst Rev. 2012 Feb 15;(2):CD007476.

148. Phenotype. In [cited 2016 Jul 30]. Available from: http://www.oxforddictionaries.com/definition/english/phenotype

149. Donzelli M, Derungs A, Serratore M-G, Noppen C, Nezic L, Krähenbühl S, et al. The basel cocktail for simultaneous phenotyping of human cytochrome P450 isoforms in plasma, saliva and dried blood spots. Clin Pharmacokinet. 2014 Mar;53(3):271–82.

150. Camblin M, Berger B, Haschke M, Krähenbühl S, Huwyler J, Puchkov M. CombiCap: A novel drug formulation for the basel phenotyping cocktail. Int J Pharm. 2016 Oktober;512(1):253–61.

151. Michalet X, Pinaud FF, Bentolila LA, Tsay JM, Doose S, Li JJ, et al. Quantum Dots for Live Cells, in Vivo Imaging, and Diagnostics. Science. 2005 Jan 28;307(5709):538–44.

152. Bakalova R, Lazarova D, Nikolova B, Atanasova S, Zlateva G, Zhelev Z, et al. Delivery of size-controlled long-circulating polymersomes in solid tumours, visualized by quantum dots and optical imaging in

vivo. Biotechnol Biotechnol Equip. 2015 Jan 2;29(1):175–80.

153. Bakalova R, Zhelev Z, Nikolova B, Murayama S, Lazarova D, Tsoneva I, et al. Lymph node mapping using quantum dot-labeled polymersomes. Gen Physiol Biophys. 2015 Oct;34(4):393–8.

154. Canton I, Battaglia G. Polymersomes-mediated delivery of fluorescent probes for targeted and long-term imaging in live cell microscopy. Methods Mol Biol Clifton NJ. 2013;991:343–51.

155. Alibolandi M, Abnous K, Sadeghi F, Hosseinkhani H, Ramezani M, Hadizadeh F. Folate receptor-targeted multimodal polymersomes for delivery of quantum dots and doxorubicin to breast adenocarcinoma: In vitro and in vivo evaluation. Int J Pharm. 2016 Mar 16;500(1–2):162–78.

156. Opdam FL, Modak AS, Gelderblom H, Guchelaar H-J. Breath tests to phenotype drug disposition in oncology. Clin Pharmacokinet. 2013 Nov;52(11):919–26.

157. Vogenberg FR, Barash CI, Pursel M. Personalized Medicine. Pharm Ther. 2010 Nov;35(11):624–42.

158. Annadurai K, Danasekaran R, Mani G. Personalized medicine: A paradigm shift towards promising health care. J Pharm Bioallied Sci. 2016;8(1):77–8.

159. Miners JO, Mackenzie PI, Knights KM. The prediction of drug-glucuronidation parameters in humans: UDP-glucuronosyltransferase enzyme-selective substrate and inhibitor probes for reaction phenotyping and in vitro–in vivo extrapolation of drug clearance and drug-drug interaction potential. Drug Metab Rev. 2010 Feb 1;42(1):196–208.

7 APPENDIX

7.1 Use of nanoparticles in therapeutics

Nanomaterials: Applications in Therapeutics

Dominik Witzigmann, Marine Camblin, Jörg Huwyler, Vimalkumal Balasubramanian

Division of Pharmaceutical Technology, University of Basel, Basel, Switzerland

Encyclopedia of Biomedical Polymers and Polymer Biomaterials, 2015, Taylor & Francis

Nanomaterials: Applications in Therapeutics

Dominik Witzigmann
Marine Camblin
Jörg Huwyler
Vimalkumar Balasubramanian
Division of Pharmaceutical Technology, University of Basel, Basel, Switzerland

Abstract
In recent years, uses of engineered nanomaterials have been increased in day-to-day life, especially in biomedical applications. In this direction, advances in polymer science have significantly contributed to the development of polymeric nanomaterials for drug delivery applications. Particularly, intensive efforts have been made to develop new type of nanomaterials through self-assembly techniques. Polymers that can spontaneously self-assemble in aqueous solution into various nanoscale structures such as micelles, nanoparticles, and vesicles have huge potential to serve as nanocarriers for various therapeutic applications. By controlling number of physicochemical parameters that can influence the self-assembly process, it is possible to tailor the desired morphology of the nanostructures and to engineer different properties of the nanostructures. This entry reviews the fundamental and physicochemical properties of self-assembled morphologies like micelles, nanoparticles, vesicles (polymersomes), and layer-by-layer capsules that are driven by template-directed assembly. We covered formulation characteristics such as loading efficiency, stability, and release properties of polymeric nanocarrier systems with recent examples. We emphasized the biological properties of the polymeric nanomaterials and their therapeutic applications from the delivery of small drug molecules to proteins and gene delivery.

INTRODUCTION

Drug molecules have often unfavorable pharmacokinetic properties. Encountered problems may include low bioavailability, poor distribution to target tissues, accumulation in non-target tissues and low metabolic stability. Consequently, their therapeutic efficiency is decreased and off target toxicity is more pronounced in conventional approaches. Those issues raise the pressing need of more sophisticated and smart drug delivery systems (DDSs) to improve the performance of classical therapeutics. Nanomaterial-based formulations offer the possibility to modulate pharmacokinetic properties of delivered drugs. Unique nanoscale properties of nanomaterials such as high surface-to-volume ratio due to their nanoscale size (20–200 nm) and enhanced physicochemical properties make them an ideal candidate for nanocarriers. They can, for example, be loaded with a drug of interest. As a result, increase in the apparent solubility of the administered drug and change in the pharmacokinetic properties has the potential to improve the therapeutic efficiency and efficacy.

The main aim of the present review is to discuss the therapeutic use of nanocarriers as DDSs. A wide range of nanomaterials made of organic, inorganic, lipid, polymer, and peptide-based compounds have been proposed as nanocarriers for such therapeutic applications. As compared to clinically established nanocarriers such as liposomal DDSs, polymeric nanomaterials have recently gained attention due to their unique properties. First, physicochemical properties and chemical versatility nature of polymers can be used to combine polymers with drugs (covalent and noncovalent approach) that can dramatically improve the drug characteristics in terms of solubility, stability, and permeability. Second, polymers can be chemically modified to conjugate with targeting vectors such as antibodies, peptides, and aptamers to guide them to specific tissue or cells in the body. Third, environmental responsiveness such as pH and temperature of polymers can be used to control the release profile of the drug in a specified area of interest. It has to be emphasized that polymers can offer the biological properties to be nontoxic, biodegradable, and biocompatible. These are essential requirements for therapeutic applications. In this entry, we discuss recent developments of polymeric nanomaterials forming self-assembled nanostructures such as micelles, nanoparticles, polymersomes, and template-directed assembly-forming layer-by-layer (LbL) capsules for various therapeutic applications (Fig. 1).

POLYMERIC MICELLES

General Characteristics

Polymeric micelles are self-assembled nanostructures consisting of a compact hydrophobic core surrounded by a hydrophilic corona. Micelles are dynamic structures

Encyclopedia of Biomedical Polymers and Polymeric Biomaterials DOI: 10.1081/E-EBPP-120050055

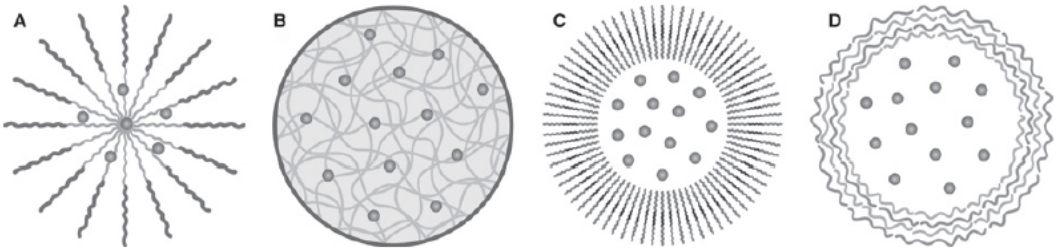

Fig. 1 Schematic illustration of different types of polymeric nanomaterial based nanocarriers (**A**) polymeric micelle, (**B**) polymeric NP, (**C**) polymersome, and (**D**) LbL capsule. Gray dots represent the transported drug.

composed of amphiphilic block copolymers possessing both hydrophilic and hydrophobic blocks. Amphiphilic copolymers begin to self-assemble in solution into micelles at a specific and narrow concentration range, which is known as critical micelle concentration (CMC). One of the main reasons why amphiphilic copolymers self-assemble themselves in aqueous solution is their tendency to isolate the hydrophobic blocks from the aqueous environment and to reach a state of minimum energy. This process is driven by an increase in entropy of water molecules interacting with hydrophobic molecules.[1] Above the CMC, micelle structures are thermodynamically stable and below the CMC, micelles are unstable. The relative size of the hydrophobic block of the copolymer is the most important factor that affects the process of micelle formation.

Amphiphilic block copolymers can form a variety of self-assembled structures in solutions where the solvent preferentially solvates one of the blocks. The most common structures formed by these amphiphilic copolymers are spherical micelles, cylindrical micelles, and vesicles. Depending on the length of the hydrophobic block, spherical micelles can be classified as star-like or crew-cut micelles. When the length of the hydrophilic block is longer than the hydrophobic block, it forms the star-like micelles. Crew-cut micelles are formed when the hydrophilic block is shorter than the hydrophobic block. As the hydrophilic block length decreases, the morphology of the micelles change from spherical to cylindrical (also called worm-like or rod micelles). Recent approaches showed that by controlling the self-assembly of the amphiphilic block copolymers different types of micellar morphologies can be obtained. These types of micellar morphologies include disk-like, toroidal, bi-continuous, cross-linked, and Janus micelles.[2,3] In most cases, polymeric micelles are prepared by two different methods. In the first method, amphiphilic copolymers are directly dissolved in water. During spontaneous self-assembly, drugs can be loaded simply by adding them to the polymers. In the second method, copolymers are dissolved in organic solvent. The solvent is removed by evaporation resulting in a thin film of copolymers. Drugs can then be loaded during the rehydration and self-assembly process of the film exposed to an aqueous solution. These techniques are referred to as direct dissolution and film rehydration method, respectively.[4]

Formulation Characteristics

Classically, polymeric micelles have been utilized to improve the solubilization and loading of hydrophobic drug molecules. When maximum solubilization capacity of the micelles is achieved, drugs cannot be loaded further into the micelles. Thus, solubilization and drug loading efficiency are directly linked parameters.[1] To improve drug solubilization, hydrotropic polymers can be used instead of conventional amphiphilic copolymers.[5,6] Furthermore, solubilization and loading efficiency can also be dependent on the hydrophobicity level of the drugs. For instance, conventional poly(ethylene glycol)–polylactide acid (PEG–PLA) micelles improved the solubilization of paclitaxel (PTX) by a factor of 50, compared to the less hydrophobic nifedipine (factor of 20), due to a higher hydrophobicity level. Similarly, hydrotropic polymer based poly(ethylene glycol)–poly(2-amino-2-methyl-butyl)acrylamide (PEG-PDMBA) micelles showed the dramatic solubility enhancement for PTX (6000-fold increased solubility) compared with nifedipine (60-fold increased solubility). Interestingly, poly(ethylene glycol)–poly [2-(4-vinylbenzyloxy)-*N*,*N*-diethylnicotinamide] (PEG-PDENA) micelles showed high specificity toward the solubilizing properties for PTX (about 9000-fold increased loading) than for the other drugs.[6]

Compatibility between drug molecules and the micelle core is the major determinant of drug solubility and loading efficiency.[5] In one study, the influence of copolymer was investigated on the solubilization of PTX. In this study, PEG-PDENA (hydrotropic polymer) micelles showed the highest loading capacity of PTX (37.4%) compared to the conventional poly(ethylene glycol)–polyphosphoramidate (PEG-PPA) and PEG-PLA micelles that showed 14.7% and 27.6% of PTX loading due to the compatibility between PTX and PDENA.[5] In addition to the single drug loading, micelles offer the possibility to load multiple drugs into single micelles at clinically relevant doses. PTX, etoposide (ETO), docetaxel (DTXL), and 17-allylamino-17-demethyoxygeldanamycin (17-AAG) were solubilized in PEG-PLA micelles within the combinations PTX/17-AAG, ETO/17-AAG, DTXL/17-AAG, and PTX/ETO/17-AAG. Two-drug and three-drug combinations in micelles

retained the 94% and 97% of loaded drugs, respectively, compared to the single drug micelles that retained 16% to 32% of the loaded drugs. The presence of 17-AAG in those micelles helped to stabilize the formulation and to offer greater stability of the drugs at the same level of solubilization as single drug micelles.[7]

Stability of micelles is crucial for drug delivery applications. To improve the stability of drug loaded micelles, several strategies have been explored such as enhancing the compatibility between the drug and the block copolymer, cross-linking of the micelle core/corona, and lowering the CMC by altering the polymer.[4] Classical PEG-PLA micelles loaded with PTX showed stability over a period of 4–5 days. To overcome this limitation, hydrotropic polymers have been linked to PEG to develop PEG-PDENA micelles that increase the micellar stability for a period of 25 days due to the compatibility of PDENA and PTX.[5] Polymeric micelles cross-linked with ionic cores by using block ionomer complexes of poly(ethylene oxide)–poly(methacrylic acid) (PEO-PMA) and divalent metal cations showed colloidal stability for a prolonged period of time.[8] Moreover, cross-linking of micelles increased the stability without affecting the drug loading capacity.[4]

Therapeutic Applications

Polymeric micelles are one of the widely used nano-carrier systems due to their unique properties, usually ranging from 20 to 200 nm in size for drug delivery application.[1] High colloidal stability of polymeric micelles is mainly due to the low CMC of the polymers that prevents the dissociation of micelles and offers high stability in biological systems, where it is diluted after intravenous injection. Polymeric micelles have better rigidity and stability than phospholipid micelles due to the covalent link between the polymeric blocks.[4] The hydrophobicity of the micellar core permits the incorporation and stabilization of wide range of small drug molecules, such as doxorubicin (DOX), PTX, amphothericin B, cisplatin, cyclosporine, and hydroxyl camptothecin.[9] Hydrophilic corona of the micelle offers the stealth properties to escape the reticuloendothelial system (RES). These properties lead to a significant increase in the blood residence time of micelles, allow them to permeate the blood vessels, and to accumulate efficiently at the tumor site.[10] The nano-size of polymeric micelles may also facilitate the deep penetration of carrier to tumor tissue and ease of their uptake by tumor cells.[9]

Anticancer drugs such as DOX and PTX are commonly used cancer therapeutics. However, low water solubility, acute toxicity to normal cells, and multidrug resistance are the major issues that can be surmounted by using polymeric micelles. For instance, poloxamer micelles [poly(ethylene oxide–poly(propylene oxide)] loaded with DOX entered clinical trials in Canada in 1999 and completed phase II in esophageal adenocarcinoma.[11] Pharmacokinetic and biodistribution of these micelles in healthy mice showed a 2.1-fold increase of area under the curve (AUC), 2.1-fold decrease in clearance, and 1.5-fold decrease in volume of distribution compared to the free DOX. In-vivo (in mice) and at equal dose, poloxamer micelles showed to be more effective than free DOX in solid tumor models. In another approach, use of polymeric micelles made of PEO–poly(D,L-lactic acid) [PDLLA] hamper the unwanted toxic side effects associated with solubilizing agent, Cremophor EL®, which is present in the commercial PTX formulations (Taxol®). Intravenous administration of PTX micelles in nude mice caused 91% decrease in the tumor volume that showed high therapeutic efficiency. Additionally, polymeric micelles offer the possibility of introducing high dose of PTX without any potential side effects.[12] In another study, PEO-poly(4-phenyl-L-butanoate)-L-aspartamide) (PPBA) micelles loaded with PTX (NK-105) showed 87-fold increase in AUC, 86-fold decrease in clearance, and 15-fold decrease in volume of distribution compared with marketed product Taxol® after intravenous injection. Micelles had a long circulation time in blood and were able to evade serum protein binding. Enhanced accumulation in the tumor (25-fold) and stronger antitumor activity in C-26 tumor bearing mice model at a single administration of NK-105 leads to the efficient tumor regression.[13]

In addition to the delivery of small hydrophobic molecules, micelles can serve to deliver large therapeutic proteins. Different PEG-PLA diblock copolymer-based micelles have been investigated for the delivery of recombinant human erythropoietin (rhEPO) in Sprague-Dawley rats.[14] This study showed a twofold increase of AUC with the micelles (from 23 μg/L·hr to 33 μg/L·hr) compared to the native rhEPO (16 μg/L·hr). Plasma concentration of rhEPO was twofold higher with the micelles (i.e., 39.88 ng/mL) than with the native rhEPO. Micelles increased the half-life of rhEPO in blood circulation from 2.0 hr (native rhEPO) to 4.4 hr due to the stealth property of the PEG.[14] Micellar formulation of rhEPO enhanced the pharmacological effect of the drug (i.e., increased level of hemoglobin by 48.72%) demonstrating that micellar delivery of the protein did not affect protein functionality. In an alternative approach, human serum albumin (HSA) was loaded into poly(ethylene glycol)–poly(amino ester) (PEG-PAE) micelles and the delivery was enhanced by a pH-dependent stimulus at reduced pH in ischemic tissue. Accumulation of labeled albumin in ischemic brain areas of rats after IV injection indicated that this type of formulation can be used for targeted protein delivery in experimental models of cerebral ischemia (Fig. 2).[15]

Polycationic-based polymeric micelles have an ability to form complexes with negatively charged plasmid DNA (pDNA). Thus, DNA can be packed into micelles for gene delivery. DNA is thereby protected from enzymatic and hydrolytic degradation. Intravenous injection of pDNA/PEG–poly-L-lysine (PLL) micelles showed circulation of intact pDNA in the blood circulation for 3 hr when compared to naked pDNA that is eliminated from the

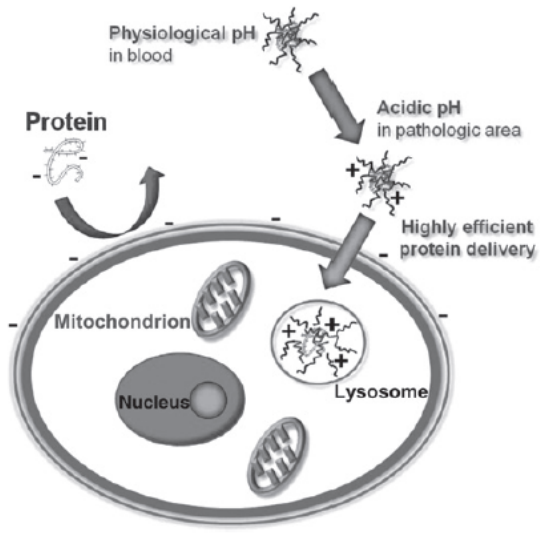

Fig. 2 Schematic representation of pH-tunable micelles loaded with a therapeutic protein to implement a drug targeting strategy. At appropriate pH for noninvasive administration (pH 7 or over), the protein-loaded micelles are stable. If the pH turns acidic (pH < 7), the ionized amino groups of the PAE block forming the micelles are positively charged. This promotes uptake into a diseased tissue, which is characterized by a low pH (e.g., ischemic tissue). At low pH, block copolymers from micelles dissolve and release the transported protein.
Source: Reprinted from Gao et al.,[15] © 2012 with permission from Elsevier.

circulation within 5 min.[16] Micelles are also capable of co-delivering DNA and other drugs. Micelles composed of copolymer poly(*N*-methyldietheneamine sebacate)-[(cholesteryl oxocarbonylamido ethyl) methyl bis(ethylene) ammonium bromide] sebacate (PMDS-CES) were shown to transport PTX within the hydrophobic core and pDNA within the corona. Combined delivery of PTX and pDNA suppressed the tumor growth in a 4T1 mouse breast cancer model three times more efficiently than the single delivery of drug and pDNA in micelles.[17] Furthermore, a combination of small interfering ribonucleic acid (siRNA) and PTX demonstrated synergistic effects. MDA-MB-231 human breast carcinoma cells were incubated with micelles containing drug and siRNA. After 4 hr, cell viability decreased from 78% to 58%. As the siRNA cytotoxicity was only about 8%, there was a clear synergistic effect associated with the co-delivery of PTX and siRNA.[17]

POLYMERIC NANOPARTICLES

General Characteristics

Polymeric nanoparticles (NPs) are spherical, colloidal particles consisting of macromolecular materials, in which the active pharmaceutical ingredient (API) is dissolved, entrapped, encapsulated, and/or adsorbed or attached.[18] Although NP size ranges from 10 to 1000 nm, the optimal requirement for drug delivery applications is <200 nm. Three approaches are used to prepare polymeric NPs: (i) dispersion of preformed polymers; (ii) polymerization of monomers for synthetic polymers; and (iii) ionic gelation or coazervation for hydrophilic polymers. Depending on the method of preparation, nanospheres or nanocapsules are designed to tune the release profile (Fig. 3). In general, the process of drug release from NPs is mediated by (i) drug solubility; (ii) diffusion through the NP matrix/polymer wall; (iii) NP matrix erosion; (iv) desorption of adsorbed drug; or (v) a combination of all these factors.[20]

Nanospheres are matrix systems, in which the drug is physically and uniformly dispersed and released by diffusion and erosion.[21] If the erosion of the matrix is faster than the diffusion process, the release mainly depends on the degradation kinetics of the material and results typically in a first order kinetics. Biodegradable polymers have the advantage that they degrade in vivo either enzymatically or nonenzymatically to nontoxic, biocompatible products. One of the disadvantages of nanospheres is the direct contact of the API to the environment at the surface, which can lead to degradation of the compound and burst release. From a drug delivery point of view, nanocapsules can overcome these negative characteristics. Nanocapsules are vesicular systems, in which the drug is encapsulated in a cavity surrounded by a polymer membrane.[22] Depending on the inner core liquid, aqueous or lipophilic, variations of drug solubility are possible. As compared to nanospheres, nanocapsules have the advantage of: (i) increased drug protection; (ii) advanced controlled release; and (iii) higher drug loading capacity. Nanocapsules release drugs by a zero order diffusion driven process, which is influenced by the preparation method for these nanocarriers.[23]

Formulation Characteristics

Two different types of polymers have been employed for the development of NPs, namely natural and synthetic materials. The most commonly used natural polymers are gelatin, alginate, albumin, and chitosan, which are considered to be biodegradable and nontoxic.[24] To prepare albumin-bound nanoparticles (NAB), the API is mixed with HSA in a solvent and pressed through a jet to form NPs in the size range of 50–200 nm. The first polymeric NP product, which is used clinically, is the NAB-formulation Abraxane® (ABI-007) containing the mitotic inhibitor PTX. This technology is approved for the treatment of breast cancer and non-small cell lung cancer (NSCLC). Additional clinical trials are ongoing.[25,26]

Another commonly used natural polymer is chitosan, which offers additional advantages like increased paracellular permeability and excellent mucoadhesive properties.[27,28] pDNA-loaded chitosan NPs demonstrated nasal

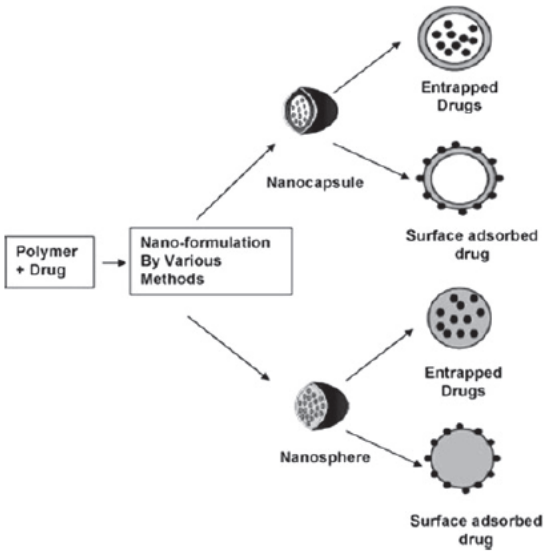

Fig. 3 Schematic representation of methods used to prepare different types of NPs (e.g., nanocapsules and nanospheres). Drug is entrapped within particles or absorbed to the surface. Black dots represent the transported drug.
Source: Reprinted from Kumari et al.,[19] © 2010 with permission from Elsevier.

mucosal immunization against hepatitis B at low pH.[29] However, at physiological pH, the permeation effect by interactions with components of the tight junctions is limited due to the decreased charge (pK_a of amine groups is 6.2). Therefore, quaternary chitosan derivatives such as *N*-trimethyl chitosan (TMC) have been evaluated to overcome this limitation. This derivative has a positive charge independent of the pH and is soluble over a wide pH range, which affects the mucoadhesive and penetration-enhancing properties.[30] Nasal administration of mucoadhesive and rapid antigen-releasing TMC NPs demonstrated the promise of noninvasive vaccination.[31] Furthermore, chitosan has a high loading capacity for nucleic acids with an encapsulation efficiency of 96.2%, owing to ionic interactions.[29]

The use of synthetic polymers in place of natural polymers can offer a wide range of chemical versatility. This includes improved loading efficiency, functionalization properties, and pharmacokinetic profiles. Synthetic polymers like PLA, polyglycolide acid (PGA), polylactide-*co*-glycolide acid (PLGA), poly(ε-caprolactone) (PCL), polyalkylcyanoacrylate (PACA), polyanhydrides, or polymethacrylates have been prepared from a great pool of synthetic and readily available monomers. Depending on the material, different release characteristics from hours up to weeks could be achieved.[19] The polyester PLGA/PLA and PCL are the most commonly used synthetic materials since they are biocompatible, biodegradable, and nontoxic. They are approved for clinical use by the Food and Drug Administration (FDA) and European Medicines Agency (EMA).[32,33] In presence of water, the ester linkages of PLGA and PLA are hydrolyzed and the drug is released. The metabolites (monomers), lactide acid and glycolide acid, are not toxic and are removed by endogenous metabolic pathways such as the citric acid or cori cycle.[34] An interesting property of PLGA is its degradation kinetic, which is a function of the copolymer ratio. Higher glycolide content lowers the time required for its degradation.[35] A significant decrease in the release rate and enhanced entrapment efficiency of estradiol in PLGA NPs were observed with increase in lactide content and molecular weight.[36] However, an acidic microenvironment is generated during degradation that may negatively affect the stability of the loaded API.[37] Common PLGA copolymer ratios (lactide/glycolide molar ratio) are 50:50 and 75:25.[38] To overcome the limitation of hydrolytic stability of polylactides, PCL is often preferred for long-lasting DDSs. A drug release of up to 20 days was achieved with vinblastin loaded PCL-NPs.[39]

Therapeutic Applications

During the last decades, polymeric NPs were used to deliver small molecules, larger peptides and proteins, and expression plasmids.[40] For instance, the natural compound curcumin has chemotherapeutic activity in cancer but a poor bioavailability and suboptimal pharmacokinetic characteristics are limiting factors. However, the encapsulation into PLGA-NPs enhanced the therapeutic efficacy in-vitro compared to free curcumin.[41] The IC50 of curcumin-NPs was 9.1 μM in MDA-MB-231 cells compared to 16.4 μM for the free curcumin. In another study, coencapsulation of the anticancer drug vincristine and chemosensitizer verapamil into PLGA-NPs showed moderate reversion of multidrug resistance in breast cancer cells in vitro.[42] In an alternative approach, DOX combined with the thermal-optical agent indocyanine green (ICG) allows dual application of chemotherapy and hyperthermia for improved cytotoxicity. The DOX-ICG-PLGA-NPs resulted in enhanced cytotoxicity in Dx5 human uterine cancer cells in vitro.[43]

NPs have to be sterically protected in order to prolong their half-life in the circulation. Using PEG, a hydrophilic protective layer can be created to block and delay the opsonization process.[44] To further increase the therapeutic efficacy, targeted delivery of the NPs to specific cells is performed. A aptamer-funtionalized polymeric NP (BIND-014), which is a PEG-PLGA formulation of DTXL, currently completed a phase I clinical study (Fig. 4).[45] In another study, stealth PEG-PLGA-NPs were used as a delivery vehicle for cisplatin,[46] resulting in an 80 times increased toxicity of the cytotoxic agent. Another aptamer-funtionalized PEG-PLGA-NP containing PTX showed a significant decrease in tumor growth and an increase in survival in a glioma xenograft model compared to the

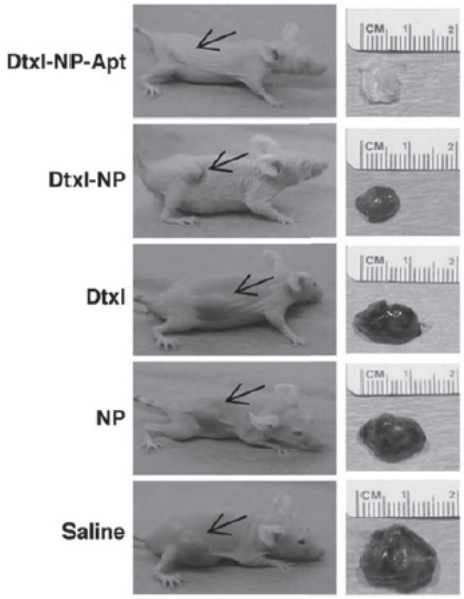

Fig. 4 Comparative prostate tumor regression study in a xenograft mouse model. The left panel shows mice of each treatment group. Black arrows indicate the position of the prostate cancer cell tumor. The right side indicates the tumor size at the endpoint. In the DTXL-NP-Apt group (i.e., mice treated with DTXL loaded PEG-NPs with prostate specific membrane antigen (PSMA) targeting aptamers) the tumor was completely regressed compared with the control treated mice, which received placebo (Saline), empty nanoparticles (NP), DTXL, or nontargeting DTXL-NPs.
Source: Reprinted from Farokhzad et al.,[45] © 2006 with permission from National Academy of Sciences.

unmodified counterparts.[47] Therapeutic proteins and peptides have very limited gastrointestinal bioavailability. They are sensitive to proteolytic enzymes and do not cross passively the biological barriers. NPs can be used to overcome issues associated with peptide and protein delivery. Oral administered insulin-Eudragit-PCL-NPs showed a 52% reduction in blood glucose level in diabetic rats. Their mucoadhesive properties were proposed to enhance gastrointestinal bioavailability.[48] In another study, erythropoietin loaded into oligochitosan NPs was investigated in rats for neuroprotection.[49,50]

Polymeric NPs also have a great potential for the application of nucleic acid gene delivery, because they can overcome the major drawbacks of their viral counterparts like immunogenicity and toxicity. Additionally, they offer the possibility of cheaper large-scale production. The natural polysaccharide chitosan and the noncationic polymer PLGA are the most commonly used nonviral gene vectors for siRNA and pDNA. The inhibition of tumor angiogenesis and growth by PLGA-NP-mediated p53 gene therapy in mice was evaluated recently.[51] In this study, xenografts of p53 mutant tumors were treated with a single intratumoral injection of p53-gene-loaded NPs. Greater levels of apoptosis, antiproliferative activity, decreased angiogenic activity, and finally improved survival indicate that PLGA has potential for sustained gene delivery. The effectiveness of gene silencing with siRNA loaded PLGA-NPs have been evaluated to overcome tumor drug resistance.[52] Silencing of the multidrug resistance protein 1 (MDR1) gene sensitized resistant tumor cells to chemotherapy, as demonstrated by increased PTX accumulation. In a recent study, RGD (Arg-Gly-Asp) peptide-labeled chitosan NPs loaded with siRNA were used for targeted silencing of multiple growth-promoting genes.[53] An inhibition of tumor growth (87% reduction, $P<0.001$) in an $\alpha v\beta 3$-integrin tumor mouse model was shown with siRNA targeting plexin domain-containing protein 1 (PLXDC-1) that is upregulated in ovarian cancer vasculature. A promising approach for the treatment of NSCLC based on the inhibition of telomerase in cancer cells was carried out with chitosan-coated PLGA-NPs. These NPs with a mean size of 160 nm enhanced the delivery of the antisense oligonucleotide 2′-*O*-methyl-RNA to human lung cancer cells. Telomerase inhibition (80%) and telomere shortening (from 5.8 kb to 4 kb) in A549 indicated the potential for in-vivo applications. The cationic NPs showed no cytotoxicity and could be easily modified for active tumor-cell targeting.[54]

POLYMERSOMES

General Characteristics

Polymersomes are artificial vesicles made of synthetic amphiphilic block copolymers and form via a self-assembly process. Generally speaking, polymersomes are hollow spheres, containing an aqueous core that is surrounded by a bilayer membrane. This membrane is composed of a hydrophobic layer sandwiched between internal and external hydrophilic layer forming coronas.[55] Polymersomes were developed as DDS for the transport of either hydrophilic and/or hydrophobic molecules. Compared with liposomes that are lipid analogs, polymersomes have a thick and strong synthetic membrane, conferring a better physicochemical stability as well as lower elasticity and permeability.[2] Polymersomes can be prepared from various types of block copolymers such as nonbiodegradable polymers, degradable polymers, and biocompatible polymers.[56] Depending on the type of polymerization used for synthesis, di-block copolymers (AB), tri-block copolymers (ABA, BAB, or ABC), or even multiblock copolymers can be designed, allowing to tune different properties of the polymersomes.[2] Many factors influence the formation of polymersomes including hydrophilic/hydrophobic block lengths of the copolymer, solvent ratios, concentration of the polymer, and method of preparation. More importantly, volume ratio of hydrophilic to hydrophobic block copolymer fraction influences the formation of polymersomes.

It has been reported that hydrophilic to hydrophobic ratio of less than 1:2 highly favors the formation of polymersomes followed by the ratio of less than 1:3 and ratio more than 1:1 favor the micelle formation.[55] However, the hydrophilic to hydrophobic ratio is not the only determining parameter for polymersome formation.

Although several techniques have been employed to prepare polymersomes, solvent switch and film rehydration techniques are the commonly used methods. In solvent switch amphiphilic block copolymer is dissolved in a suitable organic solvent that is slowly exchanged by an aqueous solution either by adding water to organic polymer solution or vice versa. This technique makes the hydrophobic blocks insoluble, generating copolymer self-assembly into polymersomes as a result of increasing interfacial tension between the hydrophobic blocks and water. In film rehydration, amphiphilic copolymers are dissolved in an organic solvent that is removed by evaporation to form a thin film. An aqueous solution is used to rehydrate the film. Upon mixing, the aqueous phase permeates through defects in the film layers that inflate and finally form vesicles upon separation from the surface.[55,57] Different mechanisms have been reported and proposed for the formation of polymersomes.[58,59] Conventionally, copolymers form a bilayer and close-up to form a vesicular structure. In another mechanism, spherical micelles are formed and then changed into rods, which become flattened and form paddle shape structures. Then these structures transform to circular lamellae that finally close-up to form polymersomes.[60]

Formulation Characteristics

High loading efficiency is a prerequisite for polymersome-based formulation in drug delivery. Loading efficiency can be dependent on preparation method, formation mechanism, and molecular composition of the copolymers. In one study, PEO- poly(benzyl-L-aspartate) (PEO-PBLA) and PEO-poly (2,4,6-trimethoxybenzylidene pentaerythritol carbonate) (PEO-PTMBPEC) based polymersomes were loaded with DOX and showed loading efficiencies of 12% and 8%, respectively.[61] Loading efficiency can be improved using poly(trimethylene carbonate) if the pH of the loading solution is raised to a pH above the pK_a of DOX during the loading process.[62] Using direct dissolution of PEG-polypropylene sulfide (PPS) copolymers, polymersomes achieved higher encapsulation efficiencies for larger protein molecules such as ovalbumin (37%), bovine serum albumin (19%), and bovine gamma-globulin (15%). This method requires a short time for encapsulation, is solvent-free, and simple as compared to methods used for loading of liposomes and other polymersomes.[63] It should be noted that the hollow core of the polymersomes encapsulate the surrounding environment during the self-assembly. Therefore, encapsulation efficiency can also be dependent on the formation mechanism of the polymersomes.

Polymersomes usually exhibit higher stability than polymeric micelles and liposomes due to their thicker membrane. For example, polymersomes made of poly(γ-benzyl L-glutamate)-hyaluronan (PBLG-HYA) loaded with DTXL have shown excellent colloidal stability both at room temperature and at 4°C for one month. More than 90% of DTXL was recovered after storage of DTXL-loaded polymersomes and can be readily lyophilized without alternation in loading content of DTXL for a period of six months storage at 4°C. However, redispersion of lyophilized polymersomes needed a sonication step to accelerate the dispersion time and eliminate the few aggregates still present in solution.[64]

Polymersomes release the loaded drugs through various mechanisms. Furthermore, recently third generation smart systems were designed, where release of drugs from polymersomes can be controlled with external environmental stimuli such as UV light, temperature, and oxidation-reduction.[65] The widely used mechanism for release is degradation of hydrophobic blocks of the polymersomes mediated by simple hydrolysis. This type of degradation is accelerated at acidic pH as found within the endolysosomal compartments of cells.[65] Another possible release mechanism involves the diffusion based permeation of the loaded drug through the polymersome membrane. PEO-PCL polymersomes loaded with DOX showed immediate burst release of 20% of DOX (from 0 hr to 8 hr) by diffusion, followed by a sustained release (up to 14 days) facilitated by pH-driven hydrolysis of the polymersome membrane.[66] The advantages of using stimuli-responsive polymersomes for DDSs have been reviewed extensively elsewhere.[67]

Therapeutic Applications

Polymersomes can readily accommodate a number of drug molecules in the aqueous compartment as well as in their hydrophobic membrane. For instance, to overcome the limitations of DTXL such as low solubility and side effects, this chemotherapeutic drug was incorporated in PBLG-HYA polymersomes. New Zealand rabbits received an IV injection of either polymersome-encapsulated DTXL or free drug. Comparing the plasma profiles, the DTXL-loaded PBLG-HYA polymersomes exhibited a higher maximal concentration (17.97 μg/mL) than the DTXL solution (11.72 μg/mL). The polymersome formulation significantly improved half-life and AUC of DTXL ($t_{1/2}$ = 19.90 hr and AUC = 209.32 μg/mL) compared to the DTXL solution ($t_{1/2}$ = 4.79 hr and AUC = 60.6 μg/mL). Hemolysis tests were performed on human blood and about 30% red blood cell hemolysis (DTXL side-effect) was observed with DTXL solution while less than 5% hemolysis occurred with DTXL-loaded PBLG-HYA polymersomes. Biodistribution studies showed an accumulation of the polymersome formulation at the tumor site in BalB/c mice, and a significantly higher uptake by tumor cells with the polymersomes than with the free drug.[64]

In another series of experiments, biodegradable polymersomes based on PEO-PLA block copolymers were prepared. A hydrophobic drug (PTX) was incorporated into the vesicle membrane. Alternatively, a hydrophilic drug (DOX) was encapsulated within the vesicle core. DOX-PTX loaded into polymersomes showed higher maximum tolerated doses (MDT) of 3 mg/kg for DOX and 7.5 mg/kg for PTX, which is increased by the factor of two compared to free DOX and PTX. In-vitro studies in MDA-MB231 human breast cancer cells with DOX-PTX polymersomes showed a potent antitumor activity without any other toxic side-effects. Polymersomes loaded with DOX-PTX showed 16-fold increased toxicity in tumor cells as compared to both free drugs, leading to a high tumor apoptosis and ultimately increased therapeutic efficacy (Fig. 5).[68]

Therapeutic applications of proteins are challenging due to poor tissue distribution, rapid elimination by renal clearance, and enzymatic degradation. Polymersomes may be promising candidate for delivering a wide range of proteins without affecting their functionality. Polymersomes formed by film rehydration are able to incorporate transmembrane proteins in the bilayer as well as encapsulate proteins in the aqueous core without loss of their functional conformation.[65,69]

Recently, polymersomes were utilized to encapsulate DNA for delivering into cells. Biomimetic, pH-sensitive polymersomes were prepared using poly[2-(methacryloyloxy) ethyl-phosphorylcholine]-*co*-poly[2-(diisopropylamino) ethyl methcrylate] (PMPC-PDPA) diblock copolymers.[70] Under mild acidic condition, pDNA formed a complex with PMPC-PDPA copolymer by electrostatic interaction and the pDNA was encapsulated into the polymersomes at pH 7.5.[70] The pDNA-encapsulated polymersomes used the endocytic pathway to enter the cells and the pDNA escaped to the cytosol due to low pH in the endosomal environment. Experiments with DNA-encapsulated polymersomes clearly showed that the pH-dependent release of plasmid and the transfection efficiency was comparable with the commercially available transfection agent Lipofectamine® (Fig. 6).[70] In addition, the polymeric vesicles exhibited less toxicity and no proinflammatory response with less leakage. The biomimetic surface reduces nonspecific interactions with blood plasma proteins and thereby increases the half-life in the circulation of the polymersomes.[70] In another approach, polymersomes forming diblock copolymer poly(oligoethylene glycol methacrylate)–poly(2-(diisopropylamino)ethyl methacrylate) (POEGMA–PDPA) were used to incorporate pDNA into multicompartment capsules via a LbL technique. By this method, very high loading (60% efficiency) was achieved due to cationic amine groups on the PDPA block, which are protonated at low pH.[71] In another experiment, siRNA was encapsulated into PEO-b-PLA and antisense oligonucleotides (AON) were encapsulated into PEG-b-PCL by a co-solvent method. Loaded oligos were released and escaped from the endosomes by hydrolytic degradation of the polymersomes.[72] In gene silencing experiments, siRNA-(PEO-b-PLA) based polymersomes showed a knockdown efficiency of 40% and

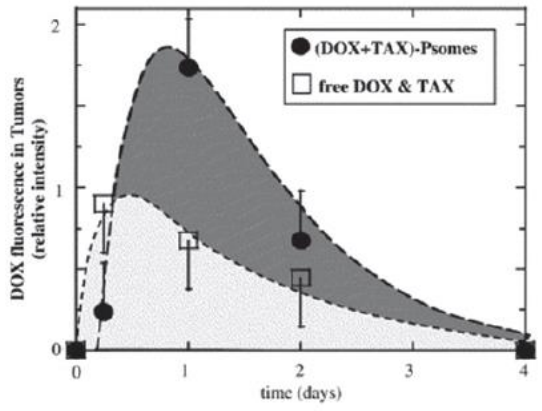

Fig. 5 Tissue accumulation profile of DOX loaded polymersomes in breast cancer tumors. Fluorescence intensity analysis of DOX reveals that accumulation of polymersomes in tumors regions was higher (dark grey) compared to the free drugs (DOX & PTX). Maximal release and tumor tissue accumulation of DOX + PTX loaded polymersomes occur within one day.
Source: Reprinted from Ahmed et al.,[68] © 2012 with permission from Elsevier.

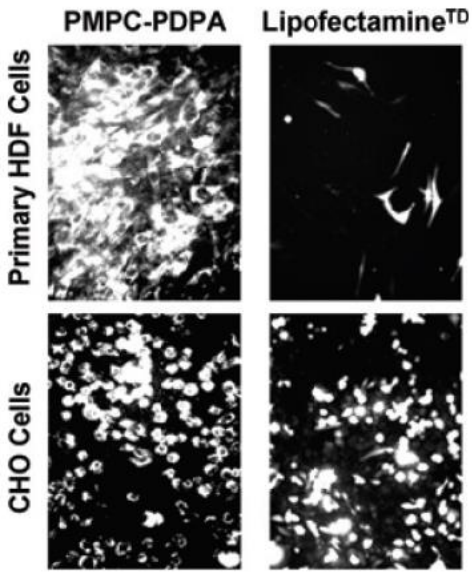

Fig. 6 Delivery of pDNA using pH-dependent polymersomes made of PMPC-PDPA. Polymersomes showed the efficient expression of green fluorescent protein in primary HDF cells and CHO cells and compared with the commercially available LipofectamineTD.
Source: Reprinted from Lomas et al.,[70] © 2007 with permission from WILEY-VCH.

the result was similar to that of Lipofectamine 2000. AON polymeric vesicles were successfully delivered in-vivo to dystrophin-deficient mice with delivery efficiency above 50% and significantly expressed the dystrophin.[72] It was also reported that PMPC-PDPA polymersomes loaded with enhanced green fluorescent protein (EGFP) siRNA showed significant decrease in the EGFP production in cells. After 48 hr, a 70% EGFP expression silencing was observed without affecting the proliferation of the cells.[73]

LAYER-BY-LAYER CAPSULES

General Characteristics

LbL capsules are polymeric multilayer capsules (PMLC) prepared by alternate adsorption of polymers onto a template via complementary interactions such as electrostatic interactions, hydrogen bonding, and covalent linkage.[74–77] In brief, the colloidal template is immersed into an aqueous solution of polymers to build the first surrounding layer. Subsequently, the excess polymer is removed and a second layer of an interacting polymer is absorbed.[78] These two steps are repeated alternately, resulting in a core–shell particle. By altering the number of layer depositions, the film thickness can be easily regulated. The template is finally dissolved to form a multilayered hollow capsule.[79] Dissolution of organic templates like polystyrene or melamine formaldehyde requires strong acids or organic solvents that can hamper the applicability for therapeutics and particularly biomolecules. Moreover, organic solvents can influence the carrier stability by destroying the capsule shell.[80] To overcome these problems, inorganic templates like silica (0.5–5 μm), calcium carbonate (3–5 μm), manganese carbonate, or metal particles are preferred. Inorganic templates are easily dissolved under mild conditions that do not affect the encapsulated drug.[81,82] The initial template strongly influences size distribution and shape of the PMLC.

The constituents of the capsule shell can tailor the chemical and mechanical properties of the PMLCs. For polyelectrolyte capsules, a large variety of charged compounds like synthetic polymers, polypeptides, polysaccharides, nucleic acids, or NPs are used.[83–85] The negative charge of the polyanions is often achieved by sulfonate or carbonate groups whereas polycations mostly have amino or imino groups.[86] Thus, the selected buffer for the synthesis should maintain a high degree of ionization. Phosphate-buffered saline at pH 7.4 offers the maintenance of the charge as well as the physiological condition for many biotherapeutics. Well-studied polyanion/polycation systems for multilayer assembly are polystyrene sulfonate (PSS)/poly allylamine (PAH), PSS/chitosan, heparin/albumin, heparin/poly(ethylene imine) (PEI), dextran sulfate (DS)/chitosan, DS/poly (L-arginine), DS/PEI, and alginate/PLL. To avoid cytotoxic effects of some polycations, hydrogen bonding offers an alternative interaction for LbL assembly. PEI and PLL showed mitochondrial-mediated cell death in a range of human cell lines in-vitro.[87–89] Therefore, poly(*N*-vinylpyrrolidone (PVPON) as hydrogen-bond acceptor and PMA as hydrogen-bond donor have been successfully used. At the end of the production process, it is necessary to cross-link the capsule shell to prevent its destruction at physiological pH and to entrap the drug inside the NP cavity. Carbodiimide chemistry and thiol oxidation are commonly used methods for cross-linking.[90,91]

Formulation Characteristics

Drugs are encapsulated into the carrier mainly by two procedures: (i) postloading or (ii) preloading (Fig. 7). Capsules can be prepared without a compound and the capsule shell can be permeabilized for a postloading process.[93] The capsule wall can be opened by changing pH, ionic strength, solvent polarity, or temperature to allow the diffusion of therapeutics into the capsule interior.[94–97] Returning to the original medium conditions can entrap the drugs inside the capsules. For example, the permeability of biodegradable dextran/chitosan capsules for protein encapsulation can be regulated by variations in pH. At pH values >8, electrostatic repulsion of the polymers leads to an opening of the capsule wall. However, in acidic conditions, the membrane tightens and drugs of interest are entrapped inside the micron-sized hollow capsules.[98] In general, the encapsulation efficiency of the postloading procedure is low. Additionally, the conditions for inducing pores may not be suitable for many biomolecules. An improved variation of this technique is the preloading of the capsule with a sequestering agent, which has a high affinity to the drug. Therefore, the loading process during the diffusion can be increased. Examples include the use of dextran sulfate to increase the encapsulation of DOX.[99]

In contrast to the postloading procedure, porous inorganic templates like mesoporous silica particles offer the possibility of drug preloading due to their large surface area. The polymeric layers adsorb onto the preloaded template.[100,101] Drug crystals as initial template have attracted attention owing to their high encapsulation efficiency.[102–106] For instance, proteins can be directly encapsulated by LbL assembly onto protein crystals.[107] Moreover, other techniques are reported for the drug incorporation. Hydrophobic association is an encapsulation strategy, which was successfully used for natural polyphenols. The anticancer compounds were incorporated into gelatin-based 200 nm NPs surrounded by a 5–20 nm thick LbL shell of polyelectrolytes. The polyphenol loading varied from 20% to 70%.[108] Apart from single drug delivery, polymeric capsules offer the possibility to formulate a DDS, which can release two or more incorporated drugs gradually from a single carrier.[109] Encapsulation of two proteins in separate positions of the capsule showed a time-modulated release. One protein was

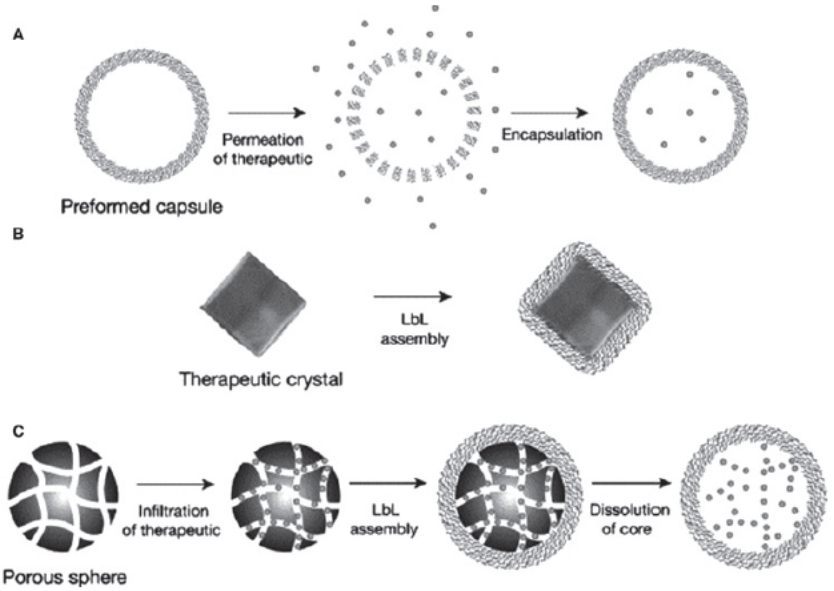

Fig. 7 Different encapsulation methods for loading drugs into LbL capsules: (**A**) postloading procedure of a preformed capsule, (**B**) encapsulation of drug crystals, and (**C**) preloading of porous templates. Gray dots represent loaded drug.
Source: Reprinted from Johnston et al.,[92] © 2006 with permission from Elsevier.

incorporated inside the cavity and the second one between the layers of the shell.[110]

Therapeutic Applications

A versatile spectrum of therapeutics can be incorporated into LbL capsules. Recently, the effect of anticancer drug-loaded capsules has been investigated. Gold NPs coated with a PAH/PSS multilayer were modified with *N*-(2-hydroxypropyl)methacrylamide (HPMA) and a pro-drug of DOX was linked onto the surface.[111] Specific cleavage of the peptide linker by cathepsin B could release DOX from the stealth core-shell-particle after endocytosis in-vitro. Another successfully used encapsulation strategy for DOX is emulsion templating.[112] DOX/oleic acid–loaded PMA capsules (500 nm) demonstrated an enhanced toxicity in a human colorectal cancer cell line in vitro as compared to the free drug. A further improvement of LbL capsules is the smart system that releases the payload by environmental stimuli.[113] Different formulation techniques and polymer combinations can trigger drug release depending on pH or reducing conditions. Redox-responsive capsules demonstrated a novel release method for DOX PMLCs. The disulfide cross-linked shell was stabilized in an oxidizing environment but disrupted under reducing conditions releasing an anticancer drug into the cytoplasm. By this technique, the cytotoxicity of the drug was increased 5000 times compared with the free drug.[114] In a pH-triggered release study LbL-containing quantum dots with a pH-responsible layer were passively navigated to hypoxic regions of solid tumors in vivo and showed a pH-triggered response.[115] PEG was linked to the PLL layer using an iminobiotin-neutravidin interaction, which can be destablized at low pH.[116]

Macromolecules like proteins can also be loaded into PMLCs. Biodegradable multilayered capsules loaded with the cytokine bFGF prolonged the proliferation of L929 fibroblast cells due to sustained release.[98] In general, the LbL technique used for proteins results in micrometer-sized particles. This size is big compared to other nanoparticulate technologies and therefore not suitable for intravenous application.[117] The delivery of nucleic acids like pDNA and siRNA with multilayered capsules is a promising research area. The first successful gene transfection using functional DNA-loaded PMLCs was demonstrated with silica-assisted LbL assembly of dextran and protamine.[118] Recently, single-polyelectrolyte capsules were investigated for the transfection of melanoma cells with pDNA in vitro.[119] Cross-linked PLL particles were co-loaded with pDNA of a nuclear transcription factor and alpha-melanocyte-stimulating hormone as a reporter hormone. The gene expression was significantly increased (70%). In another study, RNA interference was studied by incorporating siRNA into PEI layers on gold NPs.[120] The production of EGFP in CHO-K1 cells was knocked down to about 28%. The versatility and modularity of LbL assembly can be used to introduce multiple functionalities. Drug encapsulation, triggered release, active targeting, and imaging could be achieved with one

single carrier.[121] Furthermore, polymer capsules containing liposomal subcompartments, so-called capsosomes, can co-encapsulate different drugs and trigger the release by encapsulated enzymatic catalysis.[122,123] Nevertheless, the production of capsules <1 μm without aggregation is quite challenging and would be not acceptable for various applications.[124] Further improvements are necessary to produce capsules less than 200 nm in diameter, which is a common size used in DDSs.

CONCLUSION

Over the last two decades, considerable efforts were paid to the development of self-assembling and template-directed copolymer-based nanostructures. These new and innovative nanomaterials can be used for different types of therapeutic drug delivery applications. Polymeric nanomaterial-based DDSs including micelles, NPs, polymersomes and LbL capsules have been extensively studied. Mechanistic studies of the self-assembly process of different types of copolymers have demonstrated the possibility to modulate the physicochemical properties and morphology of resultant nanostructures. Numerous strategies have been explored to improve drug loading, to control drug release, and to improve the stability of nanocarriers in biological systems. Advanced technologies include the design of polymeric nanomaterials with the possibility to introduce multifunctionalities, responsiveness to environmental stimuli, active targeting, biocompatible, and biodegradable properties. Although numerous studies have been reported using polymeric nanomaterials, the clinical realization of drug targeting strategies remains a challenge.

ACKNOWLEDGMENTS

Financial support of the Swiss Centre of Applied Human Toxicology (SCAHT) and the "Freie Akademische Gesellschaft Basel (FAG)" is acknowledged. We thank Annette Roulier for graphical assistance with the figures.

REFERENCES

1. Letchford, K.; Burt, H. A review of the formation and classification of amphiphilic block copolymer nanoparticulate structures: Micelles, nanospheres, nanocapsules and polymersomes. Eur. J. Pharm. Biopharm. **2007**, *65* (3), 259–269.
2. Blanazs, A.; Armes, S.P.; Ryan, A.J. Self-assembled block copolymer aggregates: From micelles to vesicles and their biological applications. Macromol. Rapid Commun. **2009**, *30* (4–5), 267–277.
3. Holder, S.J.; Sommerdijk, N.A.J.M. New micellar morphologies from amphiphilic block copolymers: Disks, toroids and bicontinuous micelles. Polym. Chem. **2011**, *2* (5), 1018–1028.
4. Kulthe, S.S.; Choudhari, Y.M.; Inamdar, N.N.; Mourya, V. Polymeric micelles: Authoritative aspects for drug delivery. Des. Monomers Polym. **2012**, *15* (5), 465–521.
5. Huh, K.M.; Lee, S.C.; Cho, Y.W.; Lee, J.; Jeong, J.H.; Park, K. Hydrotropic polymer micelle system for delivery of paclitaxel. J Control. Release **2005**, *101* (1–3), 59–68.
6. Kim, J.Y.; Kim, S.; Pinal, R.; Park, K. Hydrotropic polymer micelles as versatile vehicles for delivery of poorly water-soluble drugs. J. Control. Release **2011**, *152* (1), 13–20.
7. Shin, H.-C.; Alani, A.W.; Rao, D.A.; Rockich, N.C.; Kwon, G.S. Multi-drug loaded polymeric micelles for simultaneous delivery of poorly soluble anticancer drugs. J. Control. Release **2009**, *140* (3), 294–300.
8. Bronich, T.K.; Keifer, P.A.; Shlyakhtenko, L.S.; Kabanov, A.V. Polymer micelle with cross-linked ionic core. J. Am. Chem. Soc. **2005**, *127* (23), 8236–8237.
9. Aliabadi, H.M.; Lavasanifar, A. Polymeric micelles for drug delivery. Expert Opin. Drug Deliv. **2006**, *3* (1), 139–162.
10. Kim, S.; Shi, Y.; Kim, J.Y.; Park, K.; Cheng, J.X. Overcoming the barriers in micellar drug delivery: Loading efficiency, in vivo stability, and micelle-cell interaction. Expert Opin Drug Deliv **2010**, *7* (1), 49–62.
11. Batrakova, E.V.; Kabanov, A.V. Pluronic block copolymers: Evolution of drug delivery concept from inert nanocarriers to biological response modifiers. J. Control. Release **2008**, *130* (2), 98–106.
12. Leung, S.Y.L.; Jackson, J.; Miyake, H.; Burt, H.; Gleave, M.E. Polymeric micellar paclitaxel phosphorylates Bcl-2 and induces apoptotic regression of androgen-independent LNCaP prostate tumors. Prostate **2000**, *44* (2), 156–163.
13. Hamaguchi, T.; Matsumura, Y.; Suzuki, M.; Shimizu, K.; Goda, R.; Nakamura, I.; Nakatomi, I.; Yokoyama, M.; Kataoka, K.; Kakizoe, T. NK105, a paclitaxel-incorporating micellar nanoparticle formulation, can extend in vivo antitumour activity and reduce the neurotoxicity of paclitaxel. Br. J. Cancer **2005**, *92* (7), 1240–1246.
14. Shi, Y.; Huang, W.; Liang, R.; Sun, K.; Zhang, F.; Liu, W.; Li, Y. Improvement of in vivo efficacy of recombinant human erythropoietin by encapsulation in PEG-PLA micelle. Int. J. Nanomed. **2013**, *8* (1), 1–11.
15. Gao, G.H.; Park, M.J.; Li, Y.; Im, G.H.; Kim, J.H.; Kim, H.N.; Lee, J.W.; Jeon, P.; Bang, O.Y.; Lee, J.H.; Lee, D.S. The use of pH-sensitive positively charged polymeric micelles for protein delivery. Biomaterials **2012**, *33* (35), 9157–9164.
16. Nishiyama, N.; Jang, W.D.; Date, K.; Miyata, K.; Kataoka, K. Photochemical enhancement of transgene expression by polymeric micelles incorporating plasmid DNA and dendrimer-based photosensitizer. J. Drug Target. **2006**, *14* (6), 413–424.
17. Wang, L.; Chierico, L.; Little, D.; Patikarnmonthon, N.; Yang, Z.; Azzouz, M.; Madsen, J.; Armes, S.P.; Battaglia, G. Encapsulation of biomacromolecules within polymersomes by electroporation. Angew. Chem. Int. Ed. **2012**, *51* (44), 11122–11125.
18. Kreuter, J. Nanoparticles—a historical perspective. Int. J. Pharm. **2007**, *331* (1), 1–10.

51. Prabha, S.; Sharma, B.; Labhasetwar, V. Inhibition of tumor angiogenesis and growth by nanoparticle-mediated p53 gene therapy in mice. Cancer Gene Ther. **2012**, *19* (8), 530–537.
52. Patil, Y.B.; Swaminathan, S.K.; Sadhukha, T.; Ma, L.; Panyam, J. The use of nanoparticle-mediated targeted gene silencing and drug delivery to overcome tumor drug resistance. Biomaterials **2010**, *31* (2), 358–365.
53. Han, H.D.; Mangala, L.S.; Lee, J.W.; Shahzad, M.M.; Kim, H.S.; Shen, D.; Nam, E.J.; Mora, E.M.; Stone, R.L.; Lu, C.; Lee, S.J.; Roh, J.W.; Nick, A.M.; Lopez-Berestein, G.; Sood, A.K. Targeted gene silencing using RGD-labeled chitosan nanoparticles. Clin. Cancer Res. **2010**, *16* (15), 3910–3922.
54. Beisner, J.; Dong, M.; Taetz, S.; Nafee, N.; Griese, E.U.; Schaefer, U.; Lehr, C.M.; Klotz, U.; Mürdter, T.E. Nanoparticle mediated delivery of 2'-O-methyl-RNA leads to efficient telomerase inhibition and telomere shortening in human lung cancer cells. Lung Cancer **2010**, *68* (3), 346–354.
55. Lee, J.S.; Feijen, J. Polymersomes for drug delivery: Design, formation and characterization. J. Control. Release **2012**, *161* (2), 473–483.
56. Jain, J.P.; Ayen, W.Y.; Kumar, N. Self assembling polymers as polymersomes for drug delivery. Curr. Pharm. Des. **2011**, *17* (1), 65–79.
57. Howse, J.R.; Jones, R.A.; Battaglia, G.; Ducker, R.E.; Leggett, G.J.; Ryan, A.J. Templated formation of giant polymer vesicles with controlled size distributions. Nat. Mater. **2009**, *8* (6), 507–511.
58. Uneyama, T. Density functional simulation of spontaneous formation of vesicle in block copolymer solutions. J. Chem. Phys. **2007**, *126* (11), 114902.
59. He, X.; Schmid, F. Dynamics of spontaneous vesicle formation in dilute solutions of amphiphilic diblock copolymers. Macromolecules **2006**, *39* (7), 2654–2662.
60. Chen, L.; Shen, H.; Eisenberg, A. Kinetics and mechanism of the rod-to-vesicle transition of block copolymer aggregates in dilute solution. J. Phys. Chem. B **1999**, *103* (44), 9488–9497.
61. Kataoka, K.; Matsumoto, T.; Yokoyama, M.; Okano, T.; Sakurai, Y.; Fukushima, S.; Okamoto, K.; Kwon, G.S. Doxorubicin-loaded poly(ethylene glycol)–poly(β-benzyl-l-aspartate) copolymer micelles: Their pharmaceutical characteristics and biological significance. J. Control. Release **2000**, *64* (1–3), 143–153.
62. Sanson, C.; Schatz, C.; Le Meins, J.F.; Soum, A.; Thévenot, J.; Garanger, E.; Lecommandoux, S. A simple method to achieve high doxorubicin loading in biodegradable polymersomes. J. Control. Release **2010**, *147* (3), 428–435.
63. O'Neil, C.P.; Suzuki, T.; Demurtas, D.; Finka, A.; Hubbell, J.A. A novel method for the encapsulation of biomolecules into polymersomes via direct hydration. Langmuir **2009**, *25* (16), 9025–9029.
64. Upadhyay, K.K.; Bhatt, A.N.; Castro, E.; Mishra, A.K.; Chuttani, K.; Dwarakanath, B.S.; Schatz, C.; Le Meins, J.F.; Misra, A.; Lecommandoux, S. In vitro and in vivo evaluation of docetaxel loaded biodegradable polymersomes. Macromol. Biosci. **2010**, *10* (5), 503–512.
65. Christian, D.A.; Cai, S.; Bowen, D.M.; Kim, Y.; Pajerowski, J.D.; Discher, D.E. Polymersome carriers: From self-assembly to siRNA and protein therapeutics. Eur. J. Pharm. Biopharm. **2009**, *71* (3), 463–474.
66. Ghoroghchian, P.P.; Li, G.; Levine, D.H.; Davis, K.P.; Bates, F.S.; Hammer, D.A.; Therien, M.J. Bioresorbable vesicles formed through spontaneous self-assembly of amphiphilic poly(ethylene oxide)-block-polycaprolactone. Macromolecules **2006**, *39* (5), 1673–1675.
67. Onaca, O.; Enea, R.; Hughes, D.W.; Meier, W. Stimuli-responsive polymersomes as nanocarriers for drug and gene delivery. Macromol. Biosci. **2009**, *9* (2), 129–139.
68. Ahmed, F.; Pakunlu, R.I.; Brannan, A.; Bates, F.; Minko, T.; Discher, D.E. Biodegradable polymersomes loaded with both paclitaxel and doxorubicin permeate and shrink tumors, inducing apoptosis in proportion to accumulated drug. J. Control. Release **2006**, *116* (2), 150–158.
69. Tanner, P.; Baumann, P.; Enea, R.; Onaca, O.; Palivan, C.; Meier, W. Polymeric vesicles: From drug carriers to nanoreactors and artificial organelles. Acc. Chem. Res. **2011**, *44* (10), 1039–1049.
70. Lomas, H.; Canton, I.; MacNeil, S.; Du, J.; Armes, S.P.; Ryan, A.J.; Lewis, A.L.; Battaglia, G. Biomimetic pH sensitive polymersomes for efficient DNA encapsulation and delivery. Adv. Mater. **2007**, *19* (23), 4238–4243.
71. Lomas, H.; Johnston, A.P.; Such, G.K.; Zhu, Z.; Liang, K.; Van Koeverden, M.P.; Alongkornchotikul, S.; Caruso, F. Polymersome-loaded capsules for controlled release of DNA. Small **2011**, *7* (14), 2109–2119.
72. Kim, Y.; Tewari, M.; Pajerowski, J.D.; Cai, S.; Sen, S.; Williams, J.H.; Sirsi, S.R.; Lutz, G.J.; Discher, D.E. Polymersome delivery of siRNA and antisense oligonucleotides. J. Control. Release **2009**, *134* (2), 132–140.
73. Lewis, A.L.; Battaglia, G.; Canton, I.; Stratford, P.W. Amphiphilic Block Copolymers For Nucleic Acid Delivery, http://patent.ipexl.com/U2S/20110151013.html (accessed Mar 27, 2013).
74. Quinn, J.F.; Johnston, A.P.; Such, G.K.; Zelikin, A.N.; Caruso, F. Next generation, sequentially assembled ultrathin films: Beyond electrostatics. Chem. Soc. Rev. **2007**, *36* (5), 707–718.
75. Zhang, Y.J.; Guan, Y.I.N.G.; Yang, S.; Xu, J.; Han, C.C. Fabrication of hollow capsules based on hydrogen bonding. Adv. Mater. **2003**, *15* (10), 832–835.
76. Kozlovskaya, V.; Ok, S.; Sousa, A.; Libera, M.; Sukhishvili, S.A. Hydrogen-bonded polymer capsules formed by layer-by-layer self-assembly. Macromolecules **2003**, *36* (23), 8590–8592.
77. Such, G.K.; Tjipto, E.; Postma, A.; Johnston, A.P.; Caruso, F. Ultrathin, responsive polymer click capsules. Nano Lett. **2007**, *7* (6), 1706–1710.
78. Decher, G.; Hong, J. Buildup of ultrathin multilayer films by a self-assembly process .1. Consecutive adsorption of anionic and cationic bipolar amphiphiles on charged surfaces. Makromol. Chem. Macromol. Symp. **1991**, *46* (1) 321–327.
79. Caruso, F.; Caruso, R.A.; Möhwald, H. Nanoengineering of inorganic and hybrid hollow spheres by colloidal templating. Science **1998**, *282* (5391), 1111–1114.
80. Dejugnat, C.; Sukhorukov, G.B. pH-responsive properties of hollow polyelectrolyte microcapsules templated on various cores. Langmuir **2004**, *20* (17), 7265–7269.

81. Volodkin, D.V.; Larionova, N.I.; Sukhorukov, G.B. Protein encapsulation via porous CaCO3 microparticles templating. Biomacromolecules **2004**, *5* (5), 1962–1972.
82. Itoh, Y.; Matsusaki, M.; Kida, T.; Akashi, M. Enzyme-responsive release of encapsulated proteins from biodegradable hollow capsules. Biomacromolecules **2006**, *7* (10), 2715–2718.
83. Peyratout, C.S.; Dahne, L. Tailor-made polyelectrolyte microcapsules: From multilayers to smart containers. Angew. Chem. Int. Ed. **2004**, *43* (29), 3762–3783.
84. De Geest, B.G.; Sanders, N.N., Sukhorukov, G.B.; Demeester, J.; De Smedt, S.C. Release mechanisms for polyelectrolyte capsules. Chem. Soc. Rev. **2007**, *36* (4), 636–649.
85. De Cock, L.J.; De Koker, S.; De Geest, B.G.; Grooten, J.; Vervaet. C.; Remon, J.P.; Sukhorukov. G.B.; Antipina, M.N. Polymeric multilayer capsules in drug delivery. Angew. Chem. Int. Ed. **2010**, *49* (39), 6954–6973.
86. Ai, H.; Jones, S.A.; Lvov, Y.M. Biomedical applications of electrostatic layer-by-layer nano-assembly of polymers, enzymes, and nanoparticles. Cell Biochem. Biophys. **2003**, *39* (1), 23–43.
87. Fischer, D.; Li, Y.; Ahlemeyer, B.; Krieglstein, J.; Kissel, T. In vitro cytotoxicity testing of polycations: Influence of polymer structure on cell viability and hemolysis. Biomaterials **2003**, *24* (7), 1121–1131.
88. Moghimi, S.M.; Symonds, P.; Murray, J.C.; Hunter, A.C.; Debska, G.; Szewczyk, A. A two-stage poly(ethylenimine)-mediated cytotoxicity: Implications for gene transfer/therapy. Mol. Ther. **2005**, *11* (6), 990–995.
89. Symonds, P.; Murray, J.C.; Hunter, A.C.; Debska, G.; Szewczyk, A.; Moghimi, S.M. Low and high molecular weight poly(L-lysine)s/poly(L-lysine)-DNA complexes initiate mitochondrial-mediated apoptosis differently. FEBS Lett. **2005**, *579* (27), 6191–6198.
90. Kozlovskaya, V.; Kharlampieva, E.; Mansfield, M.L.; Sukhishvili, S.A. Poly(methacrylic acid) hydrogel films and capsules: Response to pH and ionic strength, and encapsulation of macromolecules. Chem. Mater. **2006**, *18* (2), 328–336.
91. Zelikin, A.N.; Li, Q.; Caruso, F. Disulfide-stabilized poly(methacrylic acid) capsules: Formation, cross-linking, and degradation behavior. Chem. Mat. **2008**, *20* (8), 2655–2661.
92. Johnston, A.P.R.; Cortez, C.; Angelatos, A.S.; Caruso, F. Layer-by-layer engineered capsules and their applications. Curr. Opin. Colloid Interface Sci. **2006**, *11* (4), 203–209.
93. De Koker, S.; Hoogenboom, R.; De Geest, B.G. Polymeric multilayer capsules for drug delivery. Chem. Soc. Rev **2012**, *41* (7), 2867–2884.
94. Shutava, T.; Prouty, M.; Kommireddy, D.; Lvov, Y. pH responsive decomposable layer-by-layer nanofilms and capsules on the basis of tannic acid. Macromolecules **2005**, *38* (7), 2850–2858.
95. Ibarz, G.; Dähne, L.; Donath, E.; Moehwald, H. Smart micro- and nanocontainers for storage, transport, and release. Adv. Mater. **2001**, *13* (17), 1324–1327.
96. Lvov, Y.; Antipov, A.A.; Mamedov, A.; Möhwald, H.; Sukhorukov, G.B. Urease encapsulation in nanoorganized microshells. Nano Lett. **2001**, *1* (3), 125–128.
97. Koehler, K.; Sukhorukov, G.B. Heat treatment of polyelectrolyte multilayer capsules: A versatile method for encapsulation. Adv. Funct. Mater. **2007**, *17* (13), 2053–2061.
98. Itoh, Y.; Matsusaki, M.; Kida, T.; Akashi, M. Locally controlled release of basic fibroblast growth factor from multilayered capsules. Biomacromolecules **2008**, *9* (8), 2202–2206.
99. Khopade, A.J.; Caruso, F. Stepwise self-assembled poly(amidoamine) dendrimer and poly(styrenesulfonate) microcapsules as sustained delivery vehicles. Biomacromolecules **2002**, *3* (6), 1154–1162.
100. Wang, Y.; Yu, A.; Caruso, F. Nanoporous polyelectrolyte spheres prepared by sequentially coating sacrificial mesoporous silica spheres. Angew. Chem. Int. Ed. **2005**, *44* (19), 2888–2892.
101. Yu, A.; Wang, Y.; Barlow, E.; Caruso, F. Mesoporous silica particles as templates for preparing enzyme-loaded biocompatible microcapsules. Adv. Mater. **2005**, *17* (14), 1737–1741.
102. Zheng, Z.; Zhang, X.; Carbo, D.; Clark, C.; Nathan, C.; Lvov, Y. Sonication-assisted synthesis of polyelectrolyte-coated curcumin nanoparticles. Langmuir **2010**, *26* (11), 7679–7681.
103. Chen, Y.; Lin, X.; Park, H.; Greever, R. Study of artemisinin nanocapsules as anticancer drug delivery systems. Nanomed. Nanotechnol. Biol. Med. **2009**, *5* (3), 316–322.
104. Zhang, F.; Wu, Q.; Chen, Z.C.; Zhang, M.; Lin, X.F. Hepatic-targeting microcapsules construction by self-assembly of bioactive galactose-branched polyelectrolyte for controlled drug release system. J. Colloid Interface Sci. **2008**, *317* (2), 477–484.
105. Pargaonkar, N.; Lvov, Y.M.; Li, N.; Steenekamp, J.H.; de Villiers, M.M. Controlled release of dexamethasone from microcapsules produced by polyelectrolyte layer-by-layer nanoassembly. Pharm. Res. **2005**, *22* (5), 826–835.
106. Caruso, F.; Trau, D.; Möhwald, H.; Renneberg, R. Enzyme encapsulation in layer-by-layer engineered polymer multilayer capsules. Langmuir **2000**, *16* (4), 1485–1488.
107. Balabushevitch, N.G.; Sukhorukov, G.B.; Moroz, N.A.; Volodkin, D.V.; Larionova, N.I.; Donath, E.; Mohwald, H. Encapsulation of proteins by layer-by-layer adsorption of polyelectrolytes onto protein aggregates: Factors regulating the protein release. Biotechnol. Bioeng. **2001**, *76* (3), 207–213.
108. Shutava, T.G.; Balkundi, S.S.; Vangala, P.; Steffan, J.J.; Bigelow, R.L.; Cardelli, J.A.; O'Neal, D.P.; Lvov, Y.M. Layer-by-layer-coated gelatin nanoparticles as a vehicle for delivery of natural polyphenols. ACS Nano **2009**, *3* (7), 1877–1885.
109. Matsusaki, M.; Akashi, M. Functional multilayered capsules for targeting and local drug delivery. Expert Opin. Drug Deliv. **2009**, *6* (11), 1207–1217.
110. Itoh, Y.; Matsusaki, M.; Kida, T.; Akashi, M. Time-modulated release of multiple proteins from enzyme-responsive multilayered capsules. Chem. Lett. **2008**, *37* (3), 238–239.
111. Schneider, G.F.; Subr, V.; Ulbrich, K.; Decher, G. Multifunctional cytotoxic stealth nanoparticles. A model approach with potential for cancer therapy. Nano Lett. **2009**, *9* (2), 636–642.

112. Sivakumar, S.; Bansal, V.; Cortez, C.; Chong, S.F.; Zelikin, A.N.; Caruso, F. Degradable, surfactant-free, monodisperse polymer-encapsulated emulsions as anticancer drug carriers. Adv. Mater. **2009**, *21* (18), 1820–1824.
113. Sukhishvili, S.A. Responsive polymer films and capsules via layer-by-layer assembly. Curr. Opin. Colloid Interface Sci. **2005**, *10* (1–2), 37–44.
114. Yan, Y.; Johnston, A.P.; Dodds, S.J.; Kamphuis, M.M.; Ferguson, C.; Parton, R.G.; Nice, E.C.; Heath, J.K.; Caruso, F. Uptake and intracellular fate of disulfide-bonded polymer hydrogel capsules for doxorubicin delivery to colorectal cancer cells. ACS Nano **2010**, *4* (5), 2928–2936.
115. Poon, Z.; Chang, D.; Zhao, X.; Hammond, P.T. Layer-by-layer nanoparticles with a ph-sheddable layer for in vivo targeting of tumor hypoxia. ACS Nano **2011**, *5* (6), 4284–4292.
116. Wohl, B.M.; Engbersen, J.F.J. Responsive layer-by-layer materials for drug delivery. J. Control. Release **2012**, *158* (1), 2–14.
117. Staedler, B.; Price, A.D.; Zelikin, A.N. A critical look at multilayered polymer capsules in biomedicine: Drug carriers, artificial organelles, and cell mimics. Adv. Funct. Mater. **2011**, *21* (1), 14–28.
118. Reibetanz, U.; Claus, C.; Typlt, E.; Hofmann, J.; Donath, E. Defoliation and plasmid delivery with layer-by-layer coated colloids. Macromol. Biosci. **2006**, *6* (2), 153–160.
119. Zhang, X.; Oulad-Abdelghani, M.; Zelkin, A.N.; Wang, Y.; Haîkel, Y.; Mainard, D.; Voegel, J.C.; Caruso, F.; Benkirane-Jessel, N. Poly(L-lysine) nanostructured particles for gene delivery and hormone stimulation. Biomaterials **2010**, *31* (7), 1699–1706.
120. Elbakry, A.; Zaky, A.; Liebl, R.; Rachel, R.; Goepferich, A.; Breunig, M. Layer-by-layer assembled gold nanoparticles for siRNA delivery. Nano Lett. **2009**, *9* (5), 2059–2064.
121. del Mercato, L.L.; Rivera-Gil, P.; Abbasi, A.Z.; Ochs, M.; Ganas, C.; Zins, I.; Sönnichsen, C.; Parak, W.J. LbL multilayer capsules: Recent progress and future outlook for their use in life sciences. Nanoscale **2010**, *2* (4), 458–467.
122. Staedler, B.; Chandrawati, R.; Price, A.D.; Chong, S.F.; Breheney, K.; Postma, A.; Connal, L.A.; Zelikin, A.N.; Caruso, F. A microreactor with thousands of subcompartments: Enzyme-loaded liposomes within polymer capsules. Angew. Chem. Int. Ed. **2009**, *48* (24), 4359–4362.
123. Chandrawati, R.; Odermatt, P.D.; Chong, S.F.; Price, A.D; Städler, B.; Caruso, F. Triggered cargo release by encapsulated enzymatic catalysis in capsosomes. Nano Lett. **2011**, *11* (11), 4958–4963.
124. De Geest, B.G.; Sukhorukov, G.B.; Möhwald, H. The pros and cons of polyelectrolyte capsules in drug delivery. Expert Opin. Drug Deliv. **2009**, *6* (6), 613–624.